

Proxy-Normalizing Activations to Match Batch Normalization while Removing Batch Dependence

Antoine Labatie Dominic Masters Zach Eaton-Rosen Carlo Luschi
 Graphcore Research, UK
 antoine.labatie@centraliens.net
 {dominicm, zacher, carlo}@graphcore.ai

Abstract

We investigate the reasons for the performance degradation incurred with batch-independent normalization. We find that the prototypical techniques of layer normalization and instance normalization both induce the appearance of failure modes in the neural network’s pre-activations: (i) layer normalization induces a collapse towards channel-wise constant functions; (ii) instance normalization induces a lack of variability in instance statistics, symptomatic of an alteration of the expressivity. To alleviate failure mode (i) without aggravating failure mode (ii), we introduce the technique “Proxy Normalization” that normalizes post-activations using a proxy distribution. When combined with layer normalization or group normalization, this batch-independent normalization emulates batch normalization’s behavior and consistently matches or exceeds its performance.

1 Introduction

Normalization plays a critical role in deep learning as it allows successful scaling to large and deep models. In vision tasks, the most well-established normalization technique is Batch Normalization (BN) [1]. At every layer in the network, BN normalizes the intermediate activations to have zero mean and unit variance in each channel. While indisputably successful when training with large batch size, BN incurs a performance degradation in the regime of small batch size [2, 3, 4, 5, 6, 7]. This performance degradation is commonly attributed to an excessive or simply unwanted regularization stemming from the noise in the approximation of full-batch statistics by mini-batch statistics.

Many techniques have been proposed to avoid this issue, while at the same time retaining BN’s benefits. Some techniques mimic BN’s principle while decoupling the computational batch from the normalization batch [2, 8, 7]. Other techniques are “batch-independent” in that they operate independently of the batch in various modalities: through an explicit normalization either in activation space [9, 10, 11, 12, 13, 3, 5, 14, 15, 6] or in weight space [16, 17, 18, 19, 20]; through the use of an analytic proxy to track activation statistics [21, 22, 23]; through a change of activation function [24, 5, 15].

In this paper, we push the endeavor to replace BN with a batch-independent normalization a step further. Our main contributions are as follows: (i) we introduce a novel framework to finely characterize the various neural network properties affected by the choice of normalization; (ii) using this framework, we show that BN’s beneficial properties *are not* retained when using solely the prototypical batch-independent normalization techniques, but *are* retained when combining some of these techniques with Proxy Normalization, a novel technique that we hereby introduce; (iii) we demonstrate on an extensive set of experiments that, by reproducing BN’s beneficial properties, our batch-independent normalization approach consistently matches or exceeds BN’s performance.

As a starting point of our analysis, we need to gain a better understanding of those beneficial properties of BN that we aim at reproducing.

2 Batch Normalization’s beneficial properties

We consider throughout this paper a convolutional neural network with $d = 2$ spatial axes. This neural network receives an input $\mathbf{x} \in \mathbb{R}^{H \times W \times C_0}$ which, unless otherwise stated, is assumed sampled from a finite dataset \mathcal{D} . The neural network maps its input \mathbf{x} to intermediate activations $\mathbf{x}^l \in \mathbb{R}^{H \times W \times C_l}$ of height H , width W and number of channels C_l at each layer l . The value of \mathbf{x}^l at spatial position $\alpha \in \{1, \dots, H\} \times \{1, \dots, W\}$ and channel $c \in \{1, \dots, C_l\}$ is denoted as $\mathbf{x}_{\alpha,c}^l$, with the dependency on \mathbf{x} kept *implicit* to avoid overloading notations.

The inclusion of BN at layer l leads in the full-batch setting to adding the following operations $\forall \alpha, c$:

$$\mathbf{y}_{\alpha,c}^l = \frac{\mathbf{x}_{\alpha,c}^l - \mu_c(\mathbf{x}^l)}{\sigma_c(\mathbf{x}^l)}, \quad \tilde{\mathbf{y}}_{\alpha,c}^l = \gamma_c^l \mathbf{y}_{\alpha,c}^l + \beta_c^l, \quad (1)$$

where $\mu_c(\mathbf{x}^l)$, $\sigma_c(\mathbf{x}^l)$ are the mean and standard deviation of \mathbf{x}^l in channel c , and γ_c^l, β_c^l are channel-wise scale and shift parameters restoring the degrees of freedom lost in the standardization. In the mini-batch setting, the full-batch statistics $\mu_c(\mathbf{x}^l)$, $\sigma_c(\mathbf{x}^l)$ are approximated by mini-batch statistics.

Table 1 summarizes the beneficial properties that result from including BN in the neural network. Below, we provide details on each of these properties, and we discuss whether each property is reproduced with batch-independent norms.

Scale invariance. When BN is present, the input-output mapping of the neural network is invariant to the scale of the weights preceding any BN layer. With such scale invariance plus weight decay, the scale of weights during training reaches an equilibrium with an effective learning rate depending on both the learning rate and the weight decay strength [25, 26, 27, 8, 28, 29, 30]. Such mechanism of “auto rate-tuning” has been shown to provide optimization benefits [31, 26, 32].

This property is easy to reproduce. It is already obtained with most existing batch-independent norms.

Control of activation scale in residual networks. To be trainable, residual networks require the scale of activations to remain well-behaved at initialization [33, 34, 35, 20, 36, 37]. While this property naturally arises when BN is present on the residual path, when BN is not present it can also be enforced by a proper scaling decaying with the depth of the residual path. This “dilution” of the residual path with respect to the skip connection path reduces the effective depth of the network and thereby enables to avoid coarse-grained failures modes [38, 39, 40, 41, 42, 35].

This property is easy to reproduce. It is already obtained with most existing batch-independent norms.

Regularizing noise. Due to the stochasticity of the approximation of $\mu_c(\mathbf{x}^l)$, $\sigma_c(\mathbf{x}^l)$ by mini-batch statistics, training a neural network with BN in the mini-batch setting can be seen as equivalent to performing Bayesian inference [43, 44] or as adding a regularizing term to the training of the same network with full-batch statistics [45]. As a result, BN induces a specific form of regularization.

This regularization is not reproduced with batch-independent norms, but we leave it out of the scope of this paper. To help minimize the bias in our analysis and “subtract away” this effect, we perform all our experiments without and with extra degrees of regularization. This procedure can be seen as a coarse disentanglement of normalization’s effects from regularization’s effects.

Avoidance of collapse. Unnormalized networks with non-saturating nonlinearities are subject to a phenomenon of “collapse” whereby the distribution with respect to \mathbf{x} , α of the intermediate activation vectors $(\mathbf{x}_{\alpha,1}^l, \dots, \mathbf{x}_{\alpha,C_l}^l)^T$ becomes close to zero- or one-dimensional in deep layers [39, 46, 41, 47, 48, 49, 37]. This means that deep in an unnormalized network: (i) layers tend to have their channels imbalanced; (ii) nonlinearities tend to become channel-wise linear with respect to \mathbf{x} , α and not add any effective capacity [39, 50, 51]. Consequently, unnormalized networks can neither effectively use their whole width (imbalanced channels) nor effectively use their whole depth (channel-wise linearity).

Conversely, when BN is used, the standardization at each layer prevents this collapse from happening. Even in deep layers, channels remain balanced and nonlinearities remain channel-wise nonlinear with respect to \mathbf{x} , α . Consequently, networks with BN can effectively use their whole width and depth.

The collapse is, on the other hand, not always avoided with batch-independent norms [39, 18, 49]. Most notably, it is *not* avoided with Layer Normalization (LN) [9] and Group Normalization (GN) [3], as we show both theoretically and experimentally on commonly found networks in Section 4.

To the extent possible, we aim at designing a batch-independent norm that avoids this collapse.

Table 1: **BN’s beneficial properties.** We show whether each property is (at least approximately) present (✓) or absent (✗) with different batch-independent norms: Instance Normalization (IN), Layer Normalization (LN), Layer Normalization + Proxy Normalization (LN+PN, cf Section 5). In this categorization, BN is considered in the mini-batch setting but still close to the full-batch setting, such that it approximately preserves expressivity [53].

	Scale invariance	Control of activation scale	Regularizing noise	Avoidance of collapse	Preservation of expressivity
BN	✓	✓	✓	✓	✓
IN	✓	✓	✗	✓	✗
LN	✓	✓	✗	✗	✓
LN+PN	✓	✓	✗	✓	✓

Preservation of expressivity. We can always express the identity with Eq. (1) by choosing $\beta_c^l = \mu_c(\mathbf{x}^l)$ and $\gamma_c^l = \sigma_c(\mathbf{x}^l)$. Conversely, for any choice of β_c^l, γ_c^l , we can always “re-absorb” Eq. (1) into a preceding convolution with bias. This means that BN in the full-batch setting *does not alter the expressivity* compared to an unnormalized network, i.e. it amounts to a plain reparameterization of the hypothesis space.

The expressivity is, on the other hand, not always preserved with batch-independent norms. In activation space, the dependence of batch-independent statistics on the input \mathbf{x} turns the standardization into a channel-wise nonlinear operation that cannot be “re-absorbed” into a preceding convolution [18]. This phenomenon is most pronounced when statistics get computed over few components. This means e.g. that Instance Normalization (IN) [10] induces a greater change of expressivity than GN, which itself induces a greater change of expressivity than LN.

In weight space, the expressivity can also be altered, namely by the removal of degrees of freedom. This is the case with Weight Standardization (WS) [18, 20] and Centered Weight Normalization [17] that remove degrees of freedom (one per unit) that *cannot* be restored in a succeeding affine transformation. This reduction of expressivity could explain the ineffectiveness of these techniques in EfficientNets [52], as observed in previous works [20] and as we confirm in Section 6.

To the extent possible, we aim at designing a batch-independent norm that preserves expressivity.

3 Theoretical framework of analysis

We outlined the properties that we wish to retain in our design of batch-independent normalization: (i) scale invariance, (ii) control of activation scale; (iii) avoidance of collapse; (iv) preservation of expressivity. We now introduce a framework to quantify the presence or absence of the specific properties (iii) and (iv) with various choices of normalization.

Propagation. For simplicity, we assume in our theoretical setup that any layer l up to depth L consists of the following three steps: (i) convolution step with weights $\omega^l \in \mathbb{R}^{K_l \times K_l \times C_{l-1} \times C_l}$; (ii) normalization step; (iii) activation step sub-decomposed into an affine transformation with scale and shift parameters $\gamma^l, \beta^l \in \mathbb{R}^{C_l}$ and an activation function ϕ which, unless otherwise stated, is assumed positive homogeneous and nonzero (e.g. $\phi = \text{ReLU}$). If we denote $\mathbf{x}^l, \mathbf{y}^l, \mathbf{z}^l \in \mathbb{R}^{H \times W \times C_l}$ the intermediate activations situated just after (i), (ii), (iii) with the convention $\mathbf{z}^0 \equiv \mathbf{x}$, we may write the propagation through layer l as

$$\mathbf{x}^l = \text{Conv}(\mathbf{z}^{l-1}), \quad \forall \alpha, c : \quad \text{Conv}(\mathbf{z}^{l-1})_{\alpha, c} = (\omega^l * \mathbf{z}^{l-1})_{\alpha, c}, \quad (2)$$

$$\mathbf{y}^l = \text{Norm}(\mathbf{x}^l), \quad \forall \alpha, c : \quad \text{Norm}(\mathbf{x}^l)_{\alpha, c} = \frac{\mathbf{x}_{\alpha, c}^l - \mu_{I_{\mathbf{x}, c}}(\mathbf{x}^l)}{\sigma_{I_{\mathbf{x}, c}}(\mathbf{x}^l)}, \quad (3)$$

$$\mathbf{z}^l = \text{Act}(\mathbf{y}^l), \quad \forall \alpha, c : \quad \text{Act}(\mathbf{y}^l)_{\alpha, c} = \phi(\tilde{\mathbf{y}}_{\alpha, c}^l) = \phi(\gamma_c^l \mathbf{y}_{\alpha, c}^l + \beta_c^l), \quad (4)$$

where $\mu_{I_{\mathbf{x}, c}}(\mathbf{x}^l), \sigma_{I_{\mathbf{x}, c}}(\mathbf{x}^l)$ denote the mean and standard deviation of \mathbf{x}^l conditionally on $I_{\mathbf{x}, c} \equiv \{c\}, \{\mathbf{x}\}, \{\mathbf{x}, c\}, \{\mathbf{x}, c \bmod G\}$ for the respective cases Norm = BN, LN, IN, GN with G groups.

¹We omit the numerical stability constant and adopt the convention $\text{Norm}(\mathbf{x}^l)_{\alpha, c} = 0, \forall \alpha$ if $\sigma_{I_{\mathbf{x}, c}}(\mathbf{x}^l) = 0$.

Moments. Extending the previous notations, we use μ, σ, \mathcal{P} indexed with a (possibly empty) subset of variables to denote the operators of conditional mean, standard deviation and power. If we apply these operators to the intermediate activations \mathbf{y}^l that implicitly depend on the input \mathbf{x} and that depend on the spatial position α and the channel c , we get e.g.

$$\begin{aligned}\mu_c(\mathbf{y}^l) &= \mathbb{E}_{\mathbf{x}, \alpha}[\mathbf{y}_{\alpha, c}^l], & \sigma_c(\mathbf{y}^l) &= \sqrt{\text{Var}_{\mathbf{x}, \alpha}[\mathbf{y}_{\alpha, c}^l]}, & \mathcal{P}_c(\mathbf{y}^l) &= \underbrace{\mathbb{E}_{\mathbf{x}, \alpha}[(\mathbf{y}_{\alpha, c}^l)^2]}_{\sigma_c(\mathbf{y}^l)^2 + \mu_c(\mathbf{y}^l)^2}, \\ \mu_{\mathbf{x}, c}(\mathbf{y}^l) &= \mathbb{E}_{\alpha}[\mathbf{y}_{\alpha, c}^l], & \sigma_{\mathbf{x}, c}(\mathbf{y}^l) &= \sqrt{\text{Var}_{\alpha}[\mathbf{y}_{\alpha, c}^l]}, & \mathcal{P}_{\mathbf{x}, c}(\mathbf{y}^l) &= \underbrace{\mathbb{E}_{\alpha}[(\mathbf{y}_{\alpha, c}^l)^2]}_{\sigma_{\mathbf{x}, c}(\mathbf{y}^l)^2 + \mu_{\mathbf{x}, c}(\mathbf{y}^l)^2}\end{aligned}$$

where, by convention, \mathbf{x}, α, c are considered uniformly sampled among inputs of \mathcal{D} , spatial positions and channels, whenever they are considered as random.

Power decomposition. Using these notations, we may gain important insights by decomposing the power in channel c of \mathbf{y}^l , just after the normalization, as

$$\mathcal{P}_c(\mathbf{y}^l) = \underbrace{\mathbb{E}_{\mathbf{x}}[\mu_{\mathbf{x}, c}(\mathbf{y}^l)]^2}_{\mathcal{P}_c^{(1)}(\mathbf{y}^l)} + \underbrace{\text{Var}_{\mathbf{x}}[\mu_{\mathbf{x}, c}(\mathbf{y}^l)]}_{\mathcal{P}_c^{(2)}(\mathbf{y}^l)} + \underbrace{\mathbb{E}_{\mathbf{x}}[\sigma_{\mathbf{x}, c}(\mathbf{y}^l)]^2}_{\mathcal{P}_c^{(3)}(\mathbf{y}^l)} + \underbrace{\text{Var}_{\mathbf{x}}[\sigma_{\mathbf{x}, c}(\mathbf{y}^l)]}_{\mathcal{P}_c^{(4)}(\mathbf{y}^l)}. \quad (5)$$

Since this four-terms *power decomposition* will be at the core of our analysis, we detail two useful views of it. The first view is that of a *hierarchy of scales*: $\mathcal{P}_c^{(1)}(\mathbf{y}^l)$ measures the power of $\mu_c(\mathbf{y}^l)$ at the dataset scale; $\mathcal{P}_c^{(2)}(\mathbf{y}^l)$ measures the power of $\mu_{\mathbf{x}, c}(\mathbf{y}^l) - \mu_c(\mathbf{y}^l)$ at the instance scale; the sum of $\mathcal{P}_c^{(3)}(\mathbf{y}^l), \mathcal{P}_c^{(4)}(\mathbf{y}^l)$ measures the power of $\mathbf{y}_{\alpha, c}^l - \mu_{\mathbf{x}, c}(\mathbf{y}^l)$ at the pixel scale. A particular situation where the power would be concentrated at the dataset scale with $\mathcal{P}_c^{(1)}(\mathbf{y}^l)$ equal to $\mathcal{P}_c(\mathbf{y}^l)$ would thus imply that \mathbf{y}^l has its distribution fully “collapsed” in channel c , i.e. that \mathbf{y}^l is constant in channel c .

The second view is that of a *two-level binary tree*: on one half of the tree, the sum of $\mathcal{P}_c^{(1)}(\mathbf{y}^l)$ and $\mathcal{P}_c^{(2)}(\mathbf{y}^l)$ measures the power coming from $\mu_{\mathbf{x}, c}(\mathbf{y}^l)$, with the relative proportions of $\mathcal{P}_c^{(1)}(\mathbf{y}^l)$ and $\mathcal{P}_c^{(2)}(\mathbf{y}^l)$ functions of the inter- \mathbf{x} similarity and inter- \mathbf{x} variability of $\mu_{\mathbf{x}, c}(\mathbf{y}^l)$; on the other half of the tree, the sum of $\mathcal{P}_c^{(3)}(\mathbf{y}^l)$ and $\mathcal{P}_c^{(4)}(\mathbf{y}^l)$ measures the power coming from $\sigma_{\mathbf{x}, c}(\mathbf{y}^l)$, with the relative proportions of $\mathcal{P}_c^{(3)}(\mathbf{y}^l)$ and $\mathcal{P}_c^{(4)}(\mathbf{y}^l)$ functions of the inter- \mathbf{x} similarity and inter- \mathbf{x} variability of $\sigma_{\mathbf{x}, c}(\mathbf{y}^l)$. A particular situation where $\mathcal{P}_c^{(2)}(\mathbf{y}^l), \mathcal{P}_c^{(4)}(\mathbf{y}^l)$ would be equal to zero would thus imply that $\mu_{\mathbf{x}, c}(\mathbf{y}^l), \sigma_{\mathbf{x}, c}(\mathbf{y}^l)$ have zero inter- \mathbf{x} variability, i.e. that $\mu_{\mathbf{x}, c}(\mathbf{y}^l), \sigma_{\mathbf{x}, c}(\mathbf{y}^l)$ are constant for all \mathbf{x} .

A version of Eq. (5) at the layer level instead of channel level will be easier to work with. Defining $\mathcal{P}^{(i)}(\mathbf{y}^l)$ as the averages of $\mathcal{P}_c^{(i)}(\mathbf{y}^l)$ over c for $i \in \{1, 2, 3, 4\}$, we obtain

$$\mathcal{P}(\mathbf{y}^l) = \mathcal{P}^{(1)}(\mathbf{y}^l) + \mathcal{P}^{(2)}(\mathbf{y}^l) + \mathcal{P}^{(3)}(\mathbf{y}^l) + \mathcal{P}^{(4)}(\mathbf{y}^l).$$

It should be noted that $\mathcal{P}(\mathbf{y}^l) = 1$ for any choice of Norm $\in \{\text{BN}, \text{LN}, \text{IN}, \text{GN}\}$, as long as the denominator of Eq. (3) is nonzero for all \mathbf{x}, c [D.2]. Consequently, the terms $\mathcal{P}^{(i)}(\mathbf{y}^l)$ sum to one, meaning they can be conveniently seen as the proportion of each term $i \in \{1, 2, 3, 4\}$ into $\mathcal{P}(\mathbf{y}^l)$.

Revisiting BN’s avoidance of collapse. When BN is used, \mathbf{y}^l is normalized not only layer-wise but also channel-wise with $\mathcal{P}_c^{(1)}(\mathbf{y}^l) = 0$ and $\mathcal{P}_c(\mathbf{y}^l) = 1$. As a first consequence, $\tilde{\mathbf{y}}^l$ (that is only one affine transformation away from \mathbf{y}^l) is *unlikely* to have its channel-wise distributions collapsed. This means that the nonlinearity ϕ acting on $\tilde{\mathbf{y}}^l$ is *likely* to be effectively nonlinear with respect to $\tilde{\mathbf{y}}^l$ ’s channel-wise distributions.² As a result, each layer adds capacity and the network effectively uses its whole *depth*. This is opposite to the situation where $\tilde{\mathbf{y}}^l$ has its channel-wise distributions collapsed with $\mathcal{P}_c(\tilde{\mathbf{y}}^l) - \mathcal{P}_c^{(1)}(\tilde{\mathbf{y}}^l) \ll \mathcal{P}_c(\tilde{\mathbf{y}}^l)$ for all c , which results in ϕ being close to linear with respect to $\tilde{\mathbf{y}}^l$ ’s channel-wise distributions. This is illustrated in Figure 1 and formalized in Appendix D.3.

²Note that: (i) this likeliness could be quantified in the context of random nets of Definition 1 with “reasonable” choices of β, γ ; (ii) BN still only guarantees an intra-task nonlinearity and not an intra-mode nonlinearity in contexts such as adversarial training [54, 55] or conditional GANs [56], unless the modes are decoupled in BN’s computation [57, 58, 59, 60, 61].

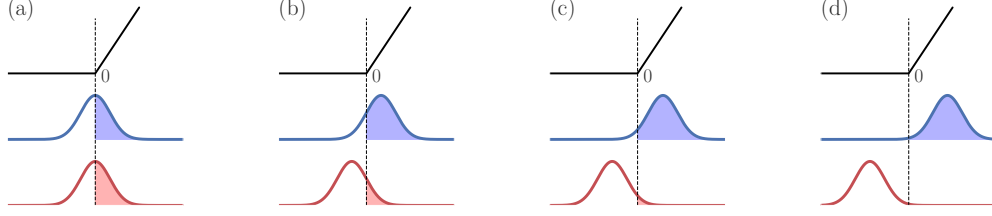


Figure 1: **Channel-wise collapse implies channel-wise linearity.** Each subplot shows $\phi = \text{ReLU}$ (black activation function) as well as two channel-wise distributions (red and blue distributions) positioned symmetrically around 0 with $\frac{\mathcal{P}_c(\tilde{\mathbf{y}}^l) - \mathcal{P}_c^{(1)}(\tilde{\mathbf{y}}^l)}{\mathcal{P}_c(\tilde{\mathbf{y}}^l)} = 1, \frac{1}{2}, \frac{1}{4}, \frac{1}{8}$ for (a), (b), (c), (d), respectively. When progressing from (a) to (d), the part of the distribution corresponding to active ReLU (shaded region) becomes either overly dominant (blue distribution) or negligible (red distribution). In either case, the channel-wise distribution ends up concentrated on only one side of piece-wise linearity.

As an additional consequence, \mathbf{y}^l is guaranteed to have its channels well balanced with equal power $\mathcal{P}_c(\mathbf{y}^l)$ for all c . As a result, the network effectively uses its whole *width*. This is opposite to the situation where a single channel c becomes overly dominant over the others with $\mathcal{P}_c(\mathbf{y}^l) \gg \mathcal{P}_{c'}(\mathbf{y}^l)$ for $c' \neq c$, which results in downstream layers only “seeing” this channel c and the network behaving as if it had a width equal to one at layer l .

Revisiting BN’s preservation of expressivity. When BN is used, $\mathcal{P}_c^{(1)}(\mathbf{y}^l) = 0$ implies for all c that the terms $\mathcal{P}_c^{(2)}(\mathbf{y}^l), \mathcal{P}_c^{(3)}(\mathbf{y}^l), \mathcal{P}_c^{(4)}(\mathbf{y}^l)$ sum to one. Apart from that, BN does not impose any particular constraints on the relative proportions of each term into the sum. This means that the relative proportions of $\mathcal{P}_c^{(i)}(\mathbf{y}^l)$ and $\mathcal{P}^{(i)}(\mathbf{y}^l)$ for $i \in \{2, 3, 4\}$ are free to evolve as naturally dictated by the task and the optimizer during learning.

This absence of constraints seems sensible. Indeed, imposing constraints on these relative proportions would *alter the expressivity*, which would not have any obvious justification in general and could even be detrimental in some cases, as we discuss in Section 4.

4 Failure modes with batch-independent normalization

With our theoretical framework in hand, we now turn to showing that the prototypical batch-independent norms are subject to failures modes opposite to BN’s beneficial properties.

In the case of LN, the failure mode does not manifest in an absolute sense but rather as a “soft” inductive bias, i.e. as a preference or a favoring in the hypothesis space. This “soft” inductive bias is quantified by Theorem 1 in the context of networks with random model parameters.

Definition 1 (random net). *We define a “random net” as a neural network having an input \mathbf{x} sampled from the dataset \mathcal{D} and implementing Eq. (2), (3), (4) in every layer up to depth L , with the components of $\omega^l, \gamma^l, \beta^l$ at each layer $l \in \{1, \dots, L\}$ sampled i.i.d. from the fixed distributions $\nu_\omega, \nu_\gamma, \nu_\beta$ (up to a fan-in’s square root scaling for ω^l).*

In such networks, we assume that: (i) none of the inputs of the dataset \mathcal{D} is identically zero; (ii) $\nu_\omega, \nu_\beta, \nu_\gamma$ have well-defined moments, with strictly positive associated root mean squares $\omega, \gamma, \beta > 0$; (iii) ν_ω, ν_β are symmetric around zero.

Theorem 1 (layer-normalized networks collapse (informal)). [E.3] *Fix a layer $l \in \{1, \dots, L\}$ and $\nu_\omega, \nu_\beta, \nu_\gamma, \mathcal{D}$ in Definition 1. Further suppose Norm = LN and suppose that the convolution of Eq. (2) uses periodic boundary conditions.*

Then for random nets of Definition 1 with large widths, it holds that

$$\mathcal{P}(\mathbf{y}^l) - \mathcal{P}^{(1)}(\mathbf{y}^l) \lesssim \rho^{l-1}, \quad \mathcal{P}(\mathbf{y}^l) \simeq 1, \quad (6)$$

where $\rho \equiv \gamma^2 / (\gamma^2 + \beta^2) < 1$, and \lesssim and \simeq denote inequality and equality up to arbitrarily small constants with probability arbitrarily close to 1 when $\min_{1 \leq k \leq l} C_k$ is large enough.

Discussion on LN’s failure mode. Theorem 1 implies that, with high probability, \mathbf{y}^l is subject to *channel-wise collapse* in deep layers ($l \gg 1$) with $\mathcal{P}(\mathbf{y}^l) - \mathcal{P}^{(1)}(\mathbf{y}^l) \ll \mathcal{P}(\mathbf{y}^l)$. This means that $\tilde{\mathbf{y}}^l$ (that is only one affine transformation away from \mathbf{y}^l) is likely to have its channel-wise distributions collapsed with $\mathcal{P}_c(\tilde{\mathbf{y}}^l) - \mathcal{P}_c^{(1)}(\tilde{\mathbf{y}}^l) \ll \mathcal{P}_c(\tilde{\mathbf{y}}^l)$ for most c . The nonlinearity ϕ acting on $\tilde{\mathbf{y}}^l$ is then likely to be close to linear with respect to $\tilde{\mathbf{y}}^l$ ’s channel-wise distributions [D.3]. Being close to channel-wise linear in deep layers, layer-normalized networks are unable to effectively use their whole depth.

Since the inequality \lesssim can be replaced by an equality \simeq in the case $\phi = \text{identity}$ of Theorem 1 [E.4], the aggravation at each layer l of the upper bound of Eq. (6) does not stem from the activation function itself but rather by the preceding affine transformation. The phenomenon of channel-wise collapse — also known under the terms of “domain collapse” [39] or “elimination singularity” [18] — is therefore not only induced by a “mean-shifting” activation function such as $\phi = \text{ReLU}$ [62, 20], but also by the injection of non-centeredness through the application of the channel-wise shift parameter β^l at each layer l . The fact that the general case of positive-homogeneous ϕ is upper-bounded by the case $\phi = \text{identity}$ in Eq. (6) still means that the choice $\phi = \text{ReLU}$ can only be an aggravating factor.

Crucially, in the context of random nets of large width, LN’s operation at each layer l does not compensate this “mean shift”. This stems from the fact that LN’s mean and variance statistics can be approximated by zero and a constant value independent of \mathbf{x} , respectively. This means that LN’s operation can be approximated by a layer-wise constant scaling independent of \mathbf{x} .³

The predominance of LN’s failure mode in the hypothesis space, implied by its predominance in random nets, is expected to have at least two negative effects on the actual learning and final performance: (i) being expected to “linger” along the training trajectory and being associated with reduced effective capacity, the failure mode is expected to cause degraded performance on the training loss; (ii) even if avoided to some extent during training, the failure mode is still expected to be present in the vicinity of the training trajectory, implying an ill-conditioning of the loss landscape [62, 64] and a prohibition of large learning rates that could have led otherwise to generalization benefits [65].

After detailing LN’s failure mode, we now detail IN’s failure mode.

Theorem 2 (instance-normalized networks lack variability in instance statistics). [F] *Fix a layer $l \in \{1, \dots, L\}$ and lift any assumption on ϕ . Further suppose $\text{Norm} = \text{IN}$, with Eq. (3) having nonzero denominator at layer l for all inputs and channels.*

Then it holds that

- \mathbf{y}^l is normalized in each channel c with

$$\mathcal{P}_c^{(1)}(\mathbf{y}^l) = 0, \quad \mathcal{P}_c(\mathbf{y}^l) = 1;$$

- \mathbf{y}^l lacks variability in instance statistics in each channel c with

$$\mathcal{P}_c^{(2)}(\mathbf{y}^l) = 0, \quad \mathcal{P}_c^{(3)}(\mathbf{y}^l) = 1, \quad \mathcal{P}_c^{(4)}(\mathbf{y}^l) = 0.$$

Discussion on IN’s failure mode. We see in Theorem 2 that \mathbf{y}^l ’s power decomposition with IN is constrained to be such that $\mathcal{P}^{(1)}(\mathbf{y}^l), \mathcal{P}^{(2)}(\mathbf{y}^l), \mathcal{P}^{(4)}(\mathbf{y}^l) = 0$ and $\mathcal{P}^{(3)}(\mathbf{y}^l) = 1$. While the constraints on $\mathcal{P}^{(1)}(\tilde{\mathbf{y}}^l), \mathcal{P}^{(3)}(\tilde{\mathbf{y}}^l)$ are removed by the affine transformation between \mathbf{y}^l and $\tilde{\mathbf{y}}^l$, the constraints on $\mathcal{P}^{(2)}(\tilde{\mathbf{y}}^l), \mathcal{P}^{(4)}(\tilde{\mathbf{y}}^l)$, on the other hand, remain even after the affine transformation. These constraints on $\mathcal{P}^{(2)}(\tilde{\mathbf{y}}^l), \mathcal{P}^{(4)}(\tilde{\mathbf{y}}^l)$ translate into $2C_l$ fixed constraints in activation space that apply to each $\tilde{\mathbf{y}}^l \in \mathbb{R}^{H \times W \times C_l}$ associated with each choice of input \mathbf{x} in the dataset \mathcal{D} [53].

Such constraints on $\tilde{\mathbf{y}}^l$ are symptomatic of an alteration of expressivity. In particular, they entail that some network mappings that can be expressed without normalization cannot be expressed with IN. One such example is the identity mapping [D.1]. Another such example is a network mapping that would provide in channel c through $\tilde{\mathbf{y}}_{\alpha,c}^l$, just before the nonlinearity, a detector of a given concept at position α in the input \mathbf{x} . With IN, the lack of variability in instance statistics implies that the mean $\mu_{\mathbf{x},c}(\tilde{\mathbf{y}}^l)$ and standard deviation $\sigma_{\mathbf{x},c}(\tilde{\mathbf{y}}^l)$ of the feature map in channel c are necessarily constant for all \mathbf{x} , equal to β_c and γ_c , respectively. This does not allow to express for some inputs \mathbf{x} the presence

³In this view, we expect layer-normalized networks to be equally subject to a phenomenon of increasingly imbalanced channels with depth. This phenomenon would be driven by the succession of affine transformations and activation functions mainly, but also by the succession of convolutions [46, 63, 48].

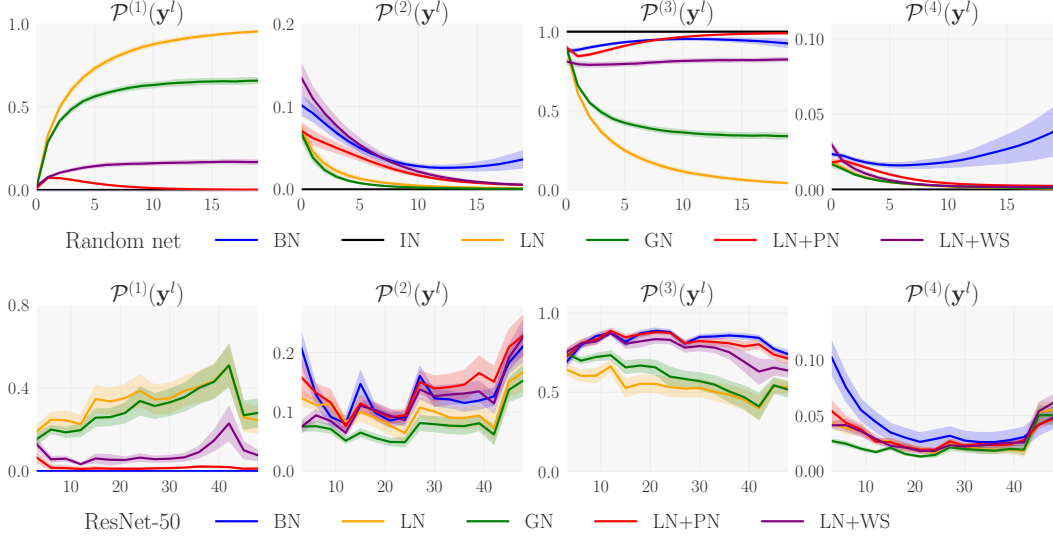


Figure 2: **“Power plots”**. The power decomposition of \mathbf{y}^l is shown as a function of the depth l for BN and different batch-independent norms: IN, LN, GN, LN+PN, LN+WS. Top row: Random net of Definition 1 with $\phi = \text{ReLU}$, widths $C_l = 1024$, kernel sizes $K_l = 3$, convolutions using periodic boundary conditions and components of β^l, γ^l sampled i.i.d. from $\mathcal{N}(0, 0.2^2)$ and $\mathcal{N}(1, 0.2^2)$, respectively. Bottom row: ResNet-50 (v2) [71] during 100 epochs of training on ImageNet (IN is not shown in this row due to numerical stability issues). Further experimental details are reported in Appendix B.2.

of the concept at some position α : $\mu_{\mathbf{x},c}(\tilde{\mathbf{y}}^l) > 0, \sigma_{\mathbf{x},c}(\tilde{\mathbf{y}}^l) > 0$; and for other inputs \mathbf{x} the absence of the concept: $\mu_{\mathbf{x},c}(\tilde{\mathbf{y}}^l) = 0, \sigma_{\mathbf{x},c}(\tilde{\mathbf{y}}^l) = 0$.

This latter example is not just anecdotal. Indeed, it is accepted that networks trained on high-level conceptual tasks have their initial layers related to low-level features and their deep layers related to high-level concepts [66, 67]. This view explains the success of IN on the specific task of style transfer with fixed “style” input, IN being then incorporated inside a generator network that only acts on the low-level features of the “content” input [10, 68, 69, 70]. On high-level conceptual tasks, on the other hand, this view hints at a harmful tension between IN’s constraints and the requirement of instance variability to express high-level concepts in deep layers. In short, not only is the expressivity altered with IN, but the alteration of the expressivity results in the exclusion of useful network mappings.

Failure modes with GN. Group Normalization is a middle ground between the two extremes of LN ($G = 1$ group) and IN ($G = C_l$ groups at layer l). Networks with GN are consequently affected by both problems of Theorem 1 and Theorem 2, but to a lesser extent than networks with LN and IN. On the one hand, since GN becomes equivalent to a constant scaling when group sizes become large, networks with GN are likely to be subject to channel-wise collapse. On the other hand, since GN can be seen as removing a fraction — with an inverse dependence on the group size — of $\mathcal{P}^{(2)}(\mathbf{y}^l), \mathcal{P}^{(4)}(\mathbf{y}^l)$ in between each layer, networks with GN are likely to lack variability in instance statistics.

The balance struck by GN between the two failure modes of LN and IN could still be beneficial, which would explain GN’s superior performance in practice. It makes sense intuitively that being weakly subject to two failure modes is preferable over being strongly subject to one failure mode.

Experimental validation. The “power plots” of Figure 2 show the power decomposition of \mathbf{y}^l as a function of the depth l in both a random net of Definition 1 and ResNet-50 (v2) trained on ImageNet.⁴ Looking at the cases of BN and LN, IN, GN in these power plots, we confirm that: (i) networks with LN, and to a lesser extent GN, are subject to channel-wise collapse as depth increases, unlike networks with BN and IN (see Appendix B.2.1 for a precise verification of Theorem 1); (ii) networks with IN, and to a lesser extent GN, lack variability in instance statistics.

⁴To ensure that activation steps are directly preceded by normalization steps (cf Section 5), we always use v2 instantiations of ResNets and instantiations of ResNeXts having the same block reorderings as ResNets v2 [B.1].

5 Proxy Normalization

With the goal of remedying the failure modes of Section 4, we now introduce our novel technique “Proxy Normalization” (PN) that is at the core of our novel batch-independent normalization approach.

PN is incorporated into the neural network by replacing the activation step of Eq. (4) by the following “proxy-normalized” activation step (cf Figure 3 and the practical implementation of Appendix C):

$$\tilde{\mathbf{z}}^l = \text{PN-Act}(\mathbf{y}^l), \quad \forall \alpha, c: \quad \text{PN-Act}(\mathbf{y}^l)_{\alpha,c} = \frac{\phi(\gamma_c^l \mathbf{y}_{\alpha,c}^l + \beta_c^l) - \mathbb{E}_{Y_c^l}[\phi(\gamma_c^l Y_c^l + \beta_c^l)]}{\sqrt{\text{Var}_{Y_c^l}[\phi(\gamma_c^l Y_c^l + \beta_c^l)] + \epsilon}}, \quad (7)$$

where $\epsilon \geq 0$ is a numerical stability constant and Y_c^l is a Gaussian “proxy” variable of mean $\tilde{\beta}_c^l$ and variance $(1 + \tilde{\gamma}_c^l)^2$ depending on additional parameters $\tilde{\beta}^l, \tilde{\gamma}^l \in \mathbb{R}^{C_l}$ of PN. Unless otherwise stated, we let $\tilde{\beta}^l, \tilde{\gamma}^l$ be nonzero but still subject to weight decay and thus close to zero. We show in Section B.3.3 that it is also effective to let $\tilde{\beta}^l, \tilde{\gamma}^l$ be strictly zero and $Y_c^l \sim \mathcal{N}(0, 1)$.

If one assumes, as hinted by Section 4, that only the affine transformation and the activation function ϕ (i.e. the activation step) play a role in the aggravation at each layer l of the channel-wise collapse and channel imbalance, then PN provides the following guarantee of channel-wise normalization.

Theorem 3 (guarantee of channel-wise normalization in proxy-normalized networks (informal)). **[G]** Fix a layer $l \in \{1, \dots, L\}$ and lift any assumptions on ϕ and \mathbf{x} ’s distribution. Further suppose that the neural network implements Eq. (2), (3), (7) at every layer up to depth L , with $\epsilon = 0$ and Eq. (3), (7) having nonzero denominators for all layers, inputs and channels.

Then both \mathbf{y}^l and $\tilde{\mathbf{z}}^l$ at layer l are channel-wise normalized if the following conditions hold:

- (i) $\tilde{\mathbf{z}}^{l-1}$ at layer $l - 1$ is channel-wise normalized;
- (ii) The convolution and normalization steps at layer l do not cause any aggravation of channel-wise collapse and channel imbalance;
- (iii) \mathbf{y}^l at layer l is channel-wise Gaussian and PN’s additional parameters $\tilde{\beta}^l, \tilde{\gamma}^l$ are zero.

Our batch-independent approach: LN+PN or GN+PN. At this point, we crucially note that PN: (i) is batch-independent; (ii) does not cause any alteration of expressivity. This leads us to adopt a batch-independent normalization approach that uses either LN or GN (with few groups) in the normalization step and that replaces the activation step by the proxy-normalized activation step (+PN). With such a choice of normalization step, we guarantee three of the benefits detailed in Table 1: “scale invariance”, “control of activation scale” and “preservation of expressivity”. With the proxy-normalized activation step, we finally guarantee the fourth benefit of “avoidance of collapse” without compromising any of the benefits provided by the normalization step.

Experimental validation. We confirm in Figure 2 that BN’s behavior is emulated in a fully batch-independent manner with our approach LN+PN or GN+PN. Indeed, the power plots of networks with LN+PN resemble the power plots of networks with BN. As desired, PN remedies LN’s failure mode without incurring IN’s failure mode.

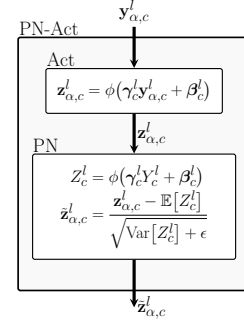


Figure 3: **Plugging PN.** PN is plugged into the activation step Act to yield the proxy-normalized activation step PN-Act.

Approach strength 1: Normalizing beyond initialization. Our batch-independent approach maintains channel-wise normalization throughout training (cf Figure 2). In contrast, many alternative approaches, either explicitly or implicitly, focus on initialization [21, 24, 17, 18, 49, 20, 72]. Centered Weight Normalization [17], PreLayerNorm [49] or WS [18, 20, 72] notably rely on the implicit assumption that different channels have the same channel-wise means after the activation function ϕ . While valid in networks at initialization with $\beta^l = 0$ and $\gamma^l = 1$ (cf Section B.2.2), this assumption becomes less valid as the affine transformation starts deviating from the identity. We see in Figure 2 that networks with LN+WS are indeed less effective in maintaining channel-wise normalization, both in networks with random β^l, γ^l (top row) and in networks considered throughout training (bottom row). Such a coarser channel-wise normalization might in turn lead to a less effective use of model capacity and a degradation of the conditioning of the loss landscape [62, 64].

Approach strength 2: Wide applicability. Our batch-independent approach matches BN with consistency across choices of model architectures, model sizes and activation functions (cf Section 6). Its only restriction, namely that activation steps should be immediately preceded by normalization steps for y^l and its associated proxy Y^l to be at the same scale, has easy workarounds. Applicability restrictions might be more serious with alternative approaches: (i) alternative approaches involving the tracking of activation statistics [21, 22, 23] might be nontrivial to apply to residual networks [73, 74]; (ii) approaches involving a normalization in weight space [16, 17, 18, 19, 20] might be ill-suited to architectures with less “dense” kernels such as EfficientNets [20]; (iii) approaches involving a change of activation function [24, 5, 15] might precisely restrict the choice of activation function.

Approach strength 3: Ease of implementation. Our approach is straightforward to implement when starting from a batch-normalized network. It simply requires replacing (i) all BN steps with LN or GN steps, and (ii) all activation steps with proxy-normalized activation steps. The proxy-normalized activation steps themselves are easily implemented (cf our implementation of Appendix C).

6 Results

We finally assess the practical performance of our batch-independent normalization approach. While we focus on ImageNet [75] in the main text of this paper, we report additional results on CIFAR [76] in Appendix B. In Appendix B, we also provide all the details on our experimental setup.

Choices of regularization and batch size. As mentioned in Section 2, we perform all our experiments with different degrees of regularization to disentangle normalization’s effects from regularization’s effects. We detail all our choices of regularization in Appendices B.1 and B.3.4.

In terms of batch size, we set: (i) the “global batch size” in between weight updates to the same value independent of the choice of norm; (ii) the “normalization batch size” to a near-optimal value with BN. These choices enable us to be conservative when concluding on a potential advantage of our approach over BN at small batch size. Indeed, while the performance of batch-independent approaches would remain the same or slightly improve at small batch size [77, 65], the performance of BN would eventually become degraded due to a regularization that eventually becomes excessive [2, 3, 4, 5, 6, 7].

Effect of adding PN. We start as a first experiment by analyzing the effect of adding PN on top of various norms in ResNet-50 (RN50). As visible in Table 2, PN is mostly beneficial when added on top of LN or GN with a small number of groups G . The consequence is that the optimal G shifts to lower values in GN+PN compared to GN. This confirms the view that PN’s benefit lies in addressing LN’s failure mode.

It is also visible in Table 2 that PN does not provide noticeable benefits to BN. This confirms again the view that PN’s benefit lies in addressing the problem, not present with BN, of channel-wise collapse. Importantly, since PN does not entail effects other than normalization that could artificially boost the performance, *GN+PN can be compared in a fair way to BN when assessing the effectiveness of normalization.*

Table 2: **Effect of adding PN.** ResNet-50 is trained on ImageNet with BN and LN, GN, GN+WS with G groups, either without or with PN added on top (plain vs. PN). Results are formatted as X / Y with X, Y the validation accuracies (%) without and with extra regularization, respectively.

	G	RN50	
		plain	+PN
BN		76.3 / 75.8	76.2 / 76.0
LN	1	74.5 / 74.6	75.9 / 76.5
GN	8	75.4 / 75.4	76.3 / 76.7
GN	32	75.4 / 75.3	75.8 / 76.1
GN+WS	8	76.6 / 76.7	76.8 / 77.1

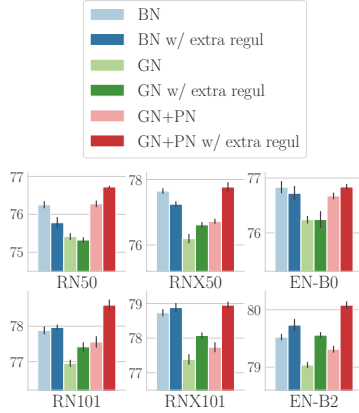
This is unlike WS which has been shown to improve BN’s performance [18]. In our results of Table 2, the high performance of GN+WS without extra regularization and the fact that PN still provides benefits to GN+WS suggests that: (i) on top of its normalization benefits, WS induces a form of regularization; (ii) GN+WS is still not fully optimal in terms of normalization.

GN+PN vs. BN. Next, we turn to comparing the performance of our batch-independent approach, GN+PN, to that of BN across a broad range of models trained on ImageNet. As visible in Figure 4 and Tables 3, 4, GN+PN outperforms BN in ResNet-50 (RN50) and ResNet-101 (RN101) [71], matches BN in ResNeXt-50 (RNx50) and ResNeXt-101 (RNx101) [78], and matches BN in EfficientNet-B0 (EN-B0) and EfficientNet-B2 (EN-B2), both in the original variant with depthwise convolutions and

expansion ratio of 6 [52] and in an approximately parameter-preserving variant with group convolutions of group size 16 and expansion ratio of 4 [79] (cf Section B.1). *In short, our batch-independent normalization approach, GN+PN, matches BN not only in behavior but also in performance.*

With regard to matching BN’s performance with alternative norms, various positive results have been reported in ResNets and ResNeXts [8, 7, 12, 13, 15, 20, 36] but only a limited number in EfficientNets [15]. In EfficientNets, we are notably not aware of any other work showing that BN’s performance can be matched with a batch-independent approach. As a confirmation, we assess the performance of various existing batch-independent approaches: GN [3], GN+WS [18], Evo-S0 [15], FRN+TLU [80, 5]. Unlike GN+PN, none of these approaches is found in Table 4 to match BN with consistency.

Normalization and regularization. Our results suggest that while an efficient normalization is not sufficient in itself to achieve good performance on ImageNet, it is still a necessary condition, together with regularization. In our results, it is always with extra regularization that GN+PN yields the most benefits. Importantly, the fact that GN+PN consistently leads to large improvements in training accuracy [B.3.2] suggests that *additional benefits would be obtained on larger datasets without the requirement of relying on regularization* [81, 72].



Acknowledgments and Disclosure of Funding

We are thankful to Simon Knowles, Luke Hudlass-Galley, Luke Prince, Alexandros Koliousis, Anastasia Dietrich and the wider research team at Graphcore for the useful discussions and feedbacks. We are also thankful to the anonymous reviewers for their insightful comments that helped improve the paper.

References

- [1] Sergey Ioffe and Christian Szegedy. Batch normalization: Accelerating deep network training by reducing internal covariate shift. In *32nd International Conference on Machine Learning, ICML 2015*, pages 448–456, 2015.
- [2] Sergey Ioffe. Batch renormalization: Towards reducing minibatch dependence in batch-normalized models. In *Advances in Neural Information Processing Systems 30: Annual Conference on Neural Information Processing Systems 2017*, pages 1945–1953, 2017.
- [3] Yuxin Wu and Kaiming He. Group normalization. In *Computer Vision - ECCV 2018 - 15th European Conference, Proceedings, Part XIII*, pages 3–19, 2018.
- [4] Chris Ying, Sameer Kumar, Dehao Chen, Tao Wang, and Youlong Cheng. Image classification at supercomputer scale. *CoRR*, abs/1811.06992, 2018.
- [5] Saurabh Singh and Shankar Krishnan. Filter response normalization layer: Eliminating batch dependence in the training of deep neural networks. In *2020 IEEE/CVF Conference on Computer Vision and Pattern Recognition, CVPR 2020*, pages 11234–11243, 2020.
- [6] Cecilia Summers and Michael J. Dinneen. Four things everyone should know to improve batch normalization. In *8th International Conference on Learning Representations, ICLR 2020*, 2020.
- [7] Junjie Yan, Ruosi Wan, Xiangyu Zhang, Wei Zhang, Yichen Wei, and Jian Sun. Towards stabilizing batch statistics in backward propagation of batch normalization. In *8th International Conference on Learning Representations, ICLR 2020*, 2020.
- [8] Vitaliy Chiley, Ilya Sharapov, Atli Kosson, Urs Köster, Ryan Reece, Sofia Samaniego de la Fuente, Vishal Subbiah, and Michael James. Online normalization for training neural networks. In *Advances in Neural Information Processing Systems 32: Annual Conference on Neural Information Processing Systems 2019, NeurIPS 2019*, pages 8431–8441, 2019.
- [9] Lei Jimmy Ba, Jamie Ryan Kiros, and Geoffrey E. Hinton. Layer normalization. *CoRR*, abs/1607.06450, 2016.
- [10] Dmitry Ulyanov, Andrea Vedaldi, and Victor S. Lempitsky. Instance normalization: The missing ingredient for fast stylization. *CoRR*, abs/1607.08022, 2016.
- [11] Mengye Ren, Renjie Liao, Raquel Urtasun, Fabian H. Sinz, and Richard S. Zemel. Normalizing the normalizers: Comparing and extending network normalization schemes. In *5th International Conference on Learning Representations, ICLR 2017, Conference Track Proceedings*, 2017.
- [12] Ping Luo, Jiamin Ren, Zhanglin Peng, Ruimao Zhang, and Jingyu Li. Differentiable learning-to-normalize via switchable normalization. In *7th International Conference on Learning Representations, ICLR 2019*, 2019.
- [13] Ping Luo, Zhanglin Peng, Wenqi Shao, Ruimao Zhang, Jiamin Ren, and Lingyun Wu. Differentiable dynamic normalization for learning deep representation. In *Proceedings of the 36th International Conference on Machine Learning, ICML 2019*, volume 97 of *Proceedings of Machine Learning Research*, pages 4203–4211, 2019.
- [14] Biao Zhang and Rico Sennrich. Root mean square layer normalization. In *Advances in Neural Information Processing Systems 32: Annual Conference on Neural Information Processing Systems 2019, NeurIPS 2019*, pages 12360–12371, 2019.

- [15] Hanxiao Liu, Andy Brock, Karen Simonyan, and Quoc Le. Evolving normalization-activation layers. In *Advances in Neural Information Processing Systems 33: Annual Conference on Neural Information Processing Systems 2020, NeurIPS 2020*, 2020.
- [16] Tim Salimans and Diederik P. Kingma. Weight normalization: A simple reparameterization to accelerate training of deep neural networks. In *Advances in Neural Information Processing Systems 29: Annual Conference on Neural Information Processing Systems 2016*, page 901, 2016.
- [17] Lei Huang, Xianglong Liu, Yang Liu, Bo Lang, and Dacheng Tao. Centered weight normalization in accelerating training of deep neural networks. In *IEEE International Conference on Computer Vision, ICCV 2017*, pages 2822–2830, 2017.
- [18] Siyuan Qiao, Huiyu Wang, Chenxi Liu, Wei Shen, and Alan L. Yuille. Weight standardization. *CoRR*, abs/1903.10520, 2019.
- [19] Brendan Ruff, Taylor Beck, and Joscha Bach. Mean shift rejection: Training deep neural networks without minibatch statistics or normalization. *CoRR*, abs/1911.13173, 2019.
- [20] Andrew Brock, Soham De, and Samuel L. Smith. Characterizing signal propagation to close the performance gap in unnormalized ResNets. In *9th International Conference on Learning Representations, ICLR 2021*, 2021.
- [21] Devansh Arpit, Yingbo Zhou, Bhargava Urala Kota, and Venu Govindaraju. Normalization propagation: A parametric technique for removing internal covariate shift in deep networks. In *Proceedings of the 33rd International Conference on Machine Learning, ICML 2016*, volume 48 of *JMLR Workshop and Conference Proceedings*, pages 1168–1176, 2016.
- [22] César Laurent, Nicolas Ballas, and Pascal Vincent. Recurrent normalization propagation. In *5th International Conference on Learning Representations, ICLR 2017, Workshop Track Proceedings*, 2017.
- [23] Alexander Shekhovtsov and Boris Flach. Normalization of neural networks using analytic variance propagation. *CoRR*, abs/1803.10560, 2018.
- [24] Günter Klambauer, Thomas Unterthiner, Andreas Mayr, and Sepp Hochreiter. Self-normalizing neural networks. In *Advances in Neural Information Processing Systems 30: Annual Conference on Neural Information Processing Systems 2017*, pages 971–980, 2017.
- [25] Twan van Laarhoven. L2 regularization versus batch and weight normalization. *CoRR*, abs/1706.05350, 2017.
- [26] Sanjeev Arora, Zhiyuan Li, and Kaifeng Lyu. Theoretical analysis of auto rate-tuning by batch normalization. In *7th International Conference on Learning Representations, ICLR 2019*, 2019.
- [27] Elad Hoffer, Ron Banner, Itay Golan, and Daniel Soudry. Norm matters: efficient and accurate normalization schemes in deep networks. In *Advances in Neural Information Processing Systems 31: Annual Conference on Neural Information Processing Systems 2018, NeurIPS 2018*, pages 2164–2174, 2018.
- [28] Zhiyuan Li and Sanjeev Arora. An exponential learning rate schedule for deep learning. In *8th International Conference on Learning Representations, ICLR 2020*, 2020.
- [29] Guodong Zhang, Chaoqi Wang, Bowen Xu, and Roger B. Grosse. Three mechanisms of weight decay regularization. In *7th International Conference on Learning Representations, ICLR 2019*, 2019.
- [30] Ruosi Wan, Zhanxing Zhu, Xiangyu Zhang, and Jian Sun. Spherical motion dynamics of deep neural networks with batch normalization and weight decay. *CoRR*, abs/2006.08419, 2020.
- [31] Minhyung Cho and Jaehyung Lee. Riemannian approach to batch normalization. In *Advances in Neural Information Processing Systems 30: Annual Conference on Neural Information Processing Systems 2017*, pages 5225–5235, 2017.

- [32] Jonas Moritz Kohler, Hadi Daneshmand, Aurélien Lucchi, Thomas Hofmann, Ming Zhou, and Klaus Neymeyr. Exponential convergence rates for batch normalization: The power of length-direction decoupling in non-convex optimization. In *The 22nd International Conference on Artificial Intelligence and Statistics, AISTATS 2019*, volume 89 of *Proceedings of Machine Learning Research*, pages 806–815, 2019.
- [33] Boris Hanin and David Rolnick. How to start training: The effect of initialization and architecture. In *Advances in Neural Information Processing Systems 31: Annual Conference on Neural Information Processing Systems 2018, NeurIPS 2018*, pages 569–579, 2018.
- [34] Hongyi Zhang, Yann N. Dauphin, and Tengyu Ma. Fixup initialization: Residual learning without normalization. In *7th International Conference on Learning Representations, ICLR 2019*, 2019.
- [35] Soham De and Samuel L. Smith. Batch normalization biases residual blocks towards the identity function in deep networks. In *Advances in Neural Information Processing Systems 33: Annual Conference on Neural Information Processing Systems 2020, NeurIPS 2020*, 2020.
- [36] Jie Shao, Kai Hu, Changhu Wang, Xiangyang Xue, and Bhiksha Raj. Is normalization indispensable for training deep neural network? In *Advances in Neural Information Processing Systems 33: Annual Conference on Neural Information Processing Systems 2020, NeurIPS 2020*, 2020.
- [37] Ekdeep Singh Lubana, Robert P. Dick, and Hidenori Tanaka. Beyond batchnorm: Towards a general understanding of normalization in deep learning. *CoRR*, abs/2106.05956, 2021.
- [38] Andreas Veit, Michael J. Wilber, and Serge J. Belongie. Residual networks behave like ensembles of relatively shallow networks. In *Advances in Neural Information Processing Systems 29: Annual Conference on Neural Information Processing Systems 2016*, pages 550–558, 2016.
- [39] George Philipp, Dawn Song, and Jaime G. Carbonell. Gradients explode - deep networks are shallow - ResNet explained. In *6th International Conference on Learning Representations, ICLR 2018, Workshop Track Proceedings*, 2018.
- [40] Greg Yang, Jeffrey Pennington, Vinay Rao, Jascha Sohl-Dickstein, and Samuel S. Schoenholz. A mean field theory of batch normalization. In *7th International Conference on Learning Representations, ICLR 2019*, 2019.
- [41] Antoine Labatie. Characterizing well-behaved vs. pathological deep neural networks. In *Proceedings of the 36th International Conference on Machine Learning, ICML 2019*, volume 97 of *Proceedings of Machine Learning Research*, pages 3611–3621, 2019.
- [42] Angus Galloway, Anna Golubeva, Thomas Tanay, Medhat Moussa, and Graham W. Taylor. Batch normalization is a cause of adversarial vulnerability. *CoRR*, abs/1905.02161, 2019.
- [43] Mattias Teye, Hossein Azizpour, and Kevin Smith. Bayesian uncertainty estimation for batch normalized deep networks. In *Proceedings of the 35th International Conference on Machine Learning, ICML 2018*, volume 80 of *Proceedings of Machine Learning Research*, pages 4914–4923, 2018.
- [44] Alexander Shekhovtsov and Boris Flach. Stochastic normalizations as Bayesian learning. In *Computer Vision - ACCV 2018 - 14th Asian Conference on Computer Vision, Revised Selected Papers, Part II*, volume 11362 of *Lecture Notes in Computer Science*, pages 463–479, 2018.
- [45] Ping Luo, Xinjiang Wang, Wenqi Shao, and Zhanglin Peng. Towards understanding regularization in batch normalization. In *7th International Conference on Learning Representations, ICLR 2019*, 2019.
- [46] Johan Bjorck, Carla P. Gomes, Bart Selman, and Kilian Q. Weinberger. Understanding batch normalization. In *Advances in Neural Information Processing Systems 31: Annual Conference on Neural Information Processing Systems 2018, NeurIPS 2018*, pages 7705–7716, 2018.

- [47] Arthur Jacot, Franck Gabriel, and Clément Hongler. Freeze and chaos for DNNs: an NTK view of batch normalization, checkerboard and boundary effects. *CoRR*, abs/1907.05715, 2019.
- [48] Hadi Daneshmand, Jonas Moritz Kohler, Francis R. Bach, Thomas Hofmann, and Aurélien Lucchi. Batch normalization provably avoids ranks collapse for randomly initialised deep networks. In *Advances in Neural Information Processing Systems 33: Annual Conference on Neural Information Processing Systems 2020, NeurIPS 2020*, 2020.
- [49] Vinay Rao and Jascha Sohl-Dickstein. Is batch norm unique? An empirical investigation and prescription to emulate the best properties of common normalizers without batch dependence. *CoRR*, abs/2010.10687, 2020.
- [50] Boris Hanin and David Rolnick. Complexity of linear regions in deep networks. In *Proceedings of the 36th International Conference on Machine Learning, ICML 2019*, volume 97 of *Proceedings of Machine Learning Research*, pages 2596–2604, 2019.
- [51] Boris Hanin and David Rolnick. Deep relu networks have surprisingly few activation patterns. In *Advances in Neural Information Processing Systems 32: Annual Conference on Neural Information Processing Systems 2019, NeurIPS 2019*, pages 359–368, 2019.
- [52] Mingxing Tan and Quoc V. Le. EfficientNet: Rethinking model scaling for convolutional neural networks. In *Proceedings of the 36th International Conference on Machine Learning, ICML 2019*, volume 97 of *Proceedings of Machine Learning Research*, pages 6105–6114, 2019.
- [53] Lei Huang, Yi Zhou, Li Liu, Fan Zhu, and Ling Shao. Group whitening: Balancing learning efficiency and representational capacity. In *IEEE Conference on Computer Vision and Pattern Recognition, CVPR 2021*, pages 9512–9521, 2021.
- [54] Cihang Xie, Mingxing Tan, Boqing Gong, Jiang Wang, Alan L. Yuille, and Quoc V. Le. Adversarial examples improve image recognition. In *2020 IEEE/CVF Conference on Computer Vision and Pattern Recognition, CVPR 2020*, pages 816–825, 2020.
- [55] Cihang Xie and Alan L. Yuille. Intriguing properties of adversarial training at scale. In *8th International Conference on Learning Representations, ICLR 2020*, 2020.
- [56] Takeru Miyato and Masanori Koyama. cGANs with projection discriminator. In *6th International Conference on Learning Representations, ICLR 2018, Conference Track Proceedings*, 2018.
- [57] Harm de Vries, Florian Strub, Jérémie Mary, Hugo Larochelle, Olivier Pietquin, and Aaron C. Courville. Modulating early visual processing by language. In *Advances in Neural Information Processing Systems 30: Annual Conference on Neural Information Processing Systems 2017*, pages 6594–6604, 2017.
- [58] Lucas Deecke, Iain Murray, and Hakan Bilen. Mode normalization. In *7th International Conference on Learning Representations, ICLR 2019*, 2019.
- [59] Ximei Wang, Ying Jin, Mingsheng Long, Jianmin Wang, and Michael I. Jordan. Transferable normalization: Towards improving transferability of deep neural networks. In *Advances in Neural Information Processing Systems 32: Annual Conference on Neural Information Processing Systems 2019, NeurIPS 2019*, pages 1951–1961, 2019.
- [60] Woong-Gi Chang, Tackgeun You, Seonguk Seo, Suha Kwak, and Bohyung Han. Domain-specific batch normalization for unsupervised domain adaptation. In *IEEE Conference on Computer Vision and Pattern Recognition, CVPR 2019*, pages 7354–7362, 2019.
- [61] Yuxin Wu and Justin Johnson. Rethinking "batch" in batchnorm. *CoRR*, abs/2105.07576, 2021.
- [62] David Page. How to train your ResNet 7: Batch norm, 2019.
- [63] Jeffrey Pennington and Pratik Worah. Nonlinear random matrix theory for deep learning. In *Advances in Neural Information Processing Systems 30: Annual Conference on Neural Information Processing Systems 2017*, pages 2637–2646, 2017.

- [64] Behrooz Ghorbani, Shankar Krishnan, and Ying Xiao. An investigation into neural net optimization via Hessian eigenvalue density. In *Proceedings of the 36th International Conference on Machine Learning, ICML 2019*, volume 97 of *Proceedings of Machine Learning Research*, pages 2232–2241, 2019.
- [65] Dominic Masters and Carlo Luschi. Revisiting small batch training for deep neural networks. *CoRR*, abs/1804.07612, 2018.
- [66] Dmitry Ulyanov, Vadim Lebedev, Andrea Vedaldi, and Victor S. Lempitsky. Texture networks: Feed-forward synthesis of textures and stylized images. In *Proceedings of the 33rd International Conference on Machine Learning, ICML 2016*, volume 48 of *JMLR Workshop and Conference Proceedings*, pages 1349–1357, 2016.
- [67] Leon A. Gatys, Alexander S. Ecker, and Matthias Bethge. Image style transfer using convolutional neural networks. In *2016 IEEE Conference on Computer Vision and Pattern Recognition, CVPR 2016*, pages 2414–2423, 2016.
- [68] Dmitry Ulyanov, Andrea Vedaldi, and Victor S. Lempitsky. Improved texture networks: Maximizing quality and diversity in feed-forward stylization and texture synthesis. In *2017 IEEE Conference on Computer Vision and Pattern Recognition, CVPR 2017*, pages 4105–4113, 2017.
- [69] Vincent Dumoulin, Jonathon Shlens, and Manjunath Kudlur. A learned representation for artistic style. In *5th International Conference on Learning Representations, ICLR 2017, Conference Track Proceedings*, 2017.
- [70] Xun Huang and Serge J. Belongie. Arbitrary style transfer in real-time with adaptive instance normalization. In *IEEE International Conference on Computer Vision, ICCV 2017*, pages 1510–1519, 2017.
- [71] Kaiming He, Xiangyu Zhang, Shaoqing Ren, and Jian Sun. Identity mappings in deep residual networks. In *Computer Vision - ECCV 2016 - 14th European Conference*, 2016.
- [72] Andy Brock, Soham De, Samuel L. Smith, and Karen Simonyan. High-performance large-scale image recognition without normalization. In *Proceedings of the 38th International Conference on Machine Learning, ICML 2021*, volume 139 of *Proceedings of Machine Learning Research*, pages 1059–1071, 2021.
- [73] Wenling Shang, Justin Chiu, and Kihyuk Sohn. Exploring normalization in deep residual networks with concatenated rectified linear units. In *Proceedings of the Thirty-First AAAI Conference on Artificial Intelligence*, pages 1509–1516, 2017.
- [74] Igor Gitman and Boris Ginsburg. Comparison of batch normalization and weight normalization algorithms for the large-scale image classification. *CoRR*, abs/1709.08145, 2017.
- [75] Jia Deng, Wei Dong, Richard Socher, Li-Jia Li, Kai Li, and Li Fei-Fei. ImageNet: A large-scale hierarchical image database. In *2009 IEEE Computer Society Conference on Computer Vision and Pattern Recognition (CVPR 2009)*, pages 248–255, 2009.
- [76] Alex Krizhevsky. Learning multiple layers of features from tiny images. Technical report, 2009.
- [77] Priya Goyal, Piotr Dollár, Ross B. Girshick, Pieter Noordhuis, Lukasz Wesolowski, Aapo Kyrola, Andrew Tulloch, Yangqing Jia, and Kaiming He. Accurate, large minibatch SGD: training ImageNet in 1 hour. *CoRR*, abs/1706.02677, 2017.
- [78] Saining Xie, Ross B. Girshick, Piotr Dollár, Zhuowen Tu, and Kaiming He. Aggregated residual transformations for deep neural networks. In *2017 IEEE Conference on Computer Vision and Pattern Recognition, CVPR 2017*, 2017.
- [79] Dominic Masters, Antoine Labatie, Zach Eaton-Rosen, and Carlo Luschi. Making EfficientNet more efficient: Exploring batch-independent normalization, group convolutions and reduced resolution training. *CoRR*, abs/2106.03640, 2021.
- [80] Sitao Xiang and Hao Li. On the effect of batch normalization and weight normalization in generative adversarial networks. *CoRR*, abs/1704.03971, 2017.

- [81] Alexander Kolesnikov, Lucas Beyer, Xiaohua Zhai, Joan Puigcerver, Jessica Yung, Sylvain Gelly, and Neil Houlsby. Big Transfer (BiT): General visual representation learning. In *Computer Vision - ECCV 2020 - 16th European Conference*, 2020.
- [82] Christian Szegedy, Vincent Vanhoucke, Sergey Ioffe, Jonathon Shlens, and Zbigniew Wojna. Rethinking the inception architecture for computer vision. In *2016 IEEE Conference on Computer Vision and Pattern Recognition, CVPR 2016*, pages 2818–2826, 2016.
- [83] Nitish Srivastava, Geoffrey E. Hinton, Alex Krizhevsky, Ilya Sutskever, and Ruslan Salakhutdinov. Dropout: a simple way to prevent neural networks from overfitting. *Journal of Machine Learning Research*, 15(1):1929–1958, 2014.
- [84] Gao Huang, Yu Sun, Zhuang Liu, Daniel Sedra, and Kilian Q. Weinberger. Deep networks with stochastic depth. In *Computer Vision - ECCV 2016 - 14th European Conference, Proceedings, Part IV*, volume 9908, pages 646–661, 2016.
- [85] Hongyi Zhang, Moustapha Cissé, Yann N. Dauphin, and David Lopez-Paz. mixup: Beyond empirical risk minimization. In *6th International Conference on Learning Representations, ICLR 2018, Conference Track Proceedings*, 2018.
- [86] Sangdoo Yun, Dongyoon Han, Sanghyuk Chun, Seong Joon Oh, Youngjoon Yoo, and Junsuk Choe. Cutmix: Regularization strategy to train strong classifiers with localizable features. In *2019 IEEE/CVF International Conference on Computer Vision, ICCV 2019*, pages 6022–6031, 2019.
- [87] Ekin D. Cubuk, Barret Zoph, Dandelion Mané, Vijay Vasudevan, and Quoc V. Le. AutoAugment: Learning augmentation strategies from data. In *IEEE Conference on Computer Vision and Pattern Recognition, CVPR 2019*, pages 113–123, 2019.
- [88] Jasmine Collins, Johannes Ballé, and Jonathon Shlens. Accelerating training of deep neural networks with a standardization loss. *CoRR*, abs/1903.00925, 2019.
- [89] Yann Dauphin and Ekin Dogus Cubuk. Deconstructing the regularization of BatchNorm. In *9th International Conference on Learning Representations, ICLR 2021*, 2021.
- [90] Shibani Santurkar, Dimitris Tsipras, Andrew Ilyas, and Aleksander Madry. How does batch normalization help optimization? In *Advances in Neural Information Processing Systems 31: Annual Conference on Neural Information Processing Systems 2018, NeurIPS 2018*, pages 2488–2498, 2018.
- [91] Moshe Leshno, Vladimir Ya. Lin, Allan Pinkus, and Shimon Schocken. Multilayer feedforward networks with a nonpolynomial activation function can approximate any function. *Neural Networks*, 6(6):861–867, 1993.

A Submission checklist

1. For all authors...
 - (a) Do the main claims made in the abstract and introduction accurately reflect the paper’s contributions and scope? [Yes] We believe the paper’s title and abstract are consistent with the theoretical results of Sections 4 and 5 and the experimental results of Sections 5 and 6.
 - (b) Did you describe the limitations of your work? [Yes] The scope and assumptions of our theoretical results are provided in Sections 3 and 4. The minor limitation of our approach stemming from the requirement that each activation step should be directly preceded by a normalization step is stated in Section 4.
 - (c) Did you discuss any potential negative societal impacts of your work? [No] Our work directly impacts the advancement of the field of computer vision. Its negative impacts could come only indirectly from the negative impacts of this field in general. We thought that this observation was not needed in the main text, as it is already implied.
 - (d) Have you read the ethics review guidelines and ensured that your paper conforms to them? [Yes]
2. If you are including theoretical results...
 - (a) Did you state the full set of assumptions of all theoretical results? [Yes] The full assumptions of our theoretical results are provided in Sections 3 and 4.
 - (b) Did you include complete proofs of all theoretical results? [Yes] Complete proofs of all our theoretical results are provided in Appendix D, E, F and G.
3. If you ran experiments...
 - (a) Did you include the code, data, and instructions needed to reproduce the main experimental results (either in the supplemental material or as a URL)? [Yes] The experimental results can be reproduced based on Appendix B and C.
 - (b) Did you specify all the training details (e.g., data splits, hyperparameters, how they were chosen)? [Yes] All the experimental details are reported in Appendix B
 - (c) Did you report error bars (e.g., with respect to the random seed after running experiments multiple times)? [Yes] The error bars associated with each of our experiments are reported in Appendix B.3.1.
 - (d) Did you include the total amount of compute and the type of resources used (e.g., type of GPUs, internal cluster, or cloud provider)? [Yes] Our experiments with batch-independent norms were run on Graphcore’s MK1 and MK2 IPU’s. We refer the reader to [79] for throughput numbers on Graphcore’s MK2 IPU’s.
4. If you are using existing assets (e.g., code, data, models) or curating/releasing new assets...
 - (a) If your work uses existing assets, did you cite the creators? [Yes]
 - (b) Did you mention the license of the assets? [No] ImageNet’s images are owned by copyright holders. We are unsure about the existence, and potentially the type, of licenses of CIFAR-10 and CIFAR-100.
 - (c) Did you include any new assets either in the supplemental material or as a URL? [N/A]
 - (d) Did you discuss whether and how consent was obtained from people whose data you’re using/curating? [N/A]
 - (e) Did you discuss whether the data you are using/curating contains personally identifiable information or offensive content? [N/A]
5. If you used crowdsourcing or conducted research with human subjects...
 - (a) Did you include the full text of instructions given to participants and screenshots, if applicable? [N/A]
 - (b) Did you describe any potential participant risks, with links to Institutional Review Board (IRB) approvals, if applicable? [N/A]
 - (c) Did you include the estimated hourly wage paid to participants and the total amount spent on participant compensation? [N/A]

B Experimental details

B.1 Experimental setup

Architectures. As stated in Section 5, we use v2 instantiations of ResNets and instantiations of ResNeXts having the same block reorderings as ResNets v2. Practically, our instantiations of ResNeXts are obtained by starting from ResNets v2 and applying the same changes in bottleneck widths and number of groups in 3×3 convolutions as the ones yielding ResNeXts v1 from ResNets v1, using a cardinality $C = 32$ and a dimension $d = 4$ [78].

As also stated in Section 6, we consider two variants of EfficientNets: (i) the original variant with one depthwise convolution per MBConv block and with expansion ratio of 6 [52], and (ii) a variant with each depthwise convolution replaced by a group convolution of group size 16 and with expansion ratio of 4 [79]. Compared to the original variant, the variant with group convolutions has roughly the same number of parameters and slightly more floating point operations (FLOPs) (cf Table 5), but it is executed more efficiently on common A.I. accelerators. Interestingly, the fact that GN+WS does not perform well even in this variant (cf Tables 4, 8 and Figure 7) suggests that the problem related to the removal of degrees of freedom by WS goes beyond just depthwise convolutions [20].

Table 5: **Number of parameters and number of FLOPs in EfficientNets.** Quantities are reported for EfficientNets-B0 (EN-B0) and EfficientNets-B2 (EN-B2) in the variant with depthwise convolutions and expansion ratio of 6 (left) and in the variant with group convolutions of group size 16 and expansion ratio of 4 (right).

	depthwise convs		group convs	
	EN-B0	EN-B2	EN-B0	EN-B2
Number of parameters	5.3M	9.1M	5.9M	9.5M
Number of FLOPs	0.4B	1.0B	0.6B	1.5B

PN. We set PN’s numerical stability constant to $\epsilon = 0.03$, as we found smaller ϵ can lead to sub-optimal performance. We use 200 samples uniformly sampled in probability in the proxy distribution (cf Section C).

In all networks, we disable the scaling part of PN in the proxy-normalized activation step just before the final mean pooling. This is to avoid an alteration of the effective learning rate. An alternative option would be to altogether remove PN before the final mean pooling.

In EfficientNets, we disable PN in squeeze-excite (SE) blocks given that no normalization step precedes each activation step in these blocks. When PN’s additional parameters $\hat{\beta}^l, \hat{\gamma}^l$ are included, we replace the final affine transformation of each MBConv block by a single channel-wise scaling (i.e. we only keep the scale parameter in the transformation). When PN’s additional parameters $\hat{\beta}^l, \hat{\gamma}^l$ are omitted, on the other hand, we leave this final affine transformation as it is.

WS. We set the numerical stability constant of WS to 0.

In all networks, we disable WS in fully-connected layers and in SE blocks. In ResNets, we add an extra scale parameter after the final convolution of each residual block with WS.

Evo-S0. In EfficientNets, the final norm and affine transformation in each MBConv block are replaced by a single affine transformation.

Initialization. We initialize the affine transformation’s parameters as $\beta^l = 0, \gamma^l = 1$, and PN’s additional parameters as $\hat{\beta}^l = 0, \hat{\gamma}^l = 0$ when they are included. We initialize weights ω^l by sampling from truncated normal distributions with inverse square root scaling with respect to fan-in (except for some kernels in EfficientNets where the scaling is with respect to fan-out).

ResNets and ResNeXts trained on ImageNet. We train for 100 epochs with SGD with a momentum of 0.9 and with a batch size of 256. We start with a learning rate of 0.1 after a linear warmup

over the first 5 epochs [77], and we decrease this learning rate four times at the epochs 30, 60, 80 and 90, each time by a factor 10. We apply weight decay with a strength of 10^{-4} to all parameters including the additional parameters β^l , γ^l of PN and the channel-wise scale and shift parameters β^l , γ^l (this is sensible as $\phi = \text{ReLU}$ is positive homogeneous).

We set the norm’s numerical stability constant to 10^{-6} and, unless otherwise specified, we use $G = 8$ groups when using GN+PN and $G = 32$ groups when using GN without PN. When using BN, we compute BN’s statistics over 32 inputs \mathbf{x} and we compute moving average statistics by exponentially weighted average with decay factor 0.97.

For the pre-processing, we follow [71]. When using extra regularization, we use label smoothing with factor 0.1 [82], dropout with rate 0.1 [83] and stochastic depth with rate 0.05 [84]. As the only exception, when changing the choice of extra regularization in Section B.3.4, we use Mixup with strength 0.1 [85] in all networks, and in ResNet-101, ResNeXt-101, we additionally use a variant of CutMix [86] that samples $U_0 \sim \text{Uniform}(0, 1)$ and $U_1 \sim \text{Uniform}(e^{-4}, 1)$ and sets the combination ratio as $\lambda = 1$ if $U_0 \leq 0.435$ and $\lambda = 1 + \frac{1}{4} \log(U_1)$ otherwise.

While we use float-16 to store and process intermediate activations (except in normalization steps), model parameters are still stored and updated in float-32. Each time we provide a result, the mean and standard deviation are computed over 3 independent runs, at the final epoch of each run. As the only exception, the mean and 1σ intervals in Figures 2, 6 are computed by “pooling together” either all 100 epochs in 5 independent runs (Figure 2) or the initialization state in 5 independent runs (Figure 6).

EfficientNets with batch-independent norms trained on ImageNet. Our experimental setup closely follows [52]. We train for 350 epochs with RMSProp with a batch size of 768. We start with a learning rate of 768×2^{-14} (i.e. using a linear scaling [65]) after a linear warmup over the first 5 epochs [77], and we decay the learning rate exponentially by a factor 0.97 every 2.4 epochs. In RMSProp, we use a momentum of 0.9, a decay of $1.0 - (768 \times 2^{-14})$ and a numerical stability constant of 10^{-3} . We apply weight decay with a strength of 10^{-5} on the convolutional weights and the additional parameters β^l , γ^l of PN, but not on other channel-wise parameters (this is sensible as ϕ is not positive homogeneous).

We set the norm’s numerical stability constant to 10^{-3} and we use $G = 4$ groups when using GN or Evo-S0.

For the baseline pre-processing, we follow [52]. In terms of regularization, we always use label smoothing with factor 0.1 [82], dropout with rate 0.2 [83] and stochastic depth with rate starting at 0.2 in the first MBConv block and decaying to zero linearly with the depth of the MBConv block [84]. When using extra regularization, we use Mixup with strength 0.1 [85] in all networks, and in EfficientNets-B2, we additionally use a variant of CutMix [86] that samples $U_0 \sim \text{Uniform}(0, 1)$ and $U_1 \sim \text{Uniform}(e^{-4}, 1)$ and sets the combination ratio as $\lambda = 1$ if $U_0 \leq 0.435$ and $\lambda = 1 + \frac{1}{4} \log(U_1)$ otherwise.

While we use float-16 to store and process intermediate activations (except in normalization steps), model parameters are still stored and updated in float-32. Each time we provide a result, the mean and standard deviation are computed over 3 independent runs. For each run, performance is evaluated at the final epoch with model parameters obtained by exponentially weighted average over checkpoints from previous epochs with a decay factor of 0.97.

EfficientNets with BN trained on ImageNet. For these experiments, we run the public EfficientNet repository with the settings recommended in the repository.⁵ When considering the variant with group convolutions, our only modifications consist in replacing depthwise convolutions with group convolutions of group size 16 and changing the expansion ratio from 6 to 4.

In addition to BN’s inherent regularization, these runs always incorporate label smoothing [82], dropout [83] and stochastic depth [84]. The runs with extra regularization additionally incorporate AutoAugment [87].

Each time we provide a result, the mean and standard deviation are computed over 3 independent runs.

⁵<https://github.com/tensorflow/tpu/tree/master/models/official/efficientnet>

Random nets. We consider a random net following Definition 1. For the cases of BN, LN, IN, GN, the random net implements Eq. (2), (3), (4) in every layer l . For the case of LN+PN, the activation step of Eq. (4) is replaced by the proxy-normalized activation step of Eq. (7). For the case of LN+WS, WS’s step of kernel standardization is added before the convolution of Eq. (2). In all cases, convolutions use periodic boundary conditions to remain consistent with the assumption of Theorem 1.

We set the activation function to $\phi = \text{ReLU}$, widths to $C_l = 1024$, kernel sizes to $K_l = 3$.

We sample the components of the affine transformation’s parameters β^l, γ^l i.i.d. from $\nu_\beta = \mathcal{N}(0, 0.2^2)$ and $\nu_\gamma = \mathcal{N}(1, 0.2^2)$, respectively. This yields $\beta^2 = 0.2^2, \gamma^2 = 1^2 + 0.2^2$ and $\rho = \frac{1^2 + 0.2^2}{1^2 + 0.2^2 + 0.2^2} \approx 0.963$ in Definition 1. We sample the components of weight parameters i.i.d. from a truncated normal distribution with $\frac{1}{\sqrt{C_l}}$ scaling. We set PN’s additional parameters $\tilde{\beta}^l, \tilde{\gamma}^l$ to 0.

We set the norm’s numerical stability constant to 10^{-6} and we use $G = 128$ groups when using GN to roughly preserve group sizes compared to ResNet-50. We use a batch size of 128 and compute BN’s statistics over all 128 inputs \mathbf{x} of the mini-batch when using BN.

We use CIFAR-10 as the dataset \mathcal{D} . We follow [71] for the pre-processing and add a downsampling in the first convolution of the network to alleviate the memory burden.

We use float-32 to store and process intermediate activations. Each time we provide a result, the mean and 1σ intervals are computed over 50 independent realizations.

ResNets trained on CIFAR-10 and CIFAR-100 (cf Section B.4). We train for 160 epochs with SGD with a momentum of 0.9 and with a batch size of 128. We start with a learning rate of 0.1 after a linear warmup over the first 5 epochs [77], and we decrease this learning rate two times at the epochs 80 and 120, each time by a factor 10. We apply weight decay with a strength of 10^{-4} to all parameters including the additional parameters $\tilde{\beta}^l, \tilde{\gamma}^l$ of PN and the channel-wise scale and shift parameters β^l, γ^l (this is sensible as $\phi = \text{ReLU}$ is positive homogeneous).

We set the norm’s numerical stability constant to 10^{-6} and we use $G = 4$ groups when using GN. When using BN, we compute BN’s statistics over 128 inputs \mathbf{x} and we compute moving average statistics by exponentially weighted average with decay factor 0.97.

For the pre-processing, we follow [71]. When using extra regularization, we use label smoothing with factor 0.1 [82], dropout with rate 0.25 [83] and stochastic depth with rate 0.1 [84].

We use float-16 to store and process intermediate activations (except in normalization steps) and to store and update model parameters. Each time we provide a result, the mean and standard deviation are computed over 10 independent runs, at the final epoch of each run.

B.2 Additional details on power plots

B.2.1 Power plots in random net

Additional experimental details. We obtain the random net’s power plots using the experimental setup described in Section B.1 for random nets. We compute the terms $\mathcal{P}^{(1)}(\mathbf{y}^l), \mathcal{P}^{(2)}(\mathbf{y}^l), \mathcal{P}^{(3)}(\mathbf{y}^l), \mathcal{P}^{(4)}(\mathbf{y}^l)$ (as well as the additional terms of Figure 5) for each layer l using the 128 randomly sampled inputs \mathbf{x} in the mini-batch as a proxy for the full dataset \mathcal{D} .

While setting the total depth to $L = 200$ in the random net, we show only the first 20 layers in Figure 2 to facilitate a side-by-side comparison with ResNet-50. That is because the “effective” depth is smaller than the “computational” depth in ResNet-50 (cf Section B.2.2), while the two notions are equivalent in the random net.

Verification of Theorem 1. The case of the random net with LN enables us to precisely verify Theorem 1. We provide this verification in the left and center subplots of Figure 5.

In the left subplot of Figure 5, we show $\mathcal{P}(\mathbf{y}^l) - \mathcal{P}^{(1)}(\mathbf{y}^l)$ (mean and 1σ intervals) and the upper bound $\rho^{l-1} = \left(\frac{1^2 + 0.2^2}{1^2 + 0.2^2 + 0.2^2} \right)^{l-1}$ from Theorem 1 for depths l up to $L = 200$. We confirm that $\mathcal{P}(\mathbf{y}^l) - \mathcal{P}^{(1)}(\mathbf{y}^l)$ is upper bounded with high probability by ρ^{l-1} as predicted by Theorem 1. The

rate of decay of $\mathcal{P}(\mathbf{y}^l) - \mathcal{P}^{(1)}(\mathbf{y}^l)$ is initially above the prediction Theorem 1 due to the aggravating effect of the activation function $\phi = \text{ReLU}$. In very deep layers ($l \gg 1$), this rate of decay ends up very slightly below the prediction of Theorem 1 due to: (i) the fact that ϕ becomes effectively close to channel-wise linear; (ii) the fact that the channel-wise collapse is slightly mitigated by LN with a finite width $C_l = 1024$.

In the center subplot of Figure 5, we show $\mathcal{P}(\mathbf{y}^l)$ (mean and 1σ intervals) for depths l up to $L = 200$. We confirm that $\mathcal{P}(\mathbf{y}^l)$ is with high probability very close to one.

Quantification of channel-wise linearity. To confirm the connection between channel-wise collapse and channel-wise linearity, we finally report the evolution with depth of an additional measure of channel-wise linearity. In the right subplot of Figure 5, we show the measure $\mathcal{P}(\phi(\tilde{\mathbf{y}}^l) - \tilde{\mathbf{z}}^l) / \mathcal{P}(\phi(\tilde{\mathbf{y}}^l))$ (mean and 1σ intervals) for depths l up to $L = 200$, with $\tilde{\mathbf{z}}^l$ the channel-wise linear best-fit of $\phi(\tilde{\mathbf{y}}^l)$ using $\tilde{\mathbf{y}}^l$, that is defined in Eq. (20) and (21). We confirm that deep in the random net, layers are effectively: (i) very close to channel-wise linear with LN; (ii) close to channel-wise linear with GN.

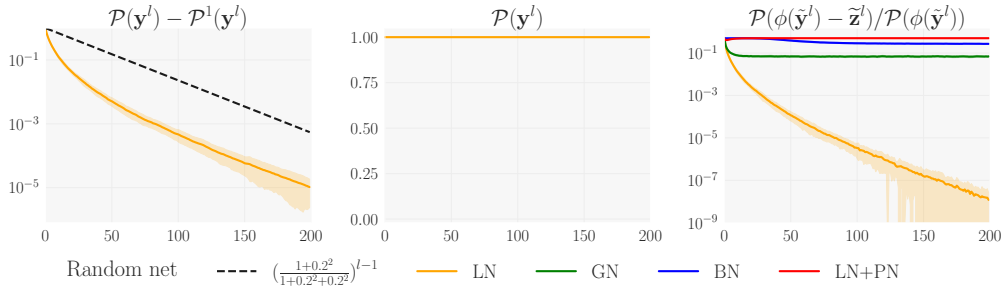


Figure 5: **Verification of Theorem 1 and quantification of channel-wise linearity.** Results are reported in a random net of Definition 1 for depths l up to $L = 200$. Left: $\mathcal{P}(\mathbf{y}^l) - \mathcal{P}^{(1)}(\mathbf{y}^l)$ (mean and 1σ intervals) and upper bound ρ^{l-1} from Theorem 1. Center: $\mathcal{P}(\mathbf{y}^l)$ (mean and 1σ intervals). Right: Additional measure of channel-wise linearity $\mathcal{P}(\phi(\tilde{\mathbf{y}}^l) - \tilde{\mathbf{z}}^l) / \mathcal{P}(\phi(\tilde{\mathbf{y}}^l))$ (mean and 1σ intervals), with $\tilde{\mathbf{z}}^l$ the channel-wise linear best-fit of $\phi(\tilde{\mathbf{y}}^l)$ using $\tilde{\mathbf{y}}^l$, that is defined in Eq. (20) and (21)

B.2.2 Power plots in ResNet-50

Additional experimental details. We obtain the ResNet-50’s power plots using the experimental setup described in Section B for ResNets on ImageNet. At each epoch, we compute the power terms $\mathcal{P}_c^{(1)}(\mathbf{y}^l)$, $\mathcal{P}_c^{(2)}(\mathbf{y}^l)$, $\mathcal{P}_c^{(3)}(\mathbf{y}^l)$, $\mathcal{P}_c^{(4)}(\mathbf{y}^l)$ for each layer l and each channel c using the last 256 inputs \mathbf{x} as a proxy for the full dataset \mathcal{D} .

When looking at each norm separately in residual networks, we noticed artefacts that we attributed to the discrepancy between the computational depth l and the “effective” depth (that oscillates with l). Indeed, the effective depth, defined in terms of the statistical properties of the intermediate activations, grows linearly inside each residual block but gets reduced each time a residual path is summed with a skip connection path (since the latter originates from earlier layers). This phenomenon is tightly connected to the property discussed in Section 2 on the control of activation scale in residual networks.

To avoid such an artefact in Figures 2, 6, we report only a single measurement of $\mathcal{P}^{(1)}(\mathbf{y}^l)$, $\mathcal{P}^{(2)}(\mathbf{y}^l)$, $\mathcal{P}^{(3)}(\mathbf{y}^l)$, $\mathcal{P}^{(4)}(\mathbf{y}^l)$ per residual block by “pooling together” all the channels from the three norms inside each block. We also do not report $\mathcal{P}^{(1)}(\mathbf{y}^l)$, $\mathcal{P}^{(2)}(\mathbf{y}^l)$, $\mathcal{P}^{(3)}(\mathbf{y}^l)$, $\mathcal{P}^{(4)}(\mathbf{y}^l)$ for the final norm just before the final mean pooling.

The presence of this artefact confirms the fact that the effective depth evolves more slowly than the computational depth l in residual networks. This explains why \mathbf{y}^l with LN and GN is not immoderately collapsed even at large l in Figures 2, 6.

Numerical stability issues with IN. As stated in the caption of Figure 2, we did not succeed at training ResNet-50 v2 with IN. We found that using float-16 to store and process intermediate activations caused divergence in these networks. When replacing float-16 by float-32, even though

divergence was avoided, instance-normalized ResNets-50 v2 still did not reach satisfactory performance. We attribute this to a plain incompatibility of IN with v2 instantiations of ResNets that could stem from the presence of a final block of normalization and activation just before the final mean pooling. Intuitively, if we denote this final block as L and if we subtract away the activation function by supposing $\phi = \text{identity}$, then $\mu_{\mathbf{x},c}(\mathbf{z}^L)$ in channel c is constant for all \mathbf{x} , equal to β_c^L (cf Section 4). Thus, if we subtract away the activation function, with IN all inputs \mathbf{x} end up mapped to the same channel-wise constants after the final mean pooling, i.e. they become indistinguishable.

Power plots at initialization. Figure 6 reports the same power plots as Figure 2, except with the mean and 1σ intervals of $\mathcal{P}^{(1)}(\mathbf{y}^l)$, $\mathcal{P}^{(2)}(\mathbf{y}^l)$, $\mathcal{P}^{(3)}(\mathbf{y}^l)$, $\mathcal{P}^{(4)}(\mathbf{y}^l)$ computed at initialization.

When comparing Figure 6 to Figure 2, it is clearly visible that the channel-wise collapse with LN+WS gets aggravated during training compared to initialization. This confirms the importance of compensating the mean shift associated with the affine transformation during training.

It is also visible that the difference between GN and LN gets narrower during training compared to initialization. This means that despite a similar behavior of $\mathcal{P}^{(1)}(\mathbf{y}^l)$ along the training trajectories with GN and LN, differences could still exist in the vicinity of these trajectories, implying a better conditioning of the loss landscape with GN. A similar argument would make us expect a better conditioning of the loss landscape when enforcing \mathbf{y}^l to be channel-wise normalized via an operation directly embedded in the network mapping [62, 64] as opposed to via an external penalty [88, 49, 89], despite the two approaches potentially leading to the same reduction of $\mathcal{P}^{(1)}(\mathbf{y}^l)$.

We believe that the notions of “channel-wise collapse” and “conditioning of the loss landscape” [62, 64] offer a more rigorous quantification of the underlying phenomena at play than the notion of “internal covariate shift” [1, 90], despite connections between the former and latter.

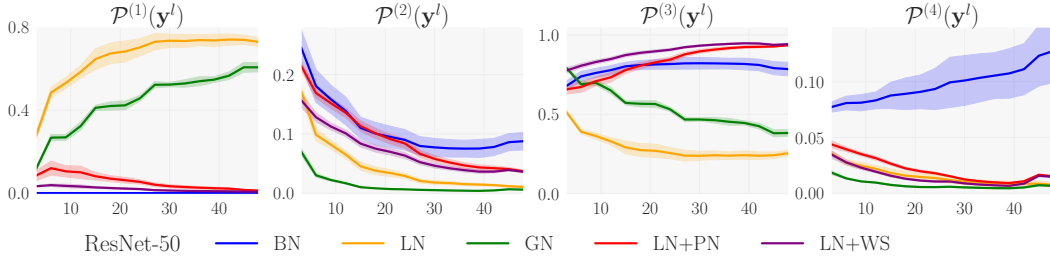


Figure 6: **Power plots at initialization.** The power decomposition of \mathbf{y}^l as a function of the depth l is shown at initialization in ResNet-50 with BN and different batch-independent norms: LN, GN, LN+PN, LN+WS.

B.3 More detailed results on ImageNet

B.3.1 Error bars

In Tables 6, 7, 8, we complement the results of Tables 2, 3, 4 with error bars. In Figure 7, we also provide a visualization of the results of Tables 4, 8.

Table 6: **Effect of adding PN.** ResNet-50 is trained on ImageNet with BN and LN, GN, GN+WS with G groups, either without or with PN added on top (plain vs. PN). Results are formatted as $X \pm \sqrt{\text{Var}X} / Y \pm \sqrt{\text{Var}Y}$ with X, Y the validation accuracies (%) without and with extra regularization, respectively.

	plain	+PN
BN	76.3 ± 0.1 / 75.8 ± 0.2	76.2 ± 0.1 / 76.0 ± 0.1
LN	74.5 ± 0.0 / 74.6 ± 0.1	75.9 ± 0.1 / 76.5 ± 0.0
GN ($G = 8$)	75.4 ± 0.1 / 75.4 ± 0.1	76.3 ± 0.1 / 76.7 ± 0.0
GN ($G = 32$)	75.4 ± 0.1 / 75.3 ± 0.1	75.8 ± 0.2 / 76.1 ± 0.1
GN+WS	76.6 ± 0.0 / 76.7 ± 0.1	76.8 ± 0.1 / 77.1 ± 0.1

Table 7: **BN vs. GN, GN+PN.** ResNets and ResNeXts are trained on ImageNet with BN and GN, GN+PN. Results are formatted as in Table 6.

	RN50	RN101	RNX50	RNX101
BN	76.3 ± 0.1 / 75.8 ± 0.2	77.9 ± 0.1 / 78.0 ± 0.1	77.6 ± 0.1 / 77.2 ± 0.1	78.7 ± 0.1 / 78.9 ± 0.1
GN	75.4 ± 0.1 / 75.3 ± 0.1	77.0 ± 0.1 / 77.4 ± 0.1	76.2 ± 0.2 / 76.6 ± 0.1	77.4 ± 0.2 / 78.1 ± 0.1
GN+PN	76.3 ± 0.1 / 76.7 ± 0.0	77.6 ± 0.2 / 78.6 ± 0.2	76.7 ± 0.1 / 77.8 ± 0.2	77.7 ± 0.2 / 79.0 ± 0.1

Table 8: **BN vs. batch-independent approaches.** EfficientNets are trained on ImageNet with BN and different batch-independent approaches: GN, GN+PN, Evo-S0, GN+WS, FRN+TLU. Results are formatted as in Table 6.

	depthwise convs		group convs	
	EN-B0	EN-B2	EN-B0	EN-B2
BN	76.9 ± 0.1 / 77.2 ± 0.1	79.4 ± 0.0 / 80.0 ± 0.0	76.8 ± 0.1 / 76.7 ± 0.2	79.5 ± 0.1 / 79.7 ± 0.1
GN	76.2 ± 0.1 / 76.2 ± 0.1	78.9 ± 0.1 / 79.4 ± 0.1	76.2 ± 0.1 / 76.2 ± 0.2	79.0 ± 0.1 / 79.6 ± 0.1
GN+PN	76.8 ± 0.0 / 77.0 ± 0.1	79.3 ± 0.1 / 80.0 ± 0.1	76.7 ± 0.1 / 76.8 ± 0.1	79.3 ± 0.1 / 80.1 ± 0.1
Evo-S0	75.8 ± 0.1 / 75.8 ± 0.2	78.5 ± 0.1 / 78.7 ± 0.1	76.2 ± 0.0 / 76.5 ± 0.1	78.9 ± 0.0 / 79.6 ± 0.0
GN+WS	74.2 ± 0.1 / 74.1 ± 0.1	77.8 ± 0.0 / 77.8 ± 0.1	76.2 ± 0.1 / 76.3 ± 0.1	79.2 ± 0.1 / 79.4 ± 0.1
FRN+TLU	75.7 ± 0.1 / 75.7 ± 0.2	78.4 ± 0.1 / 78.9 ± 0.1	74.9 ± 0.2 / 75.1 ± 0.1	78.2 ± 0.1 / 78.6 ± 0.1

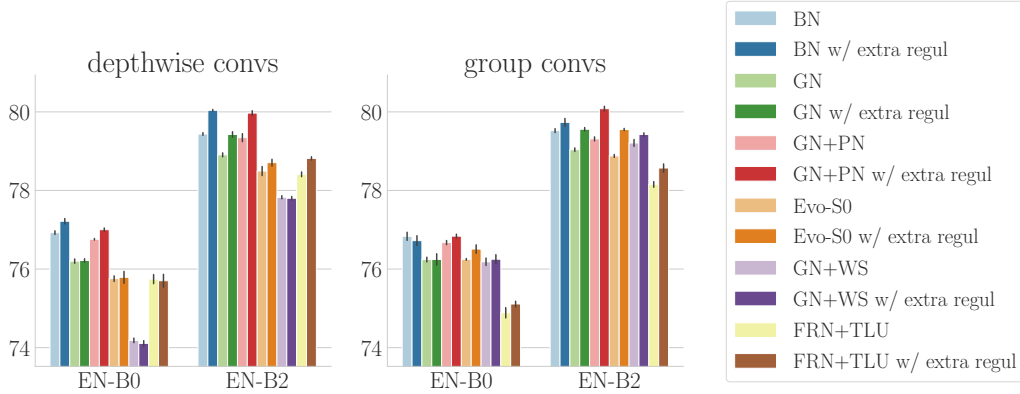


Figure 7: **BN vs. batch-independent approaches.** Validation accuracies (%) of EfficientNets trained on ImageNet with BN and different batch-independent approaches, without and with extra regularization.

B.3.2 Training accuracies

In Tables 9, 10, 11, we complement the results of Tables 2, 3, 4 with training accuracies.

We stress that these training accuracies are highly dependent on the strength of applied regularization. This leads us to: (i) always separate the training accuracies obtained without and with extra regularization; (ii) report only the training accuracies obtained with batch-independent approaches as the training accuracies obtained with BN would not be comparable due to BN’s inherent regularization.

As visible in Tables 9, 10, 11, GN+PN outperforms alternative batch-independent approaches in terms of training accuracies on ImageNet. This applies both to training without extra regularization and to training with extra regularization. This suggests that, on larger datasets, GN+PN would outperform these alternative approaches in terms of both training accuracies and validation accuracies [81, 72].

In Table 11, the fact that with extra regularization EfficientNets-B2 reach lower training accuracies than EfficientNets-B0 is explained by the different level of applied regularization (we add CutMix when training EfficientNets-B2).

Table 9: **Training accuracies, either without or with PN.** ResNet-50 is trained on ImageNet with LN, GN, GN+WS with G groups, either without or with PN added on top (plain vs. +PN). Results are formatted as $X \pm \sqrt{\text{Var} X}$ with X the training accuracies at the final epoch (%). We report separately the results without extra regularization (top) and with extra regularization (bottom).

			RN50		
			G	plain	+PN
without extra regul	LN	1	75.7 \pm 0.1	79.9 \pm 0.1	
	GN	8	77.2 \pm 0.1	80.3\pm0.1	
	GN	32	77.0 \pm 0.0	79.2 \pm 0.2	
	GN+WS	8	80.1 \pm 0.0	80.4\pm0.0	
with extra regul	LN	1	71.8 \pm 0.1	75.8 \pm 0.0	
	GN	8	73.3 \pm 0.1	76.2\pm0.1	
	GN	32	73.1 \pm 0.1	75.1 \pm 0.1	
	GN+WS	8	75.8 \pm 0.0	76.3\pm0.0	

Table 10: **Training accuracies with GN, GN+PN.** ResNets and ResNeXts are trained on ImageNet with GN, GN+PN. Results are formatted as in Table 9.

		RN50	RN101	RNX50	RNX101
without extra regul	GN	77.0 \pm 0.0	79.9 \pm 0.1	79.6 \pm 0.1	81.6 \pm 0.0
	GN+PN	80.3\pm0.1	83.5\pm0.0	84.1\pm0.1	86.2\pm0.0
with extra regul	GN	73.1 \pm 0.1	76.5 \pm 0.0	76.0 \pm 0.1	78.6 \pm 0.1
	GN+PN	76.2\pm0.1	79.7\pm0.1	79.8\pm0.0	82.7\pm0.0

Table 11: **Training accuracies with batch-independent approaches.** EfficientNets are trained on ImageNet with different batch-independent approaches: GN, GN+PN, Evo-S0, GN+WS, FRN+TLU. Results are formatted as in Table 9.

		depthwise convs		group convs	
		EN-B0	EN-B2	EN-B0	EN-B2
without extra regul	GN	75.4 \pm 0.0	80.9 \pm 0.1	74.7 \pm 0.0	80.1 \pm 0.1
	GN+PN	77.3\pm0.0	82.7\pm0.0	75.8\pm0.0	81.4\pm0.1
	Evo-S0	74.6 \pm 0.2	79.8 \pm 0.2	75.1 \pm 0.0	80.4 \pm 0.1
	GN+WS	71.4 \pm 0.0	77.6 \pm 0.0	74.5 \pm 0.0	80.2 \pm 0.1
	FRN+TLU	75.0 \pm 0.1	80.4 \pm 0.0	72.9 \pm 0.1	78.5 \pm 0.1
with extra regul	GN	71.2 \pm 0.1	66.2 \pm 0.1	70.5 \pm 0.1	65.6 \pm 0.1
	GN+PN	72.8\pm0.0	67.8\pm0.1	71.5\pm0.1	66.7\pm0.0
	Evo-S0	70.2 \pm 0.2	64.4 \pm 0.3	70.8 \pm 0.1	65.6 \pm 0.1
	GN+WS	67.3 \pm 0.1	63.4 \pm 0.1	70.4 \pm 0.1	65.4 \pm 0.0
	FRN+TLU	70.4 \pm 0.3	65.1 \pm 0.2	68.8 \pm 0.2	64.0 \pm 0.1

B.3.3 Effect of omitting PN’s additional parameters

In Tables 12, 13 and Figure 8, we report results with PN’s additional parameters $\tilde{\beta}^l, \tilde{\gamma}^l$ set to 0. In that case, $\tilde{\beta}^l, \tilde{\gamma}^l$ can be equivalently omitted and the proxy variable Y^l can be simply considered as a standardized Gaussian variable in each channel c (cf our implementation of Section C), i.e. $Y_c^l \sim \mathcal{N}(0, 1)$.

As visible in Tables 12, 13 and Figure 8, the inclusion of PN’s additional parameters $\tilde{\beta}^l, \tilde{\gamma}^l$ is indeed beneficial. The drop of performance that results from omitting $\tilde{\beta}^l, \tilde{\gamma}^l$ in GN+PN is however very small (in average less than 0.1% in validation accuracy).

Given that the omission of PN’s additional parameters $\tilde{\beta}^l, \tilde{\gamma}^l$ can lead to slight benefits in terms of computational requirements and simplicity of implementation, this variant of PN might sometimes be a better trade off.

Table 12: **Effect of omitting PN’s additional parameters.** ResNets and ResNeXts are trained on ImageNet with BN and GN, GN+PN with $\tilde{\beta}^l, \tilde{\gamma}^l$ included, and GN+PN with $\tilde{\beta}^l, \tilde{\gamma}^l$ omitted. Results are formatted as in Table 6.

	RN50	RN101	RNX50	RNX101
BN	76.3 ± 0.1 / 75.8 ± 0.2	77.9 ± 0.1 / 78.0 ± 0.1	77.6 ± 0.1 / 77.2 ± 0.1	78.7 ± 0.1 / 78.9 ± 0.1
GN	75.4 ± 0.1 / 75.3 ± 0.1	77.0 ± 0.1 / 77.4 ± 0.1	76.2 ± 0.2 / 76.6 ± 0.1	77.4 ± 0.2 / 78.1 ± 0.1
GN+PN with $\tilde{\beta}^l, \tilde{\gamma}^l$ included	76.3 ± 0.1 / 76.7 ± 0.0	77.6 ± 0.2 / 78.6 ± 0.2	76.7 ± 0.1 / 77.8 ± 0.2	77.7 ± 0.2 / 79.0 ± 0.1
GN+PN with $\tilde{\beta}^l, \tilde{\gamma}^l$ omitted	76.3 ± 0.0 / 76.7 ± 0.1	77.5 ± 0.0 / 78.5 ± 0.1	76.5 ± 0.1 / 77.6 ± 0.1	77.5 ± 0.1 / 79.0 ± 0.1

Table 13: **Effect of omitting PN’s additional parameters.** EfficientNets are trained on ImageNet with BN and GN, GN+PN with $\tilde{\beta}^l, \tilde{\gamma}^l$ included, and GN+PN with $\tilde{\beta}^l, \tilde{\gamma}^l$ omitted. Results are formatted as in Table 6.

	depthwise convs		group convs	
	EN-B0	EN-B2	EN-B0	EN-B2
BN	76.9 ± 0.1 / 77.2 ± 0.1	79.4 ± 0.0 / 80.0 ± 0.0	76.8 ± 0.1 / 76.7 ± 0.2	79.5 ± 0.1 / 79.7 ± 0.1
GN	76.2 ± 0.1 / 76.2 ± 0.1	78.9 ± 0.1 / 79.4 ± 0.1	76.2 ± 0.1 / 76.2 ± 0.2	79.0 ± 0.1 / 79.6 ± 0.1
GN+PN with $\tilde{\beta}^l, \tilde{\gamma}^l$ included	76.8 ± 0.0 / 77.0 ± 0.1	79.3 ± 0.1 / 80.0 ± 0.1	76.7 ± 0.1 / 76.8 ± 0.1	79.3 ± 0.1 / 80.1 ± 0.1
GN+PN with $\tilde{\beta}^l, \tilde{\gamma}^l$ omitted	76.6 ± 0.2 / 77.0 ± 0.1	79.2 ± 0.0 / 79.9 ± 0.1	76.7 ± 0.1 / 76.7 ± 0.1	79.3 ± 0.1 / 80.0 ± 0.2

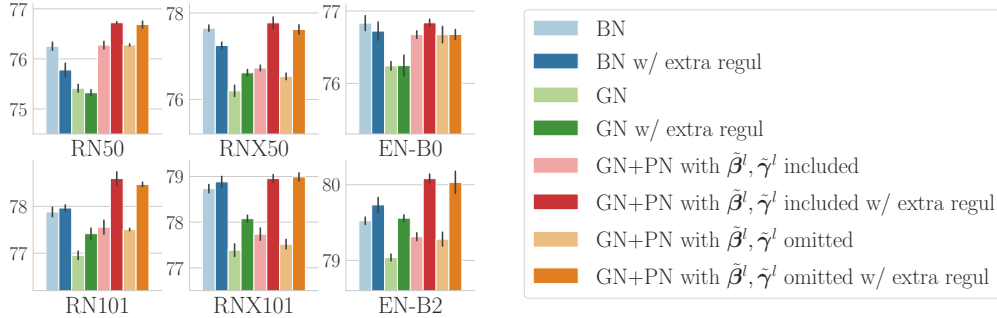


Figure 8: **Effect of omitting PN’s additional parameters.** Validation accuracies (%) of ResNets, ResNeXts and EfficientNets trained on ImageNet with BN and GN, GN+PN with $\tilde{\beta}^l, \tilde{\gamma}^l$ included, and GN+PN with $\tilde{\beta}^l, \tilde{\gamma}^l$ omitted, without and with extra regularization. EfficientNets are considered in the variant with group convolutions.

B.3.4 Effect of changing the choice of extra regularization

In Table 14 and Figure 9 we report results on ResNets and ResNeXts with a change of the choice of extra regularization. When using extra regularization, instead of using label smoothing [82], dropout [83] and stochastic depth [84], we use Mixup [85] in all networks, and in ResNet-101, ResNeXt-101, we additionally use CutMix [86] (cf Section B.1).

We reach similar conclusions with these results as with the results of Table 7: (i) BN is matched or outperformed by GN+PN, except for a small gap of performance in ResNeXt-50 (this gap might due to the imperfect “abstraction” of regularization when only two degrees of regularization are being used); (ii) good performance remains tied to the combination of both an efficient normalization and sufficient regularization.

Table 14: **Effect of changing the choice of extra regularization.** ResNets and ResNeXts are trained on ImageNet with BN and GN, GN+PN. Results are formatted as $X \pm \sqrt{\text{Var}X} / Z \pm \sqrt{\text{Var}Z}$ with X, Z the validation accuracies (%) without extra regularization and with an extra regularization alternative to that of Table 7, respectively.

	RN50	RN101	RNX50	RNX101
BN	76.3 \pm 0.1 / 76.3 \pm 0.0	77.9 \pm 0.1 / 78.1 \pm 0.1	77.6 \pm 0.1 / 78.0 \pm 0.0	78.7 \pm 0.1 / 79.5 \pm 0.0
GN	75.4 \pm 0.1 / 75.9 \pm 0.1	77.0 \pm 0.1 / 77.7 \pm 0.1	76.2 \pm 0.2 / 76.7 \pm 0.1	77.4 \pm 0.2 / 78.3 \pm 0.1
GN+PN	76.3 \pm 0.1 / 77.0 \pm 0.0	77.6 \pm 0.2 / 78.9 \pm 0.1	76.7 \pm 0.1 / 77.6 \pm 0.1	77.7 \pm 0.2 / 79.6 \pm 0.1

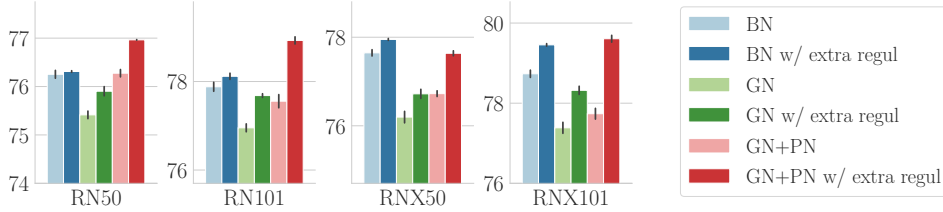


Figure 9: **Effect of changing the choice of extra regularization.** Validation accuracies (%) of ResNets and ResNeXts trained on ImageNet with BN and GN, GN+PN, without extra regularization and with an extra regularization alternative to that of Table 7.

B.4 Experiments on CIFAR-10 and CIFAR-100

In this section, we report results on CIFAR with different sizes of ResNets: ResNet-20 (RN20), ResNet-32 (RN32), ResNet-44 (RN44), ResNet-56 (RN56), ResNet-110 (RN110).

We report results on CIFAR-10 in Table 15 and on CIFAR-100 in Table 16. We further provide a visualization of these results in Figure 10.

While slightly underperforming BN on CIFAR-10, GN+PN tends to slightly outperform BN on CIFAR-100. As a possible reason, BN’s regularization could be more beneficial on the “easy” task of CIFAR-10 than on the “harder” task of CIFAR-100. To the extent that BN’s regularization can be seen as a reduction of the network’s effective capacity, such a reduction of the network’s effective capacity could be more harmful for tasks that require more capacity, i.e. for harder tasks.

Table 15: **BN vs. GN, GN+PN on CIFAR-10.** ResNets are trained on CIFAR-10 with BN and GN, GN+PN. Results are formatted as $X \pm \sqrt{\text{Var}X} / Y \pm \sqrt{\text{Var}Y}$ with X, Y the validation accuracies (%) without and with extra regularization, respectively.

	RN20	RN32	RN44	RN56	RN110
BN	91.6 \pm 0.3 / 91.8 \pm 0.2	92.4 \pm 0.1 / 92.7 \pm 0.2	92.7 \pm 0.2 / 93.1 \pm 0.2	93.0 \pm 0.1 / 93.4 \pm 0.2	93.5 \pm 0.1 / 93.7 \pm 0.2
GN	90.8 \pm 0.2 / 90.7 \pm 0.1	91.5 \pm 0.2 / 91.5 \pm 0.1	91.8 \pm 0.2 / 92.0 \pm 0.1	92.2 \pm 0.2 / 92.2 \pm 0.2	92.6 \pm 0.2 / 92.9 \pm 0.3
GN+PN	91.4 \pm 0.2 / 91.6 \pm 0.3	92.3 \pm 0.2 / 92.5 \pm 0.2	92.8 \pm 0.2 / 92.9 \pm 0.2	92.9 \pm 0.2 / 93.2 \pm 0.2	93.2 \pm 0.1 / 93.6 \pm 0.1

Table 16: **BN vs. GN, GN+PN on CIFAR-100.** ResNets are trained on CIFAR-100 with BN and GN, GN+PN. Results are formatted as in Table 15.

	RN20	RN32	RN44	RN56	RN110
BN	66.8 \pm 0.3 / 65.1 \pm 0.2	68.2 \pm 0.3 / 68.7 \pm 0.2	69.2 \pm 0.4 / 70.5 \pm 0.2	70.1 \pm 0.2 / 71.4 \pm 0.3	71.7 \pm 0.3 / 73.3 \pm 0.3
GN	65.0 \pm 0.3 / 61.7 \pm 0.3	66.5 \pm 0.4 / 65.3 \pm 0.4	67.3 \pm 0.6 / 67.0 \pm 0.3	67.8 \pm 0.4 / 68.1 \pm 0.5	69.5 \pm 0.3 / 70.2 \pm 0.4
GN+PN	66.3 \pm 0.4 / 66.7 \pm 0.2	67.8 \pm 0.4 / 69.5 \pm 0.2	68.9 \pm 0.3 / 70.8 \pm 0.4	69.8 \pm 0.3 / 71.7 \pm 0.4	71.4 \pm 0.2 / 73.1 \pm 0.4

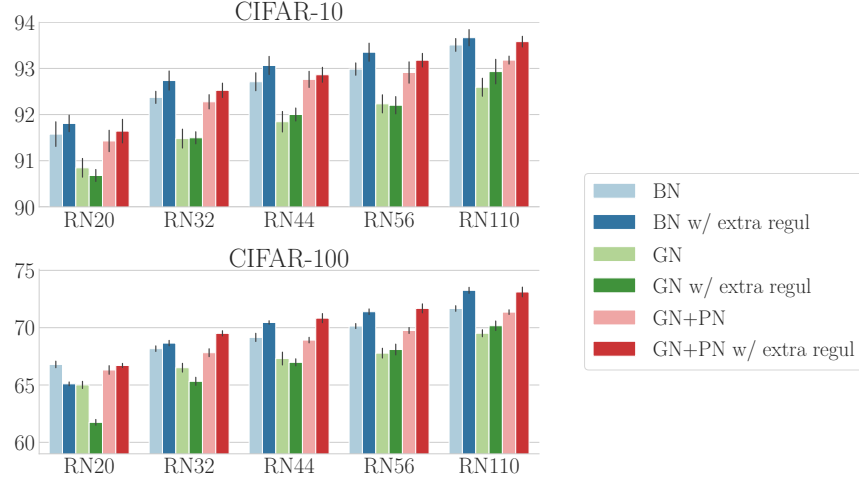


Figure 10: **BN vs. GN, GN+PN on CIFAR.** Validation accuracies (%) of ResNets trained on CIFAR-10 (left) and CIFAR-100 (right) with BN and GN, GN+PN, without and with extra regularization.

C Implementation of the proxy-normalized activation step

In this section, we provide a Tensorflow 1 implementation of the proxy-normalized activation step when PN’s additional parameters $\tilde{\beta}^l, \tilde{\gamma}^l$ are set to zero, i.e. omitted (cf Section 5).

```
import tensorflow as tf
import numpy as np
from scipy.special import erfinv
def uniformly_sampled_gaussian(num_rand):
    rand = 2 * (np.arange(num_rand) + 0.5) / float(num_rand) - 1
    return np.sqrt(2) * erfinv(rand)
```

```
def proxy_norm_act(y,
                   activation_fn=tf.nn.relu,
                   proxy_epsilon=0.03,
                   num_samples=256):
    """
    TensorFlow 1 implementation of the proxy normalized activation step.
```

Note that, as in the main text of this paper, the affine transform is applied during this step rather than the normalization step.

```
:param y: 4D activation tensor after the normalization step
:param activation_fn: Activation function
:param proxy_epsilon: PN's numerical stability constant (should not be too low)
:param num_samples: Number of samples in proxy distribution
:return tilde_z: 4D activation tensor after the proxy-normalized activation step
"""
```

```
def create_channelwise_variable(name, init):
    num_channels = int(y.get_shape()[-1])
    return tf.get_variable(name,
                           dtype=y.dtype,
                           shape=[1, 1, 1, num_channels],
                           initializer=tf.constant_initializer(init))
```

```
# scale and shift parameters after the norm
beta = create_channelwise_variable('beta', 0.0)
gamma = create_channelwise_variable('gamma', 1.0)
```

```

# activation step
z = gamma * y + beta # affine transform
z = activation_fn(z) # activation function

# proxy normalization
proxy_z = tf.constant(uniformly_sampled_gaussian(num_samples), y.dtype)
proxy_z = tf.reshape(proxy_z, [num_samples, 1, 1, 1])
proxy_z = gamma * proxy_z + beta # affine transform on proxy distribution
proxy_z = activation_fn(proxy_z) # activation function on proxy distribution
# compute proxy statistics
proxy_mean, proxy_var = tf.nn.moments(proxy_z, axes=[0], keepdims=True)
# normalize z according to proxy statistics
tilde_z = (z - proxy_mean) * tf.rsqrt(proxy_var + proxy_epsilon)
return tilde_z

```

D Proofs of results other than Theorem 1 and Theorem 2

D.1 Alteration of expressivity with IN

In this section, we first prove that, on any dataset \mathcal{D} , networks without normalization can express mappings arbitrarily close to the identity (Proposition 1). We then prove that, in general, networks with IN cannot express mappings arbitrarily close to the identity (Proposition 2)

Proposition 1. *Lift any assumptions on the activation function ϕ and suppose instead that ϕ is non-polynomial. Further suppose that each layer l up to depth L in the neural network implements the following two steps $\forall \alpha, c$:*

$$\mathbf{y}_{\alpha,c}^l = (\boldsymbol{\omega}^l * \mathbf{z}^{l-1})_{\alpha,c} + \mathbf{b}_c^l, \quad (8)$$

$$\mathbf{z}_{\alpha,c}^l = \phi(\mathbf{y}_{\alpha,c}^l), \quad (9)$$

where $\mathbf{z}^0 \equiv \mathbf{x}$, and $\boldsymbol{\omega}^l \in \mathbb{R}^{K_l \times K_l \times C_{l-1} \times C_l}$ and $\mathbf{b}^l \in \mathbb{R}^{C_l}$ are the weights and biases at layer l .

Now fix a layer $l \in \{1, \dots, L\}$, the spatial extents H, W , the widths C_0, C_l assumed equal at layer 0 and layer l , and the dataset \mathcal{D} . Further denote Φ_l the network mapping from \mathbf{x} to \mathbf{y}^l such that $\mathbf{y}^l = \Phi_l(\mathbf{x})$.

Then for any $\epsilon > 0$, there exists a choice of intermediate widths $(C_k)_{1 \leq k < l}$ and model parameters $(\boldsymbol{\omega}^1, \mathbf{b}^1, \dots, \boldsymbol{\omega}^l, \mathbf{b}^l)$ such that

$$\max_{\mathbf{x} \in \mathcal{D}} \|\Phi_l(\mathbf{x}) - \mathbf{x}\| \leq \epsilon.$$

Proof. The proof proceeds in multiple steps of increasing generality.

Case of unit spatial extents of activations and kernels. When H, W are equal to 1 and K_k is equal to one at every layer k , the propagation of Eq. (8), (9) becomes strictly equivalent to the propagation in a fully-connected network.

If l is the first layer in the network ($l = 1$), we may obtain the strict equality $\Phi_l = \text{identity}$ by choosing the reshaped matricial version $\mathbf{W}^l \in \mathbb{R}^{C_0 \times C_l}$ of $\boldsymbol{\omega}^l$ as the identity and \mathbf{b}^l as zero.

Otherwise ($l \geq 2$), we may apply the universal approximation theorem [91]. Given the assumption of non-polynomial activation function ϕ , this means that for any $\epsilon > 0$, there exists a choice of intermediate widths $(C_k)_{1 \leq k < l}$ and model parameters $(\boldsymbol{\omega}^1, \mathbf{b}^1, \dots, \boldsymbol{\omega}^l, \mathbf{b}^l)$ such that

$$\max_{\mathbf{x} \in \mathcal{D}} \|\Phi_l(\mathbf{x}) - \mathbf{x}\| \leq \epsilon. \quad (10)$$

Case of unit spatial extent of kernels. When K_k is equal to one at every layer k , the propagation of Eq. (8), (9) “occurs” strictly independently for each spatial position α .

Let us then consider the neural network that takes an input $\bar{\mathbf{x}} \in \mathbb{R}^{1 \times 1 \times C_0}$ and provides $\bar{\mathbf{y}}^l, \bar{\mathbf{z}}^l$ at every layer l by implementing the same two steps of Eq. (8), (9). Let us denote Ψ_l the network mapping

from $\bar{\mathbf{x}}$ to $\bar{\mathbf{y}}^l$ such that $\bar{\mathbf{y}}^l = \Psi_l(\bar{\mathbf{x}})$. And let us denote $\bar{\mathcal{D}} = \{\bar{\mathbf{x}}^{(\mathbf{x}, \alpha)}\}_{\mathbf{x} \in \mathcal{D}, \alpha \in \{1, \dots, H\} \times \{1, \dots, W\}}$, where $\bar{\mathbf{x}}^{(\mathbf{x}, \alpha)} \in \mathbb{R}^{1 \times 1 \times C_0}$ denotes the reshaped version of $\mathbf{x}_{\alpha,:} \in \mathbb{R}^{C_0}$ for any \mathbf{x}, α .

If we fix any $\epsilon > 0$ and if we apply Eq. (10) from the previous case with $\frac{1}{\sqrt{HW}}\epsilon$, we get that there exists a choice of intermediate widths $(C_k)_{1 \leq k < l}$ and model parameters $(\omega^1, \mathbf{b}^1, \dots, \omega^l, \mathbf{b}^l)$ such that

$$\max_{\bar{\mathbf{x}} \in \bar{\mathcal{D}}} \|\Psi_l(\bar{\mathbf{x}}) - \bar{\mathbf{x}}\| = \max_{\mathbf{x} \in \mathcal{D}, \alpha \in \{1, \dots, H\} \times \{1, \dots, W\}} \|\Psi_l(\bar{\mathbf{x}}^{(\mathbf{x}, \alpha)}) - \bar{\mathbf{x}}^{(\mathbf{x}, \alpha)}\| \leq \frac{1}{\sqrt{HW}}\epsilon. \quad (11)$$

Let us then fix $(C_k)_{1 \leq k < l}$ and $(\omega^1, \mathbf{b}^1, \dots, \omega^l, \mathbf{b}^l)$ such that Eq. (11) holds.

Due to the independence of spatial positions, the mapping Φ_l is such that $\Phi_l(\mathbf{x})_{\alpha,:}$ is a reshaped version of $\Psi_l(\bar{\mathbf{x}}^{(\mathbf{x}, \alpha)})$ for any \mathbf{x}, α . This means that $\forall \mathbf{x} \in \mathcal{D}$ and $\forall \alpha \in \{1, \dots, H\} \times \{1, \dots, W\}$:

$$\|\Phi_l(\mathbf{x})_{\alpha,:} - \mathbf{x}_{\alpha,:}\| = \|\Psi_l(\bar{\mathbf{x}}^{(\mathbf{x}, \alpha)}) - \bar{\mathbf{x}}^{(\mathbf{x}, \alpha)}\| \leq \frac{1}{\sqrt{HW}}\epsilon.$$

We then get that $\forall \mathbf{x} \in \mathcal{D}$:

$$\|\Phi_l(\mathbf{x}) - \mathbf{x}\|^2 = \sum_{\alpha \in \{1, \dots, H\} \times \{1, \dots, W\}} \|\Phi_l(\mathbf{x})_{\alpha,:} - \mathbf{x}_{\alpha,:}\|^2 \leq \sum_{\alpha \in \{1, \dots, H\} \times \{1, \dots, W\}} \frac{1}{HW}\epsilon^2 \leq \epsilon^2.$$

This immediately implies that

$$\max_{\mathbf{x} \in \mathcal{D}} \|\Phi_l(\mathbf{x}) - \mathbf{x}\| \leq \epsilon.$$

General case. Let us consider the neural network that takes $\mathbf{x} \in \mathcal{D}$ as input and provides $\bar{\mathbf{y}}^l, \bar{\mathbf{z}}^l$ at every layer l by implementing Eq. (8), (9) with weights $\bar{\omega}^l \in \mathbb{R}^{1 \times 1 \times C_{l-1} \times C_l}$, biases $\bar{\mathbf{b}}^l \in \mathbb{R}^{C_l}$ and activation function ϕ . Let us further denote Ψ_l the network mapping from \mathbf{x} to $\bar{\mathbf{y}}^l$ such that $\bar{\mathbf{y}}^l = \Psi_l(\mathbf{x})$.

If we fix any $\epsilon > 0$ and if we apply Eq. (11) from the previous case, then we get that there exists a choice of intermediate widths $(C_k)_{1 \leq k < l}$ and model parameters $(\bar{\omega}^1, \bar{\mathbf{b}}^1, \dots, \bar{\omega}^l, \bar{\mathbf{b}}^l)$ such that

$$\max_{\mathbf{x} \in \mathcal{D}} \|\Psi_l(\mathbf{x}) - \mathbf{x}\| \leq \epsilon. \quad (12)$$

Let us then fix $(C_k)_{1 \leq k < l}$ and $(\bar{\omega}^1, \bar{\mathbf{b}}^1, \dots, \bar{\omega}^l, \bar{\mathbf{b}}^l)$ such that Eq. (12) holds. Let us further define the weights and biases ω^k, \mathbf{b}^k at each layer k such that $\forall h, w, c, c'$:

$$\omega_{h,w,c,c'}^k \equiv \begin{cases} \bar{\omega}_{h,w,c,c'}^k & \text{if the multi-index } (h, w, c, c') \text{ in the weights} \\ & \text{associates spatial positions } \alpha \text{ in the convolution's input } \mathbf{z}_{\alpha,c}^{l-1}, \\ & \text{to the same spatial positions } \alpha \text{ in the convolution's output } \mathbf{y}_{\alpha,c'}^l, \\ 0 & \text{otherwise,} \end{cases}$$

$$\mathbf{b}_{c'}^k \equiv \bar{\mathbf{b}}_{c'}^k.$$

Then it holds that $\Phi_l = \Psi_l$, which in turn implies that

$$\max_{\mathbf{x} \in \mathcal{D}} \|\Phi_l(\mathbf{x}) - \mathbf{x}\| \leq \epsilon. \quad \square$$

Proposition 2. Suppose that the neural network implements Eq. (2), (3), (4) in every layer up to depth L and suppose that $\text{Norm} = \text{IN}$.

Further fix a layer $l \in \{1, \dots, L\}$, the spatial extents H, W , the widths C_0, C_l assumed equal at layer 0 and layer l , and any dataset \mathcal{D} such that there exists at least one channel in which the inputs of \mathcal{D} do not all share the same statistics of instance mean, i.e.

$$\exists c, \exists \mathbf{x}', \mathbf{x}'' \in \mathcal{D} : \quad \mathbb{E}_{\alpha}[\mathbf{x}'_{\alpha,c}] \neq \mathbb{E}_{\alpha}[\mathbf{x}''_{\alpha,c}].$$

Then there exists $\epsilon > 0$ such that for any choice of intermediate widths $(C_k)_{1 \leq k < l}$ and model parameters $(\omega^1, \beta^1, \gamma^1, \dots, \omega^l, \beta^l, \gamma^l)$, it holds that

$$\max_{\mathbf{x} \in \mathcal{D}} \|\Phi_l(\mathbf{x}) - \mathbf{x}\| > \epsilon,$$

where Φ_l denotes the network mapping from \mathbf{x} to $\tilde{\mathbf{y}}^l$ such that $\tilde{\mathbf{y}}^l = \Phi_l(\mathbf{x}), \forall \mathbf{x}$.

Proof. Let us proceed by contradiction and suppose that for any $\epsilon > 0$, there exists a choice of intermediate widths $(C_k)_{1 \leq k < l}$ and model parameters $(\omega^1, \beta^1, \gamma^1, \dots, \omega^l, \beta^l, \gamma^l)$ such that

$$\max_{\mathbf{x} \in \mathcal{D}} \|\Phi_l(\mathbf{x}) - \mathbf{x}\| \leq \epsilon. \quad (13)$$

Given the assumption on \mathcal{D} , there exists some channel c and some inputs $\mathbf{x}', \mathbf{x}'' \in \mathcal{D}$ such that

$$\mathbb{E}_\alpha[\mathbf{x}'_{\alpha,c}] \neq \mathbb{E}_\alpha[\mathbf{x}''_{\alpha,c}]. \quad (14)$$

Let us then fix c and $\mathbf{x}', \mathbf{x}'' \in \mathcal{D}$ satisfying Eq. (14) and let us define $\eta \equiv |\mathbb{E}_\alpha[\mathbf{x}'_{\alpha,c}] - \mathbb{E}_\alpha[\mathbf{x}''_{\alpha,c}]| > 0$.

Applying Eq. (13) with $\epsilon = \frac{\sqrt{HW}}{4}\eta$, we get that there exists a choice of intermediate widths $(C_k)_{1 \leq k < l}$ and model parameters $(\omega^1, \beta^1, \gamma^1, \dots, \omega^l, \beta^l, \gamma^l)$ such that

$$\max_{\mathbf{x} \in \mathcal{D}} \|\Phi_l(\mathbf{x}) - \mathbf{x}\| \leq \frac{\sqrt{HW}}{4}\eta. \quad (15)$$

Let us then fix $(C_k)_{1 \leq k < l}$ and $(\omega^1, \beta^1, \gamma^1, \dots, \omega^l, \beta^l, \gamma^l)$ such that Eq. (15) holds. It follows that

$$\begin{aligned} \sum_{\alpha} (\Phi_l(\mathbf{x}')_{\alpha,c} - \mathbf{x}'_{\alpha,c})^2 &\leq \|\Phi_l(\mathbf{x}') - \mathbf{x}'\|^2 \leq \left(\frac{\sqrt{HW}}{4}\eta\right)^2, \\ \sum_{\alpha} (\Phi_l(\mathbf{x}'')_{\alpha,c} - \mathbf{x}''_{\alpha,c})^2 &\leq \|\Phi_l(\mathbf{x}'') - \mathbf{x}''\|^2 \leq \left(\frac{\sqrt{HW}}{4}\eta\right)^2, \\ \mathbb{E}_\alpha \left[(\Phi_l(\mathbf{x}')_{\alpha,c} - \mathbf{x}'_{\alpha,c})^2 \right] + \mathbb{E}_\alpha \left[(\Phi_l(\mathbf{x}'')_{\alpha,c} - \mathbf{x}''_{\alpha,c})^2 \right] &\leq \frac{2}{HW} \left(\frac{\sqrt{HW}}{4}\eta \right)^2. \end{aligned} \quad (16)$$

At the same time, for any input \mathbf{x} , it holds that

$$\begin{aligned} \mathbb{E}_\alpha \left[(\Phi_l(\mathbf{x})_{\alpha,c} - \mathbf{x}_{\alpha,c})^2 \right] &= \mathbb{E}_\alpha \left[\Phi_l(\mathbf{x})_{\alpha,c} - \mathbf{x}_{\alpha,c} \right]^2 + \text{Var}_\alpha \left[\Phi_l(\mathbf{x})_{\alpha,c} - \mathbf{x}_{\alpha,c} \right] \\ &\geq \mathbb{E}_\alpha \left[\Phi_l(\mathbf{x})_{\alpha,c} - \mathbf{x}_{\alpha,c} \right]^2. \end{aligned} \quad (17)$$

Using $\forall a, b: (a - b)^2 \leq 2a^2 + 2b^2$, combined with Eq. (17) and Eq. (16), we get

$$\begin{aligned} &\left(\mathbb{E}_\alpha \left[\Phi_l(\mathbf{x}')_{\alpha,c} - \mathbf{x}'_{\alpha,c} \right] - \mathbb{E}_\alpha \left[\Phi_l(\mathbf{x}'')_{\alpha,c} - \mathbf{x}''_{\alpha,c} \right] \right)^2 \\ &\leq 2\mathbb{E}_\alpha \left[\Phi_l(\mathbf{x}')_{\alpha,c} - \mathbf{x}'_{\alpha,c} \right]^2 + 2\mathbb{E}_\alpha \left[\Phi_l(\mathbf{x}'')_{\alpha,c} - \mathbf{x}''_{\alpha,c} \right]^2 \\ &\leq 2\mathbb{E}_\alpha \left[(\Phi_l(\mathbf{x}')_{\alpha,c} - \mathbf{x}'_{\alpha,c})^2 \right] + 2\mathbb{E}_\alpha \left[(\Phi_l(\mathbf{x}'')_{\alpha,c} - \mathbf{x}''_{\alpha,c})^2 \right] \\ &\leq \frac{4}{HW} \left(\frac{\sqrt{HW}}{4}\eta \right)^2. \end{aligned} \quad (18)$$

Next, we note that with IN all inputs \mathbf{x} are associated with the same instance means in each channel of $\tilde{\mathbf{y}}^l = \Phi_l(\mathbf{x})$. This means in particular that

$$\mathbb{E}_\alpha \left[\Phi_l(\mathbf{x}')_{\alpha,c} \right] = \mathbb{E}_\alpha \left[\Phi_l(\mathbf{x}'')_{\alpha,c} \right]. \quad (19)$$

Combining Eq. (18) with Eq. (19), we get that

$$\begin{aligned} \left(\mathbb{E}_\alpha[\mathbf{x}''_{\alpha,c}] - \mathbb{E}_\alpha[\mathbf{x}'_{\alpha,c}] \right)^2 &\leq \frac{4}{HW} \left(\frac{\sqrt{HW}}{4}\eta \right)^2, \\ |\mathbb{E}_\alpha[\mathbf{x}'_{\alpha,c}] - \mathbb{E}_\alpha[\mathbf{x}''_{\alpha,c}]| &\leq \frac{2}{\sqrt{HW}} \frac{\sqrt{HW}}{4}\eta = \frac{\eta}{2}. \end{aligned}$$

Since we earlier defined η as $\eta \equiv |\mathbb{E}_\alpha[\mathbf{x}'_{\alpha,c}] - \mathbb{E}_\alpha[\mathbf{x}''_{\alpha,c}]| > 0$, we reach a contradiction. \square

D.2 Layer-wise power equals one

Proposition 3. *If $\sigma_{I_{\mathbf{x},c}}(\mathbf{x}^l) \neq 0$ for all $\mathbf{x} \in \mathcal{D}$ and $c \in \{1, \dots, C_l\}$, then it holds that $\mathcal{P}(\mathbf{y}^l) = 1$ for any choice of Norm $\in \{\text{BN}, \text{LN}, \text{IN}, \text{GN}\}$.*

Proof. The proof proceeds by distinguishing each case in Norm $\in \{\text{BN}, \text{LN}, \text{IN}, \text{GN}\}$.

Case of BN. If we fix a channel c , the assumption that $\sigma_c(\mathbf{x}^l) \neq 0$ implies that

$$\mathcal{P}_c(\mathbf{y}^l) = \frac{\mathbb{E}_{\mathbf{x},\alpha} \left[\left(\mathbf{x}_{\alpha,c}^l - \mu_c(\mathbf{x}^l) \right)^2 \right]}{\sigma_c(\mathbf{x}^l)^2} = \frac{\sigma_c(\mathbf{x}^l)^2}{\sigma_c(\mathbf{x}^l)^2} = 1.$$

We immediately get that $\mathcal{P}(\mathbf{y}^l) = \mathbb{E}_c \left[\mathcal{P}_c(\mathbf{y}^l) \right] = 1$.

Case of GN. Let us fix $\mathbf{x} \in \mathcal{D}$ and let us denote \mathcal{G}_g for $g \in \{1, \dots, G\}$ the G groups of channels and $I_{\mathbf{x}}^{(g)} = \{\mathbf{x}, c \in \mathcal{G}_g\}$ the conditional sets of standardization for $g \in \{1, \dots, G\}$.

The assumption that $\sigma_{I_{\mathbf{x}}^{(g)}}(\mathbf{x}^l) \neq 0$ implies for any g that

$$\mathcal{P}_{I_{\mathbf{x}}^{(g)}}(\mathbf{y}^l) = \frac{\mathbb{E}_{\alpha,c|c \in \mathcal{G}_g} \left[\left(\mathbf{x}_{\alpha,c}^l - \mu_{I_{\mathbf{x}}^{(g)}}(\mathbf{x}^l) \right)^2 \right]}{\sigma_{I_{\mathbf{x}}^{(g)}}(\mathbf{x}^l)^2} = \frac{\sigma_{I_{\mathbf{x}}^{(g)}}(\mathbf{x}^l)^2}{\sigma_{I_{\mathbf{x}}^{(g)}}(\mathbf{x}^l)^2} = 1.$$

This implies that

$$\begin{aligned} \mathcal{P}_{\mathbf{x}}(\mathbf{y}^l) &= \frac{1}{C_l} \sum_c \mathcal{P}_{\mathbf{x},c}(\mathbf{y}^l) = \frac{1}{C_l} \sum_g \sum_{c \in \mathcal{G}_g} \mathcal{P}_{\mathbf{x},c}(\mathbf{y}^l) \\ &= \frac{1}{C_l} \sum_g |\mathcal{G}_g| \mathcal{P}_{I_{\mathbf{x}}^{(g)}}(\mathbf{y}^l) = \frac{1}{C_l} \sum_g |\mathcal{G}_g| = 1, \end{aligned}$$

where we used $\mathcal{P}_{I_{\mathbf{x}}^{(g)}}(\mathbf{y}^l) = \frac{1}{|\mathcal{G}_g|} \sum_{c \in \mathcal{G}_g} \mathcal{P}_{\mathbf{x},c}(\mathbf{y}^l)$.

We immediately get that $\mathcal{P}(\mathbf{y}^l) = \mathbb{E}_{\mathbf{x}} \left[\mathcal{P}_{\mathbf{x}}(\mathbf{y}^l) \right] = 1$.

Cases of LN and IN. The cases of LN and IN immediately follow from the cases of GN with $G = 1$ group and $G = C_l$ groups. \square

D.3 Channel-wise collapse implies channel-wise linearity

Some additional notations are required in this section. We denote $\Theta^l \equiv (\omega^1, \beta^1, \gamma^1, \dots, \omega^l, \beta^l, \gamma^l)$ the aggregated model parameters up to layer l .

We further define the linearized post-activations $\tilde{\mathbf{z}}^l$ for any \mathcal{D} , Θ^l as

$$\forall \alpha, c : \quad \tilde{\mathbf{z}}_{\alpha,c}^l = \tilde{\lambda}_c \tilde{\mathbf{y}}_{\alpha,c}^l, \quad (20)$$

$$\forall c : \quad \tilde{\lambda}_c = \arg \min_{\lambda_c} \mathbb{E}_{\mathbf{x},\alpha} \left[\left(\mathbf{z}_{\alpha,c}^l - \lambda_c \tilde{\mathbf{y}}_{\alpha,c}^l \right)^2 \right] = \arg \min_{\lambda_c} \mathbb{E}_{\mathbf{x},\alpha} \left[\left(\phi(\tilde{\mathbf{y}}_{\alpha,c}^l) - \lambda_c \tilde{\mathbf{y}}_{\alpha,c}^l \right)^2 \right]. \quad (21)$$

The linearized post-activations $\tilde{\mathbf{z}}^l$ are the channel-wise linear best-fit of $\mathbf{z}^l = \phi(\tilde{\mathbf{y}}^l)$ using $\tilde{\mathbf{y}}^l$.

We start by proving that the inequality $\mathcal{P}_c(\tilde{\mathbf{y}}^l) - \mathcal{P}_c^{(1)}(\tilde{\mathbf{y}}^l) \leq \tilde{\eta} \mathcal{P}_c^{(1)}(\tilde{\mathbf{y}}^l)$ for sufficiently small $\tilde{\eta}$ implies channel-wise linearity (Proposition 4). We then prove that the inequality $\mathcal{P}_c(\tilde{\mathbf{y}}^l) - \mathcal{P}_c^{(1)}(\tilde{\mathbf{y}}^l) \leq \tilde{\eta} \mathcal{P}_c(\tilde{\mathbf{y}}^l)$ for sufficiently small $\tilde{\eta}$ implies channel-wise-linearity (Proposition 5).

Proposition 4. *If we fix some $d \in \mathbb{N}^*$, there exists $\tilde{\eta} > 0$ such that for any choice of $(\phi, H, W, \mathcal{D}, \Theta^l)$, it holds that*

$$\left(HW|\mathcal{D}| = d \right) \wedge \left(\mathcal{P}_c(\tilde{\mathbf{y}}^l) - \mathcal{P}_c^{(1)}(\tilde{\mathbf{y}}^l) \leq \tilde{\eta} \mathcal{P}_c^{(1)}(\tilde{\mathbf{y}}^l) \right) \implies \mathbf{z}_{\alpha,c}^l = \tilde{\mathbf{z}}_{\alpha,c}^l \quad \forall \mathbf{x}, \alpha,$$

where $\tilde{\mathbf{z}}^l$ are the linearized post-activations defined in Eq. (20), (21) and \wedge is the logical “and”.

Proof. Any positive homogeneous ϕ satisfies $\phi(r) = r\phi(1)$ and $\phi(-r) = r\phi(-1)$ for any $r \geq 0$. This means that any positive homogeneous ϕ is: (i) fully determined by its values at $+1$ and -1 ; (ii) linear on the intervals $(-\infty, 0]$ and $[0, +\infty)$.

A sufficient condition for the linearity with respect to \mathbf{x}, α in channel c is therefore a constant sign of $\tilde{\mathbf{y}}_{\alpha,c}^l$ for all \mathbf{x}, α . Let us see that this constant sign is implied by a sufficiently severe channel-wise collapse.

We start by proving the result with the two distinct conditionalities: (i) $\sigma_c(\tilde{\mathbf{y}}^l) = 0$ and (ii) $\sigma_c(\tilde{\mathbf{y}}^l) > 0$.

Conditionality $\sigma_c(\tilde{\mathbf{y}}^l) = 0$. If $\sigma_c(\tilde{\mathbf{y}}^l) = 0$, then $\tilde{\mathbf{y}}_{\alpha,c}^l = \mu_c(\tilde{\mathbf{y}}^l)$, $\forall \mathbf{x}, \alpha$.

Let us then define λ_c such that $\lambda_c = 0$ if $\mu_c(\tilde{\mathbf{y}}^l) = 0$, and $\lambda_c = \frac{\phi(\mu_c(\tilde{\mathbf{y}}^l))}{\mu_c(\tilde{\mathbf{y}}^l)}$ otherwise.

For any choice of positive homogeneous ϕ , it holds that $\phi(0) = 0$. Combined with the definition of λ_c , this implies $\phi(\mu_c(\tilde{\mathbf{y}}^l)) = \lambda_c \mu_c(\tilde{\mathbf{y}}^l)$ and thus $\forall \mathbf{x}, \alpha$:

$$\mathbf{z}_{\alpha,c}^l = \phi(\tilde{\mathbf{y}}_{\alpha,c}^l) = \phi(\mu_c(\tilde{\mathbf{y}}^l)) = \lambda_c \mu_c(\tilde{\mathbf{y}}^l) = \lambda_c \tilde{\mathbf{y}}_{\alpha,c}^l.$$

Given the definition of the linearized post-activations $\tilde{\mathbf{z}}^l$, this means

$$\mathbb{E}_{\mathbf{x},\alpha} \left[(\mathbf{z}_{\alpha,c}^l - \tilde{\mathbf{z}}_{\alpha,c}^l)^2 \right] \leq \mathbb{E}_{\mathbf{x},\alpha} \left[(\mathbf{z}_{\alpha,c}^l - \lambda_c \tilde{\mathbf{y}}_{\alpha,c}^l)^2 \right] = 0.$$

This immediately implies $\forall \mathbf{x}, \alpha: \mathbf{z}_{\alpha,c}^l = \tilde{\mathbf{z}}_{\alpha,c}^l$. Thus, for any $(\phi, H, W, \mathcal{D}, \Theta^l)$ such that $\sigma_c(\tilde{\mathbf{y}}^l) = 0$, it holds that $\forall \mathbf{x}, \alpha: \mathbf{z}_{\alpha,c}^l = \tilde{\mathbf{z}}_{\alpha,c}^l$.

More concisely, it holds for any choice of $(\phi, H, W, \mathcal{D}, \Theta^l)$ that

$$\sigma_c(\tilde{\mathbf{y}}^l) = 0 \implies \mathbf{z}_{\alpha,c}^l = \tilde{\mathbf{z}}_{\alpha,c}^l \quad \forall \mathbf{x}, \alpha. \quad (22)$$

Conditionality $\sigma_c(\tilde{\mathbf{y}}^l) > 0$. We start by fixing $(\phi, H, W, \mathcal{D}, \Theta^l)$. For any given $k > 0$, Chebyshev's inequality implies

$$\begin{aligned} \mathbb{P}_{\mathbf{x},\alpha} \left[|\tilde{\mathbf{y}}_{\alpha,c}^l - \mu_c(\tilde{\mathbf{y}}^l)| \geq k \sigma_c(\tilde{\mathbf{y}}^l) \right] &\leq \frac{1}{k^2}, \\ \mathbb{P}_{\mathbf{x},\alpha} \left[(\tilde{\mathbf{y}}_{\alpha,c}^l - \mu_c(\tilde{\mathbf{y}}^l))^2 \geq k^2 \sigma_c(\tilde{\mathbf{y}}^l)^2 \right] &\leq \frac{1}{k^2}. \end{aligned}$$

Thus, if $\mathcal{P}_c(\tilde{\mathbf{y}}^l) - \mathcal{P}_c^{(1)}(\tilde{\mathbf{y}}^l) \leq \eta \mathcal{P}_c^{(1)}(\tilde{\mathbf{y}}^l)$ for some $\eta > 0$, it holds for any given $k > 0$ that

$$\begin{aligned} 1 - \frac{1}{k^2} &\leq \mathbb{P}_{\mathbf{x},\alpha} \left[(\tilde{\mathbf{y}}_{\alpha,c}^l - \mu_c(\tilde{\mathbf{y}}^l))^2 < k^2 \sigma_c(\tilde{\mathbf{y}}^l)^2 \right] = \mathbb{P}_{\mathbf{x},\alpha} \left[(\tilde{\mathbf{y}}_{\alpha,c}^l - \mu_c(\tilde{\mathbf{y}}^l))^2 < k^2 (\mathcal{P}_c(\tilde{\mathbf{y}}^l) - \mathcal{P}_c^{(1)}(\tilde{\mathbf{y}}^l)) \right] \\ &\leq \mathbb{P}_{\mathbf{x},\alpha} \left[(\tilde{\mathbf{y}}_{\alpha,c}^l - \mu_c(\tilde{\mathbf{y}}^l))^2 < k^2 \eta \mathcal{P}_c^{(1)}(\tilde{\mathbf{y}}^l) \right] = \mathbb{P}_{\mathbf{x},\alpha} \left[(\tilde{\mathbf{y}}_{\alpha,c}^l - \mu_c(\tilde{\mathbf{y}}^l))^2 < k^2 \eta \mu_c(\tilde{\mathbf{y}}^l)^2 \right] \\ &\leq \mathbb{P}_{\mathbf{x},\alpha} \left[|\tilde{\mathbf{y}}_{\alpha,c}^l - \mu_c(\tilde{\mathbf{y}}^l)| < k \sqrt{\eta} |\mu_c(\tilde{\mathbf{y}}^l)| \right]. \end{aligned}$$

Choosing $k = \frac{1}{\sqrt{\eta}}$, we get

$$\mathbb{P}_{\mathbf{x},\alpha} \left[|\tilde{\mathbf{y}}_{\alpha,c}^l - \mu_c(\tilde{\mathbf{y}}^l)| \geq |\mu_c(\tilde{\mathbf{y}}^l)| \right] \leq \eta.$$

Now if we suppose that η is such that $\frac{1}{HW|\mathcal{D}|} > \eta > 0$, we get

$$\mathbb{P}_{\mathbf{x},\alpha} \left[|\tilde{\mathbf{y}}_{\alpha,c}^l - \mu_c(\tilde{\mathbf{y}}^l)| \geq |\mu_c(\tilde{\mathbf{y}}^l)| \right] < \frac{1}{HW|\mathcal{D}|}. \quad (23)$$

Eq. (23) could not hold if there existed $\mathbf{x} \in \mathcal{D}$ and $\alpha \in \{1, \dots, H\} \times \{1, \dots, W\}$ such that $|\tilde{\mathbf{y}}_{\alpha,c}^l - \mu_c(\tilde{\mathbf{y}}^l)| \geq |\mu_c(\tilde{\mathbf{y}}^l)|$. Consequently, $|\tilde{\mathbf{y}}_{\alpha,c}^l - \mu_c(\tilde{\mathbf{y}}^l)| < |\mu_c(\tilde{\mathbf{y}}^l)|$ for all \mathbf{x}, α , implying that there exists a tensor $\mathbf{r}^l \in \mathbb{R}^{H \times W \times C_l}$ with an implicit dependence on \mathbf{x} such that $\forall \mathbf{x}, \alpha$:

$$\tilde{\mathbf{y}}_{\alpha,c}^l = \mathbf{r}_{\alpha,c}^l \mu_c(\tilde{\mathbf{y}}^l), \quad \mathbf{r}_{\alpha,c}^l \geq 0. \quad (24)$$

Now if we combine $\sigma_c(\tilde{\mathbf{y}}^l) > 0$ with $\mathcal{P}_c(\tilde{\mathbf{y}}^l) - \mathcal{P}_c^{(1)}(\tilde{\mathbf{y}}^l) \leq \eta \mathcal{P}_c^{(1)}(\tilde{\mathbf{y}}^l)$, we deduce that $\mathcal{P}_c^{(1)}(\tilde{\mathbf{y}}^l) > 0$ and thus that $\mu_c(\tilde{\mathbf{y}}^l) \neq 0$. Combining this with Eq. (24), we get $\forall \mathbf{x}, \alpha$:

$$\mathbf{z}_{\alpha,c}^l = \phi(\tilde{\mathbf{y}}_{\alpha,c}^l) = \mathbf{r}_{\alpha,c}^l \phi(\mu_c(\tilde{\mathbf{y}}^l)) = \frac{\phi(\mu_c(\tilde{\mathbf{y}}^l))}{\mu_c(\tilde{\mathbf{y}}^l)} \mathbf{r}_{\alpha,c}^l \mu_c(\tilde{\mathbf{y}}^l) = \lambda_c \tilde{\mathbf{y}}_{\alpha,c}^l,$$

with the definition $\lambda_c \equiv \frac{\phi(\mu_c(\tilde{\mathbf{y}}^l))}{\mu_c(\tilde{\mathbf{y}}^l)}$.

Given the definition of the linearized post-activations $\tilde{\mathbf{z}}^l$, this means

$$\mathbb{E}_{\mathbf{x},\alpha} \left[\left(\mathbf{z}_{\alpha,c}^l - \tilde{\mathbf{z}}_{\alpha,c}^l \right)^2 \right] \leq \mathbb{E}_{\mathbf{x},\alpha} \left[\left(\mathbf{z}_{\alpha,c}^l - \lambda_c \tilde{\mathbf{y}}_{\alpha,c}^l \right)^2 \right] = 0.$$

This immediately implies $\forall \mathbf{x}, \alpha$: $\mathbf{z}_{\alpha,c}^l = \tilde{\mathbf{z}}_{\alpha,c}^l$.

Thus, if we fix some $d \in \mathbb{N}^*$ and if we define $\tilde{\eta} = \frac{1}{2d}$, it holds for any choice of $(\phi, H, W, \mathcal{D}, \Theta^l)$ such that (i) $HW|\mathcal{D}| = d$, (ii) $\mathcal{P}_c(\tilde{\mathbf{y}}^l) - \mathcal{P}_c^{(1)}(\tilde{\mathbf{y}}^l) \leq \tilde{\eta} \mathcal{P}_c^{(1)}(\tilde{\mathbf{y}}^l)$, (iii) $\sigma_c(\tilde{\mathbf{y}}^l) > 0$, that $\forall \mathbf{x}, \alpha$: $\mathbf{z}_{\alpha,c}^l = \tilde{\mathbf{z}}_{\alpha,c}^l$.

More concisely, it holds for any choice of $(\phi, H, W, \mathcal{D}, \Theta^l)$ that

$$\left(HW|\mathcal{D}| = d \right) \wedge \left(\mathcal{P}_c(\tilde{\mathbf{y}}^l) - \mathcal{P}_c^{(1)}(\tilde{\mathbf{y}}^l) \leq \tilde{\eta} \mathcal{P}_c^{(1)}(\tilde{\mathbf{y}}^l) \right) \wedge \left(\sigma_c(\tilde{\mathbf{y}}^l) > 0 \right) \implies \mathbf{z}_{\alpha,c}^l = \tilde{\mathbf{z}}_{\alpha,c}^l \quad \forall \mathbf{x}, \alpha. \quad (25)$$

General case. To wrap up, if we fix some $d \in \mathbb{N}^*$ and if we reuse the definition $\tilde{\eta} = \frac{1}{2d}$, it holds for any choice of $(\phi, H, W, \mathcal{D}, \Theta^l)$ that

$$\begin{aligned} & \left(HW|\mathcal{D}| = d \right) \wedge \left(\mathcal{P}_c(\tilde{\mathbf{y}}^l) - \mathcal{P}_c^{(1)}(\tilde{\mathbf{y}}^l) \leq \tilde{\eta} \mathcal{P}_c^{(1)}(\tilde{\mathbf{y}}^l) \right) \\ & \implies \left(\left(HW|\mathcal{D}| = d \right) \wedge \left(\mathcal{P}_c(\tilde{\mathbf{y}}^l) - \mathcal{P}_c^{(1)}(\tilde{\mathbf{y}}^l) \leq \tilde{\eta} \mathcal{P}_c^{(1)}(\tilde{\mathbf{y}}^l) \right) \wedge \left(\sigma_c(\tilde{\mathbf{y}}^l) = 0 \right) \right) \\ & \quad \vee \left(\left(HW|\mathcal{D}| = d \right) \wedge \left(\mathcal{P}_c(\tilde{\mathbf{y}}^l) - \mathcal{P}_c^{(1)}(\tilde{\mathbf{y}}^l) \leq \tilde{\eta} \mathcal{P}_c^{(1)}(\tilde{\mathbf{y}}^l) \right) \wedge \left(\sigma_c(\tilde{\mathbf{y}}^l) > 0 \right) \right) \\ & \implies \left(\mathbf{z}_{\alpha,c}^l = \tilde{\mathbf{z}}_{\alpha,c}^l \quad \forall \mathbf{x}, \alpha \right) \vee \left(\mathbf{z}_{\alpha,c}^l = \tilde{\mathbf{z}}_{\alpha,c}^l \quad \forall \mathbf{x}, \alpha \right) \\ & \implies \left(\mathbf{z}_{\alpha,c}^l = \tilde{\mathbf{z}}_{\alpha,c}^l \quad \forall \mathbf{x}, \alpha \right), \end{aligned} \quad (26)$$

where Eq. (26) is obtained using Eq. (22) and Eq. (25) and \wedge, \vee are the logical “and” and “or”. \square

Proposition 5. If we fix some $d \in \mathbb{N}^*$, there exists $\tilde{\eta} > 0$ such that for any choice of $(\phi, H, W, \mathcal{D}, \Theta^l)$, it holds that

$$\left(HW|\mathcal{D}| = d \right) \wedge \left(\mathcal{P}_c(\tilde{\mathbf{y}}^l) - \mathcal{P}_c^{(1)}(\tilde{\mathbf{y}}^l) \leq \tilde{\eta} \mathcal{P}_c^{(1)}(\tilde{\mathbf{y}}^l) \right) \implies \mathbf{z}_{\alpha,c}^l = \tilde{\mathbf{z}}_{\alpha,c}^l \quad \forall \mathbf{x}, \alpha,$$

where $\tilde{\mathbf{z}}^l$ are the linearized post-activations defined in Eq. (20), (21) and \wedge is the logical “and”.

Proof. We start by noting that for any $1 > \eta > 0$:

$$\begin{aligned} \mathcal{P}_c(\tilde{\mathbf{y}}^l) - \mathcal{P}_c^{(1)}(\tilde{\mathbf{y}}^l) \leq \eta \mathcal{P}_c(\tilde{\mathbf{y}}^l) & \iff \mathcal{P}_c(\tilde{\mathbf{y}}^l) - \mathcal{P}_c^{(1)}(\tilde{\mathbf{y}}^l) \leq \eta \left(\mathcal{P}_c(\tilde{\mathbf{y}}^l) - \mathcal{P}_c^{(1)}(\tilde{\mathbf{y}}^l) + \mathcal{P}_c^{(1)}(\tilde{\mathbf{y}}^l) \right) \\ & \iff \mathcal{P}_c(\tilde{\mathbf{y}}^l) - \mathcal{P}_c^{(1)}(\tilde{\mathbf{y}}^l) \leq \frac{\eta}{1-\eta} \mathcal{P}_c^{(1)}(\tilde{\mathbf{y}}^l). \end{aligned}$$

Thus, if we fix some $d \in \mathbb{N}^*$ and if we define $\tilde{\eta} = \frac{1}{2d}$ and $\tilde{\tilde{\eta}} = \frac{\tilde{\eta}}{1+\tilde{\eta}}$, it holds for any choice of $(\phi, H, W, \mathcal{D}, \Theta^l)$ that

$$\begin{aligned} & \left(HW|\mathcal{D}| = d \right) \wedge \left(\mathcal{P}_c(\tilde{\mathbf{y}}^l) - \mathcal{P}_c^{(1)}(\tilde{\mathbf{y}}^l) \leq \tilde{\eta} \mathcal{P}_c^{(1)}(\tilde{\mathbf{y}}^l) \right) \\ & \iff \left(HW|\mathcal{D}| = d \right) \wedge \left(\mathcal{P}_c(\tilde{\mathbf{y}}^l) - \mathcal{P}_c^{(1)}(\tilde{\mathbf{y}}^l) \leq \frac{\tilde{\eta}}{1-\tilde{\eta}} \mathcal{P}_c^{(1)}(\tilde{\mathbf{y}}^l) \right) \\ & \iff \left(HW|\mathcal{D}| = d \right) \wedge \left(\mathcal{P}_c(\tilde{\mathbf{y}}^l) - \mathcal{P}_c^{(1)}(\tilde{\mathbf{y}}^l) \leq \tilde{\tilde{\eta}} \mathcal{P}_c^{(1)}(\tilde{\mathbf{y}}^l) \right) \\ & \implies \left(\mathbf{z}_{\alpha,c}^l = \tilde{\mathbf{z}}_{\alpha,c}^l \quad \forall \mathbf{x}, \alpha \right), \end{aligned} \quad (27)$$

where Eq. (27) is obtained using Proposition 4 and \wedge is the logical “and”. \square

E Proof of Theorem 1

E.1 Additional notations

Model parameters. We introduce the notations $\theta^l \equiv (\omega^l, \beta^l, \gamma^l)$ for the model parameters at layer l and $\Theta^l \equiv (\omega^1, \beta^1, \gamma^1, \dots, \omega^l, \beta^l, \gamma^l)$ for the aggregated model parameters up to layer l .

Activation tensors. For each layer l , we define the tensors $\hat{\mathbf{z}}^{l-1}, \hat{\mathbf{x}}^l, \hat{\mathbf{y}}^l, \check{\mathbf{y}}^l, \check{\mathbf{z}}^l$ such that $\forall \alpha, c$:

$$\hat{\mathbf{z}}_{\alpha,c}^{l-1} = \sqrt{\frac{\mathcal{P}(\mathbf{z}^{l-1})}{\mathcal{P}_{\mathbf{x}}(\mathbf{z}^{l-1})}} \mathbf{z}_{\alpha,c}^{l-1}, \quad (28)$$

$$\hat{\mathbf{x}}_{\alpha,c}^l = \sqrt{\frac{\mathcal{P}(\mathbf{z}^{l-1})}{\mathcal{P}_{\mathbf{x}}(\mathbf{z}^{l-1})}} \mathbf{x}_{\alpha,c}^l = (\omega^l * \hat{\mathbf{z}}^{l-1})_{\alpha,c}, \quad (29)$$

$$\hat{\mathbf{y}}_{\alpha,c}^l = \frac{1}{\omega \sqrt{\mathcal{P}(\mathbf{z}^{l-1})}} \hat{\mathbf{x}}_{\alpha,c}^l, \quad (30)$$

$$\check{\mathbf{y}}_{\alpha,c}^l = \gamma_c^l \hat{\mathbf{y}}_{\alpha,c}^l + \beta_c^l, \quad (31)$$

$$\check{\mathbf{z}}_{\alpha,c}^l = \phi(\check{\mathbf{y}}_{\alpha,c}^l), \quad (32)$$

with the convention that, if $\mathcal{P}_{\mathbf{x}}(\mathbf{z}^{l-1}) = 0$, then $\forall \alpha, c$: $\hat{\mathbf{z}}_{\alpha,c}^{l-1} = 0$, $\hat{\mathbf{x}}_{\alpha,c}^l = 0$ and if $\mathcal{P}(\mathbf{z}^{l-1}) = 0$, then $\forall \alpha, c$: $\hat{\mathbf{y}}_{\alpha,c}^l = 0$.

Moments. We introduce the notation ϱ for the ratio of the traces of the covariance matrix and Gram matrix of the activation vectors $(\mathbf{y}_{\alpha,1}^l, \dots, \mathbf{y}_{\alpha,C_l}^l)^T$ with respect to the randomness from (\mathbf{x}, α) , i.e.

$$\varrho(\mathbf{y}^l) \equiv \frac{\mathcal{P}(\mathbf{y}^l) - \mathcal{P}^{(1)}(\mathbf{y}^l)}{\mathcal{P}(\mathbf{y}^l)} \leq 1,$$

with the convention that $\varrho(\mathbf{y}^l) = 0$ if $\mathcal{P}(\mathbf{y}^l) = 0$.

Note that with this definition, it holds that

$$\begin{aligned} \varrho(\mathbf{y}^l) = 0 &\implies \left(\mathcal{P}(\mathbf{y}^l) - \mathcal{P}^{(1)}(\mathbf{y}^l) = 0 \right) \vee \left(\mathcal{P}(\mathbf{y}^l) = 0 \right) \\ &\implies \mathcal{P}(\mathbf{y}^l) - \mathcal{P}^{(1)}(\mathbf{y}^l) = 0, \end{aligned} \quad (33)$$

where \vee is the logical “or”.

We extend the definition of the terms $\mathcal{P}_c^{(1)}(\mathbf{y}^l), \mathcal{P}_c^{(2)}(\mathbf{y}^l), \mathcal{P}_c^{(3)}(\mathbf{y}^l), \mathcal{P}_c^{(4)}(\mathbf{y}^l)$ and $\mathcal{P}^{(1)}(\mathbf{y}^l), \mathcal{P}^{(2)}(\mathbf{y}^l), \mathcal{P}^{(3)}(\mathbf{y}^l), \mathcal{P}^{(4)}(\mathbf{y}^l), \varrho(\mathbf{y}^l)$ to all other tensors of layer l , with the implication of Eq. (33) equally holding for all other tensors.

E.2 Required Lemmas

Lemma 1. Fix a layer $l \geq 1$, $\nu_\omega, \nu_\beta, \nu_\gamma, \mathcal{D}$ in Definition 1 and model parameters Θ^{l-1} up to layer $l-1$ such that $\mathcal{P}_{\mathbf{x}}(\mathbf{z}^{l-1}) > 0, \forall \mathbf{x}$. Further suppose Norm = LN and suppose that the convolution of Eq. (2) uses periodic boundary conditions.

Then for any $\eta > 0$ and any $\delta > 0$, there exists $N'(\eta, \delta) \in \mathbb{N}^*$ independent of Θ^{l-1}, l such that if $C_l \geq N'(\eta, \delta)$, it holds for random nets of Definition 1 that

$$\begin{aligned} \mathbb{P}_{\theta_l} \left[|\varrho(\hat{\mathbf{y}}^l) - \varrho(\hat{\mathbf{z}}^{l-1})| \leq \eta \right] &\geq 1 - \delta, \\ \mathbb{P}_{\theta_l} \left[|\varrho(\check{\mathbf{z}}^l) - \rho \chi(\hat{\mathbf{z}}^{l-1}) \varrho(\hat{\mathbf{z}}^{l-1})| \leq \eta \right] &\geq 1 - \delta, \end{aligned}$$

with $\hat{\mathbf{z}}^{l-1}, \hat{\mathbf{y}}^l, \check{\mathbf{z}}^l$ defined in Eq. (28), (30), (32), and with $\rho = \frac{\gamma^2}{\gamma^2 + \beta^2} < 1$ and $\chi(\hat{\mathbf{z}}^{l-1}) \in \mathbb{R}^+$ dependent on Θ^{l-1} but independent of θ^l such that $\chi(\hat{\mathbf{z}}^{l-1}) \leq 1$ in general and $\chi(\hat{\mathbf{z}}^{l-1}) = 1$ if ϕ = identity.

Proof. Let us first note that $\hat{\mathbf{x}}^l = \omega^l * \hat{\mathbf{z}}^{l-1}$. Let us then define $\hat{\mathbf{r}}^{l-1} \in \mathbb{R}^{H \times W \times K_l^2 C_{l-1}}$ the “receptive field” tensor containing at each spatial position $\alpha \in \{1, \dots, H\} \times \{1, \dots, W\}$ the $K_l^2 C_{l-1}$ elements of $\hat{\mathbf{z}}^{l-1}$ belonging to the receptive field of $(\hat{\mathbf{x}}_{\alpha,1}^l, \dots, \hat{\mathbf{x}}_{\alpha,C_l}^l)^T$.

For fixed fan-in element c' originating from channel c , the assumption of periodic boundary conditions implies that $\hat{\mathbf{r}}_{\alpha,c'}^{l-1}$ has the same distribution as $\hat{\mathbf{z}}_{\alpha,c}^{l-1}$ with respect to (\mathbf{x}, α) such that

$$\mathcal{P}_{c'}(\hat{\mathbf{r}}^{l-1}) = \mathcal{P}_c(\hat{\mathbf{z}}^{l-1}), \quad \mathcal{P}_{c'}^{(1)}(\hat{\mathbf{r}}^{l-1}) = \mathcal{P}_c^{(1)}(\hat{\mathbf{z}}^{l-1}).$$

Since the number of fan-in elements c' originating from channel c is equal to K_l^2 for any choice of c , it follows that

$$\mathcal{P}(\hat{\mathbf{r}}^{l-1}) = \mathcal{P}(\hat{\mathbf{z}}^{l-1}), \quad \mathcal{P}^{(1)}(\hat{\mathbf{r}}^{l-1}) = \mathcal{P}^{(1)}(\hat{\mathbf{z}}^{l-1}). \quad (34)$$

Now if we denote $\mathbf{W}^l \in \mathbb{R}^{C_l \times K_l^2 C_{l-1}}$ the reshaped matricial form of ω^l , we may then write $\forall \alpha$: $(\hat{\mathbf{x}}_{\alpha,1}^l, \dots, \hat{\mathbf{x}}_{\alpha,C_l}^l)^T = \mathbf{W}^l (\hat{\mathbf{r}}_{\alpha,1}^{l-1}, \dots, \hat{\mathbf{r}}_{\alpha,K_l^2 C_{l-1}}^{l-1})^T$, such that $\forall c$:

$$\mu_c(\hat{\mathbf{x}}^l) = \mathbb{E}_{\mathbf{x},\alpha} [\hat{\mathbf{x}}_{\alpha,c}^l] = \mathbb{E}_{\mathbf{x},\alpha} \left[\sum_{c'} \mathbf{W}_{cc'}^l \hat{\mathbf{r}}_{\alpha,c'}^{l-1} \right], \quad (35)$$

$$\mathcal{P}_c(\hat{\mathbf{x}}^l) = \mathbb{E}_{\mathbf{x},\alpha} [(\hat{\mathbf{x}}_{\alpha,c}^l)^2] = \mathbb{E}_{\mathbf{x},\alpha} \left[\left(\sum_{c'} \mathbf{W}_{cc'}^l \hat{\mathbf{r}}_{\alpha,c'}^{l-1} \right)^2 \right], \quad (36)$$

$$\mathcal{P}_c^{(1)}(\hat{\mathbf{x}}^l) = \mu_c(\hat{\mathbf{x}}^l)^2 = \mathbb{E}_{\mathbf{x},\alpha} \left[\sum_{c'} \mathbf{W}_{cc'}^l \hat{\mathbf{r}}_{\alpha,c'}^{l-1} \right]^2. \quad (37)$$

Further expanding Eq. (35), (36) and (37), we get $\forall c$:

$$\begin{aligned} \mu_c(\hat{\mathbf{x}}^l) &= \sum_{c'} \mathbf{W}_{cc'}^l \mathbb{E}_{\mathbf{x},\alpha} [\hat{\mathbf{r}}_{\alpha,c'}^{l-1}], \\ \mathcal{P}_c(\hat{\mathbf{x}}^l) &= \sum_{c',c''} \mathbf{W}_{cc'}^l \mathbf{W}_{cc''}^l \mathbb{E}_{\mathbf{x},\alpha} [\hat{\mathbf{r}}_{\alpha,c'}^{l-1} \hat{\mathbf{r}}_{\alpha,c''}^{l-1}], \\ \mathcal{P}_c^{(1)}(\hat{\mathbf{x}}^l) &= \sum_{c',c''} \mathbf{W}_{cc'}^l \mathbf{W}_{cc''}^l \mathbb{E}_{\mathbf{x},\alpha} [\hat{\mathbf{r}}_{\alpha,c'}^{l-1}] \mathbb{E}_{\mathbf{x},\alpha} [\hat{\mathbf{r}}_{\alpha,c''}^{l-1}], \\ \mathcal{P}_c(\hat{\mathbf{x}}^l) - \mathcal{P}_c^{(1)}(\hat{\mathbf{x}}^l) &= \sum_{c',c''} \mathbf{W}_{cc'}^l \mathbf{W}_{cc''}^l \left(\mathbb{E}_{\mathbf{x},\alpha} [\hat{\mathbf{r}}_{\alpha,c'}^{l-1} \hat{\mathbf{r}}_{\alpha,c''}^{l-1}] - \mathbb{E}_{\mathbf{x},\alpha} [\hat{\mathbf{r}}_{\alpha,c'}^{l-1}] \mathbb{E}_{\mathbf{x},\alpha} [\hat{\mathbf{r}}_{\alpha,c''}^{l-1}] \right). \end{aligned}$$

Since the components of $\sqrt{K_l^2 C_{l-1}} \mathbf{W}^l$ are sampled i.i.d. from the fixed distribution ν_ω which is assumed symmetric around zero, we get $\forall c$:

$$\mathbb{E}_{\theta^l} [\mu_c(\hat{\mathbf{x}}^l)] = 0, \quad (38)$$

$$\begin{aligned} \mathbb{E}_{\theta^l} [\mathcal{P}_c(\hat{\mathbf{x}}^l)] &= \sum_{c'} \mathbb{E}_{\theta^l} [(\mathbf{W}_{cc'}^l)^2] \mathbb{E}_{\mathbf{x},\alpha} [(\hat{\mathbf{r}}_{\alpha,c'}^{l-1})^2] \\ &= \sum_{c'} \frac{\omega^2}{K_l^2 C_{l-1}} \mathcal{P}_{c'}(\hat{\mathbf{r}}^{l-1}) \\ &= \omega^2 \mathcal{P}(\hat{\mathbf{z}}^{l-1}), \end{aligned} \quad (39)$$

$$\begin{aligned} \mathbb{E}_{\theta^l} [\mathcal{P}_c(\hat{\mathbf{x}}^l) - \mathcal{P}_c^{(1)}(\hat{\mathbf{x}}^l)] &= \sum_{c'} \mathbb{E}_{\theta^l} [(\mathbf{W}_{cc'}^l)^2] \left(\mathbb{E}_{\mathbf{x},\alpha} [(\hat{\mathbf{r}}_{\alpha,c'}^{l-1})^2] - \mathbb{E}_{\mathbf{x},\alpha} [\hat{\mathbf{r}}_{\alpha,c'}^{l-1}]^2 \right) \\ &= \sum_{c'} \frac{\omega^2}{K_l^2 C_{l-1}} \left(\mathcal{P}_{c'}(\hat{\mathbf{r}}^{l-1}) - \mathcal{P}_{c'}^{(1)}(\hat{\mathbf{r}}^{l-1}) \right) \\ &= \omega^2 \left(\mathcal{P}(\hat{\mathbf{z}}^{l-1}) - \mathcal{P}^{(1)}(\hat{\mathbf{z}}^{l-1}) \right), \end{aligned} \quad (40)$$

where we recall that $\omega \equiv \mathbb{E}_{\theta^l} \left[\left(\sqrt{K_l^2 C_{l-1}} \mathbf{W}_{cc'}^l \right)^2 \right]^{1/2} > 0$ is the L^2 norm (i.e. the root mean square) of $\sqrt{K_l^2 C_{l-1}} \mathbf{W}_{cc'}^l \sim \nu \omega$, and where we used Eq. (34) in Eq. (39) and Eq. (40).

Let us now bound $\mathbb{E}_{\theta^l} [\mu_c(\hat{\mathbf{x}}^l)^2]$ and $\mathbb{E}_{\theta^l} [\mathcal{P}_c(\hat{\mathbf{x}}^l)^2]$, with the aim of bounding $\text{Var}_{\theta^l} [\mu_c(\hat{\mathbf{x}}^l)]$ and $\text{Var}_{\theta^l} [\mathcal{P}_c(\hat{\mathbf{x}}^l)]$. We start by expanding $\mu_c(\hat{\mathbf{x}}^l)^2$ and $\mathcal{P}_c(\hat{\mathbf{x}}^l)^2$ as

$$\begin{aligned} \mu_c(\hat{\mathbf{x}}^l)^2 &= \sum_{c', c''} \mathbf{W}_{cc'}^l \mathbf{W}_{cc''}^l \mathbb{E}_{\mathbf{x}, \alpha} [\hat{\mathbf{r}}_{\alpha, c'}^{l-1}] \mathbb{E}_{\mathbf{x}, \alpha} [\hat{\mathbf{r}}_{\alpha, c''}^{l-1}], \\ \mathcal{P}_c(\hat{\mathbf{x}}^l)^2 &= \left(\sum_{c'} (\mathbf{W}_{cc'}^l)^2 \mathbb{E}_{\mathbf{x}, \alpha} [\hat{\mathbf{r}}_{\alpha, c'}^{l-1}] + \sum_{c'} \sum_{c'' \neq c'} \mathbf{W}_{cc'}^l \mathbf{W}_{cc''}^l \mathbb{E}_{\mathbf{x}, \alpha} [\hat{\mathbf{r}}_{\alpha, c'}^{l-1} \hat{\mathbf{r}}_{\alpha, c''}^{l-1}] \right)^2 \\ &= \left(\sum_{c'} (\mathbf{W}_{cc'}^l)^2 \mathbb{E}_{\mathbf{x}, \alpha} [\hat{\mathbf{r}}_{\alpha, c'}^{l-1}] + 2 \sum_{c'} \sum_{c'' < c'} \mathbf{W}_{cc'}^l \mathbf{W}_{cc''}^l \mathbb{E}_{\mathbf{x}, \alpha} [\hat{\mathbf{r}}_{\alpha, c'}^{l-1} \hat{\mathbf{r}}_{\alpha, c''}^{l-1}] \right)^2. \end{aligned}$$

When taking the expectation over θ^l , only terms in $(\mathbf{W}_{cc'}^l)^4$, $(\mathbf{W}_{cc'}^l)^2 (\mathbf{W}_{cc''}^l)^2$ and $(\mathbf{W}_{cc'}^l)^2$ remain.

For $\mathbb{E}_{\theta^l} [\mu_c(\hat{\mathbf{x}}^l)^2]$, we then get

$$\begin{aligned} \mathbb{E}_{\theta^l} [\mu_c(\hat{\mathbf{x}}^l)^2] &= \sum_{c'} \mathbb{E}_{\theta^l} [(\mathbf{W}_{cc'}^l)^2] \mathbb{E}_{\mathbf{x}, \alpha} [\hat{\mathbf{r}}_{\alpha, c'}^{l-1}]^2 \\ &= \sum_{c'} \frac{\omega^2}{K_l^2 C_{l-1}} \mu_{c'}(\hat{\mathbf{r}}^{l-1})^2 \\ &= \sum_{c'} \frac{\omega^2}{K_l^2 C_{l-1}} \mathcal{P}_{c'}^{(1)}(\hat{\mathbf{r}}^{l-1}) \\ &= \omega^2 \mathcal{P}^{(1)}(\hat{\mathbf{r}}^{l-1}) \\ &\leq \omega^2 \mathcal{P}(\hat{\mathbf{r}}^{l-1}) \\ &\leq \omega^2 \mathcal{P}(\hat{\mathbf{z}}^{l-1}), \end{aligned} \tag{41}$$

where Eq. (41) is obtained using Eq. (34).

And for $\mathbb{E}_{\theta^l} [\mathcal{P}_c(\hat{\mathbf{x}}^l)^2]$, we get

$$\begin{aligned} \mathbb{E}_{\theta^l} [\mathcal{P}_c(\hat{\mathbf{x}}^l)^2] &= \mathbb{E}_{\theta^l} \left[\left(\sum_{c'} (\mathbf{W}_{cc'}^l)^2 \mathbb{E}_{\mathbf{x}, \alpha} [\hat{\mathbf{r}}_{\alpha, c'}^{l-1}] \right)^2 + 4 \sum_{c'} \sum_{c'' < c'} (\mathbf{W}_{cc'}^l)^2 (\mathbf{W}_{cc''}^l)^2 \mathbb{E}_{\mathbf{x}, \alpha} [\hat{\mathbf{r}}_{\alpha, c'}^{l-1} \hat{\mathbf{r}}_{\alpha, c''}^{l-1}]^2 \right] \\ &\leq \mathbb{E}_{\theta^l} \left[\left(\sum_{c'} (\mathbf{W}_{cc'}^l)^2 \mathcal{P}_{c'}(\hat{\mathbf{r}}^{l-1}) \right)^2 + 4 \sum_{c'} \sum_{c'' < c'} (\mathbf{W}_{cc'}^l)^2 (\mathbf{W}_{cc''}^l)^2 \mathcal{P}_{c'}(\hat{\mathbf{r}}^{l-1}) \mathcal{P}_{c''}(\hat{\mathbf{r}}^{l-1}) \right] \tag{42} \\ &\leq \mathbb{E}_{\theta^l} \left[\sum_{c'} (\mathbf{W}_{cc'}^l)^4 \mathcal{P}_{c'}(\hat{\mathbf{r}}^{l-1})^2 + 6 \sum_{c'} \sum_{c'' < c'} (\mathbf{W}_{cc'}^l)^2 (\mathbf{W}_{cc''}^l)^2 \mathcal{P}_{c'}(\hat{\mathbf{r}}^{l-1}) \mathcal{P}_{c''}(\hat{\mathbf{r}}^{l-1}) \right] \\ &\leq \sum_{c'} \mathbb{E}_{\theta^l} [(\mathbf{W}_{cc'}^l)^4] \mathcal{P}_{c'}(\hat{\mathbf{r}}^{l-1})^2 + 3 \sum_{c'} \sum_{c'' \neq c'} \mathbb{E}_{\theta^l} [(\mathbf{W}_{cc'}^l)^2 (\mathbf{W}_{cc''}^l)^2] \mathcal{P}_{c'}(\hat{\mathbf{r}}^{l-1}) \mathcal{P}_{c''}(\hat{\mathbf{r}}^{l-1}) \\ &\leq \sum_{c'} \mathbb{E}_{\theta^l} [(\mathbf{W}_{cc'}^l)^4] \mathcal{P}_{c'}(\hat{\mathbf{r}}^{l-1})^2 + 3 \sum_{c'} \sum_{c'' \neq c'} \mathbb{E}_{\theta^l} [(\mathbf{W}_{cc'}^l)^4] \mathcal{P}_{c'}(\hat{\mathbf{r}}^{l-1}) \mathcal{P}_{c''}(\hat{\mathbf{r}}^{l-1}) \end{aligned} \tag{43}$$

where Eq. (42) and Eq. (43) are obtained using Cauchy-Schwarz inequality combined with $\mathbb{E}_{\mathbf{x}, \alpha} [\hat{\mathbf{r}}_{\alpha, c'}^{l-1}]^2 = \mathcal{P}_{c'}(\hat{\mathbf{r}}^{l-1})$ and $\mathbb{E}_{\mathbf{x}, \alpha} [\hat{\mathbf{r}}_{\alpha, c'}^{l-1} \hat{\mathbf{r}}_{\alpha, c''}^{l-1}] = \mathcal{P}_{c''}(\hat{\mathbf{r}}^{l-1})$.

We may process Eq. (43) further to get

$$\begin{aligned}
\mathbb{E}_{\theta^l} [\mathcal{P}_c(\hat{\mathbf{x}}^l)^2] &\leq 3 \sum_{c'} \mathbb{E}_{\theta^l} [(\mathbf{W}_{cc'}^l)^4] \mathcal{P}_{c'}(\hat{\mathbf{r}}^{l-1})^2 + 3 \sum_{c'} \sum_{c'' \neq c'} \mathbb{E}_{\theta^l} [(\mathbf{W}_{cc'}^l)^4] \mathcal{P}_{c'}(\hat{\mathbf{r}}^{l-1}) \mathcal{P}_{c''}(\hat{\mathbf{r}}^{l-1}) \\
&\leq 3 \sum_{c', c''} \mathbb{E}_{\theta^l} [(\mathbf{W}_{cc'}^l)^4] \mathcal{P}_{c'}(\hat{\mathbf{r}}^{l-1}) \mathcal{P}_{c''}(\hat{\mathbf{r}}^{l-1}) \\
&\leq 3 \mathbb{E}_{\theta^l} [(\mathbf{W}_{c,c'}^l)^4] (K_l^2 C_{l-1})^2 \mathcal{P}(\hat{\mathbf{r}}^{l-1})^2 \\
&\leq 3 \mathbb{E}_{\theta^l} \left[\left(\sqrt{K_l^2 C_{l-1}} \mathbf{W}_{c,c'}^l \right)^4 \right] \mathcal{P}(\hat{\mathbf{z}}^{l-1})^2 \\
&\leq 3 \tilde{\omega}^4 \mathcal{P}(\hat{\mathbf{z}}^{l-1})^2,
\end{aligned} \tag{44}$$

where $\tilde{\omega} \equiv \mathbb{E}_{\theta^l} \left[\left(\sqrt{K_l^2 C_{l-1}} \mathbf{W}_{c,c'}^l \right)^4 \right]^{1/4} \geq \omega > 0$ is the L^4 norm of $\sqrt{K_l^2 C_{l-1}} \mathbf{W}_{c,c'}^l \sim \nu_\omega$.

Now we turn to $\hat{\mathbf{y}}^l$ and $\hat{\mathbf{y}}^l$ defined in Eq. (30) and Eq. (31).

Due to $\mu_c(\hat{\mathbf{y}}^l) = \frac{1}{w\sqrt{\mathcal{P}(\hat{\mathbf{z}}^{l-1})}} \mu_c(\hat{\mathbf{x}}^l)$, $\mathcal{P}_c(\hat{\mathbf{y}}^l) = \frac{1}{w^2 \mathcal{P}(\hat{\mathbf{z}}^{l-1})} \mathcal{P}_c(\hat{\mathbf{x}}^l)$ and $\mathcal{P}_c^{(1)}(\hat{\mathbf{y}}^l) = \frac{1}{w^2 \mathcal{P}(\hat{\mathbf{z}}^{l-1})} \mathcal{P}_c^{(1)}(\hat{\mathbf{x}}^l)$

and due to $\mathcal{P}(\hat{\mathbf{z}}^{l-1}) = \mathcal{P}(\mathbf{z}^{l-1}) \mathbb{E}_{\mathbf{x}} \left[\frac{1}{\mathcal{P}_{\mathbf{x}}(\mathbf{z}^{l-1})} \mathcal{P}_{\mathbf{x}}(\mathbf{z}^{l-1}) \right] = \mathcal{P}(\mathbf{z}^{l-1})$, Eq. (38), (39) and (40) imply

$$\begin{aligned}
\mathbb{E}_{\theta^l} [\mu_c(\hat{\mathbf{y}}^l)] &= 0, \\
\mathbb{E}_{\theta^l} [\mathcal{P}_c(\hat{\mathbf{y}}^l)] &= 1,
\end{aligned} \tag{45}$$

$$\mathbb{E}_{\theta^l} [\mathcal{P}_c(\hat{\mathbf{y}}^l) - \mathcal{P}_c^{(1)}(\hat{\mathbf{y}}^l)] = \frac{\mathcal{P}(\hat{\mathbf{z}}^{l-1}) - \mathcal{P}^{(1)}(\hat{\mathbf{z}}^{l-1})}{\mathcal{P}(\hat{\mathbf{z}}^{l-1})} = \varrho(\hat{\mathbf{z}}^{l-1}). \tag{46}$$

Using Eq. (41) and Eq. (44), we further get

$$\begin{aligned}
\text{Var}_{\theta^l} [\mu_c(\hat{\mathbf{y}}^l)] &= \mathbb{E}_{\theta^l} [\mu_c(\hat{\mathbf{y}}^l)^2] \leq 1, \\
\text{Var}_{\theta^l} [\mathcal{P}_c(\hat{\mathbf{y}}^l)] &\leq \mathbb{E}_{\theta^l} [\mathcal{P}_c(\hat{\mathbf{y}}^l)^2] \leq 3 \tilde{\omega}^4 \omega^{-4}, \\
\text{Var}_{\theta^l} [\mathcal{P}_c(\hat{\mathbf{y}}^l) - \mathcal{P}_c^{(1)}(\hat{\mathbf{y}}^l)] &\leq \mathbb{E}_{\theta^l} [(\mathcal{P}_c(\hat{\mathbf{y}}^l) - \mathcal{P}_c^{(1)}(\hat{\mathbf{y}}^l))^2] \leq \mathbb{E}_{\theta^l} [\mathcal{P}_c(\hat{\mathbf{y}}^l)^2] \leq 3 \tilde{\omega}^4 \omega^{-4}.
\end{aligned} \tag{47}$$

The terms $\mu_c(\hat{\mathbf{y}}^l)$, $\mathcal{P}_c(\hat{\mathbf{y}}^l)$ and $\mathcal{P}_c(\hat{\mathbf{y}}^l) - \mathcal{P}_c^{(1)}(\hat{\mathbf{y}}^l)$ being i.i.d. with respect to θ^l in the different channels c , we get

$$\mathbb{E}_{\theta^l} [\mu(\hat{\mathbf{y}}^l)] = 0, \quad \text{Var}_{\theta^l} [\mu(\hat{\mathbf{y}}^l)] \leq \frac{1}{C_l}, \tag{48}$$

$$\mathbb{E}_{\theta^l} [\mathcal{P}(\hat{\mathbf{y}}^l)] = 1, \quad \text{Var}_{\theta^l} [\mathcal{P}(\hat{\mathbf{y}}^l)] \leq \frac{3 \tilde{\omega}^4 \omega^{-4}}{C_l}, \tag{49}$$

$$\mathbb{E}_{\theta^l} [\mathcal{P}(\hat{\mathbf{y}}^l) - \mathcal{P}^{(1)}(\hat{\mathbf{y}}^l)] = \varrho(\hat{\mathbf{z}}^{l-1}), \quad \text{Var}_{\theta^l} [\mathcal{P}(\hat{\mathbf{y}}^l) - \mathcal{P}^{(1)}(\hat{\mathbf{y}}^l)] \leq \frac{3 \tilde{\omega}^4 \omega^{-4}}{C_l}. \tag{50}$$

Combining Eq. (49) and Eq. (50) with Chebyshev's inequality, we get for any $1 \geq \eta > 0$ that

$$\begin{aligned}
\mathbb{P}_{\theta^l} \left[|\mathcal{P}(\hat{\mathbf{y}}^l) - 1| > \frac{\eta}{1+\eta} \right] &\leq \left(\frac{1+\eta}{\eta} \right)^2 \frac{3 \tilde{\omega}^4 \omega^{-4}}{C_l}, \\
\mathbb{P}_{\theta^l} \left[|\mathcal{P}(\hat{\mathbf{y}}^l) - 1| > \frac{\eta}{1-\eta} \right] &\leq \left(\frac{1-\eta}{\eta} \right)^2 \frac{3 \tilde{\omega}^4 \omega^{-4}}{C_l}, \\
\mathbb{P}_{\theta^l} \left[\left| \mathcal{P}(\hat{\mathbf{y}}^l) - \mathcal{P}^{(1)}(\hat{\mathbf{y}}^l) - \varrho(\hat{\mathbf{z}}^{l-1}) \right| > \eta \right] &\leq \left(\frac{1}{\eta} \right)^2 \frac{3 \tilde{\omega}^4 \omega^{-4}}{C_l}.
\end{aligned}$$

Thus, for any $1 > \eta > 0$ and any $\delta > 0$, there exists $N_1(\eta, \delta) \in \mathbb{N}^*$ independent of Θ^{l-1} , l , such that if $C_l \geq N_1(\eta, \delta)$, it holds that

$$\begin{aligned}\mathbb{P}_{\theta^l} \left[\mathcal{P}(\hat{\mathbf{y}}^l) \geq \frac{1}{1+\eta} \right] &\geq \mathbb{P}_{\theta^l} \left[|\mathcal{P}(\hat{\mathbf{y}}^l) - 1| \leq \frac{\eta}{1+\eta} \right] \geq 1 - \delta, \\ \mathbb{P}_{\theta^l} \left[\mathcal{P}(\hat{\mathbf{y}}^l) \leq \frac{1}{1-\eta} \right] &\geq \mathbb{P}_{\theta^l} \left[|\mathcal{P}(\hat{\mathbf{y}}^l) - 1| \leq \frac{\eta}{1-\eta} \right] \geq 1 - \delta, \\ \mathbb{P}_{\theta^l} \left[|\mathcal{P}(\hat{\mathbf{y}}^l) - \mathcal{P}^{(1)}(\hat{\mathbf{y}}^l) - \varrho(\hat{\mathbf{z}}^{l-1})| \leq \eta \right] &\geq 1 - \delta.\end{aligned}$$

Thus, if $C_l \geq N_1(\eta, \delta)$, it holds with probability greater than $1 - 3\delta$ with respect to θ^l that (i) $(1 + \eta)\mathcal{P}(\hat{\mathbf{y}}^l) \geq 1$, (ii) $(1 - \eta)\mathcal{P}(\hat{\mathbf{y}}^l) \leq 1$, (iii) $|\mathcal{P}(\hat{\mathbf{y}}^l) - \mathcal{P}^{(1)}(\hat{\mathbf{y}}^l) - \varrho(\hat{\mathbf{z}}^{l-1})| \leq \eta$, implying

$$\begin{aligned}\mathcal{P}(\hat{\mathbf{y}}^l) - \mathcal{P}^{(1)}(\hat{\mathbf{y}}^l) &\leq \varrho(\hat{\mathbf{z}}^{l-1}) + \eta \\ &\leq (\varrho(\hat{\mathbf{z}}^{l-1}) + \eta)(1 + \eta)\mathcal{P}(\hat{\mathbf{y}}^l) \\ &\leq (\varrho(\hat{\mathbf{z}}^{l-1}) + \varrho(\hat{\mathbf{z}}^{l-1})\eta + \eta + \eta^2)\mathcal{P}(\hat{\mathbf{y}}^l) \\ &\leq (\varrho(\hat{\mathbf{z}}^{l-1}) + 3\eta)\mathcal{P}(\hat{\mathbf{y}}^l), \\ \mathcal{P}(\hat{\mathbf{y}}^l) - \mathcal{P}^{(1)}(\hat{\mathbf{y}}^l) &\geq \varrho(\hat{\mathbf{z}}^{l-1}) - \eta \\ &\geq \max(0, \varrho(\hat{\mathbf{z}}^{l-1}) - \eta) \\ &\geq \max(0, \varrho(\hat{\mathbf{z}}^{l-1}) - \eta)(1 - \eta)\mathcal{P}(\hat{\mathbf{y}}^l) \\ &\geq \max(0, (\varrho(\hat{\mathbf{z}}^{l-1}) - \eta)(1 - \eta)\mathcal{P}(\hat{\mathbf{y}}^l)) \\ &\geq (\varrho(\hat{\mathbf{z}}^{l-1}) - \eta)(1 - \eta)\mathcal{P}(\hat{\mathbf{y}}^l) \\ &\geq (\varrho(\hat{\mathbf{z}}^{l-1}) - \varrho(\hat{\mathbf{z}}^{l-1})\eta - \eta + \eta^2)\mathcal{P}(\hat{\mathbf{y}}^l) \\ &\geq (\varrho(\hat{\mathbf{z}}^{l-1}) - 2\eta)\mathcal{P}(\hat{\mathbf{y}}^l)\end{aligned}$$

where we used $\varrho(\hat{\mathbf{z}}^{l-1}) \leq 1$ and $\eta^2 \leq \eta$ due to $\eta < 1$, as well as $\mathcal{P}(\hat{\mathbf{y}}^l) - \mathcal{P}^{(1)}(\hat{\mathbf{y}}^l) \geq 0$.

Given that $(1 + \eta)\mathcal{P}(\hat{\mathbf{y}}^l) \geq 1 \implies \mathcal{P}(\hat{\mathbf{y}}^l) > 0$, it follows that if $C_l \geq N_1(\eta, \delta)$, it holds with probability greater than $1 - 3\delta$ with respect to θ^l that

$$\varrho(\hat{\mathbf{z}}^{l-1}) - 2\eta \leq \varrho(\hat{\mathbf{y}}^l) \leq \varrho(\hat{\mathbf{z}}^{l-1}) + 3\eta \implies |\varrho(\hat{\mathbf{y}}^l) - \varrho(\hat{\mathbf{z}}^{l-1})| \leq 3\eta.$$

Now, let N_2 be defined independently of Θ^{l-1} , l by $N_2(\eta, \delta) = N_1\left(\min\left(\frac{\eta}{3}, \frac{1}{2}\right), \frac{\delta}{3}\right)$, $\forall \eta > 0$, $\forall \delta > 0$. Then for any $\eta > 0$ and any $\delta > 0$, if $C_l \geq N_2(\eta, \delta)$, it holds that

$$\begin{aligned}\mathbb{P}_{\theta^l} \left[|\varrho(\hat{\mathbf{y}}^l) - \varrho(\hat{\mathbf{z}}^{l-1})| \leq \eta \right] &\geq \mathbb{P}_{\theta^l} \left[|\varrho(\hat{\mathbf{y}}^l) - \varrho(\hat{\mathbf{z}}^{l-1})| \leq 3 \min\left(\frac{\eta}{3}, \frac{1}{2}\right) \right] \\ &\geq 1 - 3\frac{\delta}{3} = 1 - \delta.\end{aligned}\tag{51}$$

Let us apply a similar approach with respect to $\check{\mathbf{z}}^l$, first noting that $\forall \alpha, c$:

$$\begin{aligned}(\check{\mathbf{y}}_{\alpha,c}^l)^2 &= \left(\gamma_c^l \hat{\mathbf{y}}_{\alpha,c}^l + \beta_c^l\right)^2 = (\gamma_c^l)^2 (\hat{\mathbf{y}}_{\alpha,c}^l)^2 + (\beta_c^l)^2 + 2\gamma_c^l \beta_c^l \hat{\mathbf{y}}_{\alpha,c}^l, \\ \mathcal{P}_c(\check{\mathbf{y}}^l) &= (\gamma_c^l)^2 \mathcal{P}_c(\hat{\mathbf{y}}^l) + (\beta_c^l)^2 + 2\gamma_c^l \beta_c^l \mu_c(\hat{\mathbf{y}}^l), \\ \mathbb{E}_{\theta^l} \left[\mathcal{P}_c(\check{\mathbf{y}}^l) \right] &= \mathbb{E}_{\theta^l} \left[(\gamma_c^l)^2 \mathcal{P}_c(\hat{\mathbf{y}}^l) + (\beta_c^l)^2 \right] = \gamma^2 \mathbb{E}_{\theta^l} \left[\mathcal{P}_c(\hat{\mathbf{y}}^l) \right] + \beta^2,\end{aligned}\tag{52}$$

where we recall that γ, β are the L^2 norms (i.e. the root mean squares) of $\gamma_c^l \sim \nu_\gamma$ and $\beta_c^l \sim \nu_\beta$, and where we used the fact that γ_c^l is independent from $\mathcal{P}_c(\hat{\mathbf{y}}^l)$ with respect to θ^l , while β_c^l is independent from $\gamma_c^l \mu_c(\hat{\mathbf{y}}^l)$ with respect to θ^l , with the distribution of β_c^l symmetric around zero.

At the same time, $\forall \alpha, c$:

$$\begin{aligned} \left(\tilde{\mathbf{y}}_{\alpha,c}^l - \mu_c(\tilde{\mathbf{y}}^l)\right)^2 &= \left(\gamma_c^l \tilde{\mathbf{y}}_{\alpha,c}^l + \beta_c^l - (\gamma_c^l \mu_c(\tilde{\mathbf{y}}^l) + \beta_c^l)\right)^2 = (\gamma_c^l)^2 \left(\tilde{\mathbf{y}}_{\alpha,c}^l - \mu_c(\tilde{\mathbf{y}}^l)\right)^2, \\ \mathcal{P}_c(\tilde{\mathbf{y}}^l) - \mathcal{P}_c^{(1)}(\tilde{\mathbf{y}}^l) &= (\gamma_c^l)^2 \left(\mathcal{P}_c(\hat{\mathbf{y}}^l) - \mathcal{P}_c^{(1)}(\hat{\mathbf{y}}^l)\right), \\ \mathbb{E}_{\theta^l} \left[\mathcal{P}_c(\tilde{\mathbf{y}}^l) - \mathcal{P}_c^{(1)}(\tilde{\mathbf{y}}^l)\right] &= \gamma^2 \mathbb{E}_{\theta^l} \left[\mathcal{P}_c(\hat{\mathbf{y}}^l) - \mathcal{P}_c^{(1)}(\hat{\mathbf{y}}^l)\right], \end{aligned} \quad (53)$$

where we used the fact that γ_c^l is independent from $\mathcal{P}_c(\hat{\mathbf{y}}^l) - \mathcal{P}_c^{(1)}(\hat{\mathbf{y}}^l)$ with respect to θ^l .

Using Eq. (45) and Eq. (46), Eq. (52) and Eq. (53) imply that $\forall c$:

$$\mathbb{E}_{\theta^l} \left[\mathcal{P}_c(\tilde{\mathbf{y}}^l)\right] = \gamma^2 + \beta^2, \quad (54)$$

$$\mathbb{E}_{\theta^l} \left[\mathcal{P}_c(\tilde{\mathbf{y}}^l) - \mathcal{P}_c^{(1)}(\tilde{\mathbf{y}}^l)\right] = \gamma^2 \varrho(\hat{\mathbf{z}}^{l-1}). \quad (55)$$

We then get

$$\mathbb{E}_{\theta^l} \left[\mathcal{P}(\tilde{\mathbf{y}}^l)\right] = \gamma^2 + \beta^2, \quad (56)$$

$$\mathbb{E}_{\theta^l} \left[\mathcal{P}(\tilde{\mathbf{y}}^l) - \mathcal{P}^{(1)}(\tilde{\mathbf{y}}^l)\right] = \gamma^2 \varrho(\hat{\mathbf{z}}^{l-1}). \quad (57)$$

Now, we may bound $\mathbb{E}_{\theta^l} \left[\mathcal{P}_c(\tilde{\mathbf{y}}^l)^2\right]$ using $\forall \alpha, c$:

$$\begin{aligned} (\tilde{\mathbf{y}}_{\alpha,c}^l)^2 &= \left(\gamma_c^l \tilde{\mathbf{y}}_{\alpha,c}^l + \beta_c^l\right)^2 \leq 2 \left((\gamma_c^l)^2 (\tilde{\mathbf{y}}_{\alpha,c}^l)^2 + (\beta_c^l)^2\right), \\ \mathcal{P}_c(\tilde{\mathbf{y}}^l) &\leq 2 \left((\gamma_c^l)^2 \mathcal{P}_c(\hat{\mathbf{y}}^l) + (\beta_c^l)^2\right), \\ \mathcal{P}_c(\tilde{\mathbf{y}}^l)^2 &\leq 8 \left((\gamma_c^l)^4 \mathcal{P}_c(\hat{\mathbf{y}}^l)^2 + (\beta_c^l)^4\right), \\ \mathbb{E}_{\theta^l} \left[\mathcal{P}_c(\tilde{\mathbf{y}}^l)^2\right] &\leq 8 \left(\tilde{\gamma}^4 \mathbb{E}_{\theta^l} \left[\mathcal{P}_c(\hat{\mathbf{y}}^l)^2\right] + \tilde{\beta}^4\right), \end{aligned} \quad (58)$$

where we defined $\tilde{\gamma} \equiv \mathbb{E}_{\theta^l} \left[(\gamma_c^l)^4\right]^{1/4} > \gamma > 0$ and $\tilde{\beta} \equiv \mathbb{E}_{\theta^l} \left[(\beta_c^l)^4\right]^{1/4} > \beta > 0$ the L^4 norms of $\gamma_c^l \sim \nu_\gamma$ and $\beta_c^l \sim \nu_\beta$, and we used twice $(a+b)^2 \leq 2(a^2 + b^2)$, $\forall a, b$.

Using Eq. (47), we then get $\forall c$:

$$\mathbb{E}_{\theta^l} \left[\mathcal{P}_c(\tilde{\mathbf{y}}^l)^2\right] \leq 24\tilde{\gamma}^4 \tilde{\omega}^4 \omega^{-4} + 8\tilde{\beta}^4. \quad (59)$$

Next, we consider $\hat{\mathbf{z}}^l$. We adopt the notations $\tilde{\mathbf{y}}^{l,+}$, $\tilde{\mathbf{y}}^{l,-}$ for the positive and negative parts of $\tilde{\mathbf{y}}^l$ such that $\forall \alpha, c$:

$$\tilde{\mathbf{y}}_{\alpha,c}^{l,+} = \max(\tilde{\mathbf{y}}_{\alpha,c}^l, 0), \quad \tilde{\mathbf{y}}_{\alpha,c}^{l,-} = \max(-\tilde{\mathbf{y}}_{\alpha,c}^l, 0). \quad (60)$$

The positive homogeneity of ϕ implies that $\forall \alpha, c$:

$$\hat{\mathbf{z}}_{\alpha,c}^l = \phi(\tilde{\mathbf{y}}_{\alpha,c}^l) = \phi(1) \cdot \tilde{\mathbf{y}}_{\alpha,c}^{l,+} + \phi(-1) \cdot \tilde{\mathbf{y}}_{\alpha,c}^{l,-}, \quad (\hat{\mathbf{z}}_{\alpha,c}^l)^2 = \phi(1)^2 \cdot (\tilde{\mathbf{y}}_{\alpha,c}^{l,+})^2 + \phi(-1)^2 \cdot (\tilde{\mathbf{y}}_{\alpha,c}^{l,-})^2.$$

For any c , this implies for $\mu_c(\hat{\mathbf{z}}^l)^2$ and $\mathcal{P}_c(\hat{\mathbf{z}}^l)$ that

$$\begin{aligned} \mu_c(\hat{\mathbf{z}}^l)^2 &= \left(\phi(1) \mathbb{E}_{\mathbf{x},\alpha} [\tilde{\mathbf{y}}_{\alpha,c}^{l,+}] + \phi(-1) \mathbb{E}_{\mathbf{x},\alpha} [\tilde{\mathbf{y}}_{\alpha,c}^{l,-}]\right)^2 \\ &= \left(\phi(1) \mu_c(\tilde{\mathbf{y}}^{l,+}) + \phi(-1) \mu_c(\tilde{\mathbf{y}}^{l,-})\right)^2 \\ &= \phi(1)^2 \mu_c(\tilde{\mathbf{y}}^{l,+})^2 + \phi(-1)^2 \mu_c(\tilde{\mathbf{y}}^{l,-})^2 + 2\phi(1)\phi(-1) \mu_c(\tilde{\mathbf{y}}^{l,+}) \mu_c(\tilde{\mathbf{y}}^{l,-}), \\ \mathcal{P}_c(\hat{\mathbf{z}}^l) &= \mathbb{E}_{\mathbf{x},\alpha} \left[\phi(1)^2 (\tilde{\mathbf{y}}_{\alpha,c}^{l,+})^2 + \phi(-1)^2 (\tilde{\mathbf{y}}_{\alpha,c}^{l,-})^2\right] \\ &= \phi(1)^2 \mathcal{P}_c(\tilde{\mathbf{y}}^{l,+}) + \phi(-1)^2 \mathcal{P}_c(\tilde{\mathbf{y}}^{l,-}). \end{aligned} \quad (61)$$

As for $\check{\mathbf{y}}^l$, we have $\forall \alpha, c$:

$$\check{\mathbf{y}}_{\alpha,c}^l = \check{\mathbf{y}}_{\alpha,c}^{l,+} - \check{\mathbf{y}}_{\alpha,c}^{l,-}, \quad (\check{\mathbf{y}}_{\alpha,c}^l)^2 = (\check{\mathbf{y}}_{\alpha,c}^{l,+})^2 + (\check{\mathbf{y}}_{\alpha,c}^{l,-})^2.$$

For any c , this implies for $\mu_c(\check{\mathbf{y}}^l)^2$ and $\mathcal{P}_c(\check{\mathbf{y}}^l)$ that

$$\begin{aligned} \mu_c(\check{\mathbf{y}}^l)^2 &= \left(\mathbb{E}_{\mathbf{x},\alpha}[\check{\mathbf{y}}_{\alpha,c}^{l,+}] - \mathbb{E}_{\mathbf{x},\alpha}[\check{\mathbf{y}}_{\alpha,c}^{l,-}] \right)^2 \\ &= \left(\mu_c(\check{\mathbf{y}}^{l,+}) - \mu_c(\check{\mathbf{y}}^{l,-}) \right)^2 \\ &= \mu_c(\check{\mathbf{y}}^{l,+})^2 + \mu_c(\check{\mathbf{y}}^{l,-})^2 - 2\mu_c(\check{\mathbf{y}}^{l,+})\mu_c(\check{\mathbf{y}}^{l,-}) \end{aligned} \quad (62)$$

$$\begin{aligned} \mathcal{P}_c(\check{\mathbf{y}}^l) &= \mathbb{E}_{\mathbf{x},\alpha} \left[(\check{\mathbf{y}}_{\alpha,c}^{l,+})^2 + (\check{\mathbf{y}}_{\alpha,c}^{l,-})^2 \right] \\ &= \mathcal{P}_c(\check{\mathbf{y}}^{l,+}) + \mathcal{P}_c(\check{\mathbf{y}}^{l,-}). \end{aligned} \quad (63)$$

At this point, we note that $\hat{\mathbf{y}}^l$ and $-\hat{\mathbf{y}}^l$ have the same distribution with respect to θ^l by symmetry around zero of ν_ω . From this and the symmetry around zero of ν_β , we deduce that $\check{\mathbf{y}}^l$ and $-\check{\mathbf{y}}^l$ have the same distribution with respect to θ^l . In turn, this implies that $\check{\mathbf{y}}^{l,+}$ and $\check{\mathbf{y}}^{l,-}$ have the same distribution with respect to θ^l .

We deduce that $\forall c$:

$$\begin{aligned} \mathbb{E}_{\theta^l} \left[\mu_c(\check{\mathbf{z}}^l)^2 \right] &= \left(\phi(1)^2 + \phi(-1)^2 \right) \mathbb{E}_{\theta^l} \left[\mu_c(\check{\mathbf{y}}^{l,+})^2 \right] + 2\phi(1)\phi(-1) \mathbb{E}_{\theta^l} \left[\mu_c(\check{\mathbf{y}}^{l,+})\mu_c(\check{\mathbf{y}}^{l,-}) \right] \\ &= F_\phi \mathbb{E}_{\theta^l} \left[\mu_c(\check{\mathbf{y}}^{l,+})^2 + \mu_c(\check{\mathbf{y}}^{l,-})^2 \right] + 2\phi(1)\phi(-1) \mathbb{E}_{\theta^l} \left[\mu_c(\check{\mathbf{y}}^{l,+})\mu_c(\check{\mathbf{y}}^{l,-}) \right], \\ \mathbb{E}_{\theta^l} \left[\mathcal{P}_c(\check{\mathbf{z}}^l) \right] &= \left(\phi(1)^2 + \phi(-1)^2 \right) \mathbb{E}_{\theta^l} \left[\mathcal{P}_c(\check{\mathbf{y}}^{l,+}) \right] \\ &= F_\phi \mathbb{E}_{\theta^l} \left[\mathcal{P}_c(\check{\mathbf{y}}^{l,+}) + \mathcal{P}_c(\check{\mathbf{y}}^{l,-}) \right], \end{aligned}$$

where we defined $F_\phi \equiv \frac{\phi(1)^2 + \phi(-1)^2}{2}$, with $F_\phi > 0$ given the assumption that ϕ is nonzero.

Given $|\phi(1)\phi(-1)| \leq \frac{\phi(1)^2 + \phi(-1)^2}{2} \implies \phi(1)\phi(-1) \geq -F_\phi$, and given $\mu_c(\check{\mathbf{y}}^{l,+})\mu_c(\check{\mathbf{y}}^{l,-}) \geq 0$, we deduce that $\forall c$:

$$\begin{aligned} \mathbb{E}_{\theta^l} \left[\mu_c(\check{\mathbf{z}}^l)^2 \right] &\geq F_\phi \mathbb{E}_{\theta^l} \left[\mu_c(\check{\mathbf{y}}^{l,+})^2 + \mu_c(\check{\mathbf{y}}^{l,-})^2 - 2\mu_c(\check{\mathbf{y}}^{l,+})\mu_c(\check{\mathbf{y}}^{l,-}) \right], \\ &\geq F_\phi \mathbb{E}_{\theta^l} \left[\mu_c(\check{\mathbf{y}}^l)^2 \right], \end{aligned} \quad (64)$$

$$\begin{aligned} \mathbb{E}_{\theta^l} \left[\mathcal{P}_c(\check{\mathbf{z}}^l) \right] &= F_\phi \mathbb{E}_{\theta^l} \left[\mathcal{P}_c(\check{\mathbf{y}}^l) \right] \\ &= F_\phi (\gamma^2 + \beta^2), \end{aligned} \quad (65)$$

$$\begin{aligned} \mathbb{E}_{\theta^l} \left[\mathcal{P}_c(\check{\mathbf{z}}^l) - \mathcal{P}_c^{(1)}(\check{\mathbf{z}}^l) \right] &= \mathbb{E}_{\theta^l} \left[\mathcal{P}_c(\check{\mathbf{z}}^l) - \mu_c(\check{\mathbf{z}}^l)^2 \right] \\ &\leq F_\phi \mathbb{E}_{\theta^l} \left[\mathcal{P}_c(\check{\mathbf{y}}^l) - \mathcal{P}_c^{(1)}(\check{\mathbf{y}}^l) \right] \\ &\leq F_\phi \gamma^2 \varrho(\hat{\mathbf{z}}^{l-1}). \end{aligned} \quad (66)$$

where we used Eq. (62), (63) and Eq. (56), (57).

Let us now define $\chi(\hat{\mathbf{z}}^{l-1}) \in \mathbb{R}^+$ independently of c as

$$\chi(\hat{\mathbf{z}}^{l-1}) \equiv \begin{cases} \frac{\mathbb{E}_{\theta^l} [\mathcal{P}_c(\check{\mathbf{z}}^l) - \mathcal{P}_c^{(1)}(\check{\mathbf{z}}^l)]}{F_\phi \gamma^2 \varrho(\hat{\mathbf{z}}^{l-1})} & \text{if } \varrho(\hat{\mathbf{z}}^{l-1}) > 0, \\ 1 & \text{otherwise.} \end{cases}$$

We note that $\chi(\hat{\mathbf{z}}^{l-1})$ is independent of θ^l and that $\chi(\hat{\mathbf{z}}^{l-1}) \leq 1$ in general, and $\chi(\hat{\mathbf{z}}^{l-1}) = 1$ if $\phi = \text{identity}$ since the inequalities of Eq. (64) and Eq. (66) become equalities when $\phi = \text{identity}$.

Using this definition of $\chi(\hat{\mathbf{z}}^{l-1})$, we may rewrite $\mathbb{E}_{\theta^l} [\mathcal{P}_c(\check{\mathbf{z}}^l) - \mathcal{P}_c^{(1)}(\check{\mathbf{z}}^l)]$ for any c as

$$\mathbb{E}_{\theta^l} [\mathcal{P}_c(\check{\mathbf{z}}^l) - \mathcal{P}_c^{(1)}(\check{\mathbf{z}}^l)] = \chi(\hat{\mathbf{z}}^{l-1}) F_\phi \gamma^2 \varrho(\hat{\mathbf{z}}^{l-1}). \quad (67)$$

Now let us bound $\text{Var}_{\theta^l} [\mathcal{P}_c(\check{\mathbf{z}}^l)]$ and $\text{Var}_{\theta^l} [\mathcal{P}_c(\check{\mathbf{z}}^l) - \mathcal{P}_c^{(1)}(\check{\mathbf{z}}^l)]$. We get from Eq. (61) that $\forall c$:

$$\begin{aligned} \mathcal{P}_c(\check{\mathbf{z}}^l) &\leq \left(\phi(1)^2 + \phi(-1)^2 \right) \left(\mathcal{P}_c(\check{\mathbf{y}}^{l,-}) + \mathcal{P}_c(\check{\mathbf{y}}^{l,+}) \right) \\ &\leq 2F_\phi \mathcal{P}_c(\check{\mathbf{y}}^l), \\ \mathbb{E}_{\theta^l} [\mathcal{P}_c(\check{\mathbf{z}}^l)^2] &\leq 4F_\phi^2 \mathbb{E}_{\theta^l} [\mathcal{P}_c(\check{\mathbf{y}}^l)^2] \\ &\leq 4F_\phi^2 \left(24\tilde{\gamma}^4 \tilde{\omega}^4 \omega^{-4} + 8\tilde{\beta}^4 \right), \\ \text{Var}_{\theta^l} [\mathcal{P}_c(\check{\mathbf{z}}^l)] &\leq \mathbb{E}_{\theta^l} [\mathcal{P}_c(\check{\mathbf{z}}^l)^2] \\ &\leq 4F_\phi^2 \left(24\tilde{\gamma}^4 \tilde{\omega}^4 \omega^{-4} + 8\tilde{\beta}^4 \right), \end{aligned} \quad (68)$$

$$\begin{aligned} \text{Var}_{\theta^l} [\mathcal{P}_c(\check{\mathbf{z}}^l) - \mathcal{P}_c^{(1)}(\check{\mathbf{z}}^l)] &\leq \mathbb{E}_{\theta^l} [(\mathcal{P}_c(\check{\mathbf{z}}^l) - \mathcal{P}_c^{(1)}(\check{\mathbf{z}}^l))^2] \leq \mathbb{E}_{\theta^l} [\mathcal{P}_c(\check{\mathbf{z}}^l)^2] \\ &\leq 4F_\phi^2 \left(24\tilde{\gamma}^4 \tilde{\omega}^4 \omega^{-4} + 8\tilde{\beta}^4 \right), \end{aligned} \quad (69)$$

where we used Eq. (59).

Using Eq. (65), (67), (68), (69) and the fact that the terms $\mathcal{P}_c(\check{\mathbf{z}}^l)$ and $\mathcal{P}_c(\check{\mathbf{z}}^l) - \mathcal{P}_c^{(1)}(\check{\mathbf{z}}^l)$ are i.i.d. in the different channels c , we get

$$\mathbb{E}_{\theta^l} [\mathcal{P}(\check{\mathbf{z}}^l)] = F_\phi (\gamma^2 + \beta^2), \quad \text{Var}_{\theta^l} [\mathcal{P}(\check{\mathbf{z}}^l)] \leq \frac{4F_\phi^2 (24\tilde{\gamma}^4 \tilde{\omega}^4 \omega^{-4} + 8\tilde{\beta}^4)}{C_l}, \quad (70)$$

$$\mathbb{E}_{\theta^l} [\mathcal{P}(\check{\mathbf{z}}^l) - \mathcal{P}^{(1)}(\check{\mathbf{z}}^l)] = \chi(\hat{\mathbf{z}}^{l-1}) F_\phi \gamma^2 \varrho(\hat{\mathbf{z}}^{l-1}), \quad \text{Var}_{\theta^l} [\mathcal{P}(\check{\mathbf{z}}^l) - \mathcal{P}^{(1)}(\check{\mathbf{z}}^l)] \leq \frac{4F_\phi^2 (24\tilde{\gamma}^4 \tilde{\omega}^4 \omega^{-4} + 8\tilde{\beta}^4)}{C_l},$$

Now if we define $\check{\mathbf{z}}^l$ such that $\forall \alpha, c: \check{\mathbf{z}}_{\alpha,c}^l = \frac{\check{\mathbf{z}}_{\alpha,c}^l}{\sqrt{F_\phi(\gamma^2 + \beta^2)}}$, we get

$$\begin{aligned} \mathbb{E}_{\theta^l} [\mathcal{P}(\check{\mathbf{z}}^l)] &= 1, \quad \text{Var}_{\theta^l} [\mathcal{P}(\check{\mathbf{z}}^l)] \leq \frac{1}{C_l} \frac{4(24\tilde{\gamma}^4 \tilde{\omega}^4 \omega^{-4} + 8\tilde{\beta}^4)}{(\gamma^2 + \beta^2)^2}, \\ \mathbb{E}_{\theta^l} [\mathcal{P}(\check{\mathbf{z}}^l) - \mathcal{P}^{(1)}(\check{\mathbf{z}}^l)] &= \rho \chi(\hat{\mathbf{z}}^{l-1}) \varrho(\hat{\mathbf{z}}^{l-1}), \quad \text{Var}_{\theta^l} [\mathcal{P}(\check{\mathbf{z}}^l) - \mathcal{P}^{(1)}(\check{\mathbf{z}}^l)] \leq \frac{1}{C_l} \frac{4(24\tilde{\gamma}^4 \tilde{\omega}^4 \omega^{-4} + 8\tilde{\beta}^4)}{(\gamma^2 + \beta^2)^2}, \end{aligned}$$

where $\rho = \frac{\gamma^2}{\gamma^2 + \beta^2}$.

The reasoning that yielded Eq. (51) from Eq. (49) and Eq. (50) can be immediately transposed by replacing $\hat{\mathbf{y}}^l$ by $\check{\mathbf{z}}^l$, $\varrho(\hat{\mathbf{z}}^{l-1})$ by $\rho \chi(\hat{\mathbf{z}}^{l-1}) \varrho(\hat{\mathbf{z}}^{l-1})$ and $3\tilde{\omega}^4 \omega^{-4}$ by $\frac{4(24\tilde{\gamma}^4 \tilde{\omega}^4 \omega^{-4} + 8\tilde{\beta}^4)}{(\gamma^2 + \beta^2)^2}$.

Consequently, for any $\eta > 0$ and any $\delta > 0$, there exists $N_3(\eta, \delta) \in \mathbb{N}^*$ independent of Θ^{l-1} , l , such that if $C_l \geq N_3(\eta, \delta)$, it holds that

$$\begin{aligned} \mathbb{P}_{\theta^l} \left[|\varrho(\check{\mathbf{z}}^l) - \rho \chi(\hat{\mathbf{z}}^{l-1}) \varrho(\hat{\mathbf{z}}^{l-1})| \leq \eta \right] &\geq 1 - \delta, \\ \mathbb{P}_{\theta^l} \left[|\varrho(\check{\mathbf{z}}^l) - \rho \chi(\hat{\mathbf{z}}^{l-1}) \varrho(\hat{\mathbf{z}}^{l-1})| \leq \eta \right] &\geq 1 - \delta, \end{aligned}$$

where we used the fact that $\varrho(\tilde{\mathbf{z}}^l) = \varrho(\mathbf{z}^l)$.

Thus, if we define N' independently of Θ^l , l as $N'(\eta, \delta) = \max(N_2(\eta, \delta), N_3(\eta, \delta))$, $\forall \eta > 0$, $\forall \delta > 0$, then for any $\eta > 0$ and any $\delta > 0$, if $C_l \geq N'(\eta, \delta)$, it holds that

$$\begin{aligned}\mathbb{P}_{\theta_l} \left[|\varrho(\hat{\mathbf{y}}^l) - \varrho(\hat{\mathbf{z}}^{l-1})| \leq \eta \right] &\geq 1 - \delta, \\ \mathbb{P}_{\theta_l} \left[|\varrho(\hat{\mathbf{z}}^l) - \rho\chi(\hat{\mathbf{z}}^{l-1})\varrho(\hat{\mathbf{z}}^{l-1})| \leq \eta \right] &\geq 1 - \delta,\end{aligned}$$

where we recall that $\chi(\hat{\mathbf{z}}^{l-1}) \leq 1$ in general, and that $\chi(\hat{\mathbf{z}}^{l-1}) = 1$ if ϕ = identity. \square

Lemma 2. Fix a layer $l \geq 1$, ν_ω , ν_β , ν_γ , \mathcal{D} in Definition 1 and model parameters Θ^{l-1} up to layer $l-1$ such that $\mathcal{P}_{\mathbf{x}}(\mathbf{z}^{l-1}) > 0$, $\forall \mathbf{x}$. Further suppose Norm = LN and suppose and that the convolution of Eq. (2) uses periodic boundary conditions.

Then for any $\eta > 0$ and any $\delta > 0$, there exists $N''(\eta, \delta) \in \mathbb{N}^*$ independent of Θ^{l-1} , l such that if $C_l \geq N''(\eta, \delta)$, it holds for random nets of Definition 1 with probability greater than $1 - \delta$ with respect to θ^l that

$$\begin{aligned}|\mathcal{P}^{(1)}(\hat{\mathbf{y}}^l) - \mathcal{P}^{(1)}(\mathbf{y}^l)| &\leq \eta, & |\mathcal{P}^{(1)}(\tilde{\mathbf{z}}^l) - \mathcal{P}^{(1)}(\mathbf{z}^l)| &\leq \eta, \\ |\mathcal{P}(\hat{\mathbf{y}}^l) - \mathcal{P}(\mathbf{y}^l)| &\leq \eta, & |\mathcal{P}(\tilde{\mathbf{z}}^l) - \mathcal{P}(\mathbf{z}^l)| &\leq \eta, \\ |\mathcal{P}_{\mathbf{x}}(\hat{\mathbf{y}}^l) - 1| &\leq \eta, \quad \forall \mathbf{x} \in \mathcal{D}, & |\mathcal{P}_{\mathbf{x}}(\tilde{\mathbf{z}}^l) - F_\phi(\gamma^2 + \beta^2)| &\leq \eta, \quad \forall \mathbf{x} \in \mathcal{D},\end{aligned}$$

where $F_\phi \equiv \frac{\phi(1)^2 + \phi(-1)^2}{2} > 0$ and $\hat{\mathbf{y}}^l$, $\tilde{\mathbf{z}}^l$ are defined in Eq. (30) and Eq. (32).

Proof. Let us start by noting that $\forall \alpha, c$:

$$\hat{\mathbf{x}}_{\alpha,c}^l = \sqrt{\frac{\mathcal{P}(\mathbf{z}^{l-1})}{\mathcal{P}_{\mathbf{x}}(\mathbf{z}^{l-1})}} \mathbf{x}_{\alpha,c}^l, \quad \hat{\mathbf{y}}_{\alpha,c}^l = \frac{1}{\omega \sqrt{\mathcal{P}(\mathbf{z}^{l-1})}} \hat{\mathbf{x}}_{\alpha,c}^l = \frac{1}{\omega \sqrt{\mathcal{P}_{\mathbf{x}}(\mathbf{z}^{l-1})}} \mathbf{x}_{\alpha,c}^l.$$

This implies that $\hat{\mathbf{y}}^l$ only depends on \mathbf{x} and not on other inputs in the dataset.

Thus, Eq. (48) and Eq. (49) still hold when considering the moments conditioned on \mathbf{x} , such that $\forall \mathbf{x}$:

$$\mathbb{E}_{\theta^l} [\mu_{\mathbf{x}}(\hat{\mathbf{y}}^l)] = 0, \quad \text{Var}_{\theta^l} [\mu_{\mathbf{x}}(\hat{\mathbf{y}}^l)] \leq \frac{1}{C_l}, \quad (71)$$

$$\mathbb{E}_{\theta^l} [\mathcal{P}_{\mathbf{x}}(\hat{\mathbf{y}}^l)] = 1, \quad \text{Var}_{\theta^l} [\mathcal{P}_{\mathbf{x}}(\hat{\mathbf{y}}^l)] \leq \frac{3\tilde{\omega}^4 \omega^{-4}}{C_l}. \quad (72)$$

Similarly, Eq. (70) still holds when considering the moments conditioned on \mathbf{x} , such that $\forall \mathbf{x}, c$:

$$\mathbb{E}_{\theta^l} [\mathcal{P}_{\mathbf{x}}(\tilde{\mathbf{z}}^l)] = F_\phi(\gamma^2 + \beta^2), \quad \text{Var}_{\theta^l} [\mathcal{P}_{\mathbf{x}}(\tilde{\mathbf{z}}^l)] \leq \frac{4F_\phi^2 (24\tilde{\gamma}^4 \tilde{\omega}^4 \omega^{-4} + 8\tilde{\beta}^4)}{C_l}. \quad (73)$$

Combining Eq. (71), (72), (73), we deduce for any $\eta > 0$ and any $\delta > 0$ that there exists $N_5(\eta, \delta) \in \mathbb{N}^*$ independent of Θ^{l-1} , l , \mathbf{x} such that, if $C_l \geq N_5(\eta, \delta)$, it holds for any \mathbf{x} that

$$\mathbb{P}_{\theta^l} \left[|\mu_{\mathbf{x}}(\hat{\mathbf{y}}^l)| \leq \eta \right] \geq 1 - \delta, \quad (74)$$

$$\mathbb{P}_{\theta^l} \left[|\mathcal{P}_{\mathbf{x}}(\hat{\mathbf{y}}^l) - 1| \leq \eta \right] \geq 1 - \delta, \quad (75)$$

$$\mathbb{P}_{\theta^l} \left[|\mathcal{P}_{\mathbf{x}}(\tilde{\mathbf{z}}^l) - F_\phi(\gamma^2 + \beta^2)| \leq \eta \right] \geq 1 - \delta. \quad (76)$$

Now let us bound $|\mathcal{P}(\hat{\mathbf{y}}^l) - \mathcal{P}(\mathbf{y}^l)|$ and $|\mathcal{P}(\tilde{\mathbf{z}}^l) - \mathcal{P}(\mathbf{z}^l)|$.

We start by noting that $\mathbf{y}_{\alpha,c}^l = \frac{\mathbf{x}_{\alpha,c}^l - \mu_{\mathbf{x}}(\mathbf{x}^l)}{\sigma_{\mathbf{x}}(\mathbf{x}^l)} = \frac{\hat{\mathbf{y}}_{\alpha,c}^l - \mu_{\mathbf{x}}(\hat{\mathbf{y}}^l)}{\sigma_{\mathbf{x}}(\hat{\mathbf{y}}^l)}$, $\forall \mathbf{x}, \alpha, c$. Thus, $\forall \mathbf{x}, \alpha, c$:

$$\begin{aligned}\hat{\mathbf{y}}_{\alpha,c}^l &= \sigma_{\mathbf{x}}(\hat{\mathbf{y}}^l) \mathbf{y}_{\alpha,c}^l + \mu_{\mathbf{x}}(\hat{\mathbf{y}}^l) \\ &= \mathbf{y}_{\alpha,c}^l + (\sigma_{\mathbf{x}}(\hat{\mathbf{y}}^l) - 1) \mathbf{y}_{\alpha,c}^l + \mu_{\mathbf{x}}(\hat{\mathbf{y}}^l), \\ \tilde{\mathbf{y}}_{\alpha,c}^l &= \gamma_c^l \mathbf{y}_{\alpha,c}^l + \beta_c^l + \gamma_c^l (\sigma_{\mathbf{x}}(\hat{\mathbf{y}}^l) - 1) \mathbf{y}_{\alpha,c}^l + \gamma_c^l \mu_{\mathbf{x}}(\hat{\mathbf{y}}^l) \\ &= \tilde{\mathbf{y}}_{\alpha,c}^l + \gamma_c^l (\sigma_{\mathbf{x}}(\hat{\mathbf{y}}^l) - 1) \mathbf{y}_{\alpha,c}^l + \gamma_c^l \mu_{\mathbf{x}}(\hat{\mathbf{y}}^l).\end{aligned}$$

Now let us fix \mathbf{x} and bound $\mathcal{P}_{\mathbf{x}}(\hat{\mathbf{y}}^l - \mathbf{y}^l)$ and $\mathcal{P}_{\mathbf{x}}(\hat{\mathbf{z}}^l - \mathbf{z}^l)$. We start by noting that

$$\begin{aligned} (\hat{\mathbf{y}}_{\alpha,c}^l - \mathbf{y}_{\alpha,c}^l)^2 &\leq 2(\sigma_{\mathbf{x}}(\hat{\mathbf{y}}^l) - 1)^2(\mathbf{y}_{\alpha,c}^l)^2 + 2\mu_{\mathbf{x}}(\hat{\mathbf{y}}^l)^2, \\ (\tilde{\mathbf{y}}_{\alpha,c}^l - \hat{\mathbf{y}}_{\alpha,c}^l)^2 &\leq 2(\sigma_{\mathbf{x}}(\hat{\mathbf{y}}^l) - 1)^2(\gamma_c^l \mathbf{y}_{\alpha,c}^l)^2 + 2\mu_{\mathbf{x}}(\hat{\mathbf{y}}^l)^2(\gamma_c^l)^2, \\ (\hat{\mathbf{z}}_{\alpha,c}^l - \mathbf{z}_{\alpha,c}^l)^2 &= (\phi(\tilde{\mathbf{y}}_{\alpha,c}^l) - \phi(\hat{\mathbf{y}}_{\alpha,c}^l))^2 \\ &\leq 2F_{\phi}(\tilde{\mathbf{y}}_{\alpha,c}^l - \hat{\mathbf{y}}_{\alpha,c}^l)^2 \\ &\leq 4F_{\phi}(\sigma_{\mathbf{x}}(\hat{\mathbf{y}}^l) - 1)^2(\gamma_c^l \mathbf{y}_{\alpha,c}^l)^2 + 4F_{\phi}\mu_{\mathbf{x}}(\hat{\mathbf{y}}^l)^2(\gamma_c^l)^2, \end{aligned}$$

where we used $(a+b)^2 \leq 2a^2 + 2b^2$, $\forall a, b$ and $(\phi(a) - \phi(b))^2 \leq (F'_{\phi})^2(a-b)^2 \leq 2F_{\phi}(a-b)^2$, $\forall a, b$, by F'_{ϕ} -Lipschitzness of ϕ with $F'_{\phi} = \max(|\phi(1)|, |\phi(-1)|) \leq \sqrt{2F_{\phi}}$.

We deduce for $\mathcal{P}_{\mathbf{x}}(\hat{\mathbf{y}}^l - \mathbf{y}^l)$ and $\mathcal{P}_{\mathbf{x}}(\hat{\mathbf{z}}^l - \mathbf{z}^l)$ that

$$\begin{aligned} \mathcal{P}_{\mathbf{x}}(\hat{\mathbf{y}}^l - \mathbf{y}^l) &\leq 2(\sigma_{\mathbf{x}}(\hat{\mathbf{y}}^l) - 1)^2\mathcal{P}_{\mathbf{x}}(\mathbf{y}^l) + 2\mu_{\mathbf{x}}(\hat{\mathbf{y}}^l)^2 \\ &\leq 2\left((\sigma_{\mathbf{x}}(\hat{\mathbf{y}}^l) - 1)^2 + \mu_{\mathbf{x}}(\hat{\mathbf{y}}^l)^2\right), \end{aligned} \quad (77)$$

$$\begin{aligned} \mathcal{P}_{\mathbf{x}}(\hat{\mathbf{z}}^l - \mathbf{z}^l) &\leq 4F_{\phi}(\sigma_{\mathbf{x}}(\hat{\mathbf{y}}^l) - 1)^2\mathbb{E}_c\left[(\gamma_c^l)^2\mathcal{P}_{\mathbf{x},c}(\mathbf{y}^l)\right] + 4F_{\phi}\mu_{\mathbf{x}}(\hat{\mathbf{y}}^l)^2\mathbb{E}_c\left[(\gamma_c^l)^2\right] \\ &\leq 4F_{\phi}\left((\sigma_{\mathbf{x}}(\hat{\mathbf{y}}^l) - 1)^2 + \mu_{\mathbf{x}}(\hat{\mathbf{y}}^l)^2\right)\mathbb{E}_c\left[(\gamma_c^l)^2(\mathcal{P}_{\mathbf{x},c}(\mathbf{y}^l) + 1)\right], \end{aligned} \quad (78)$$

where we used $\mathcal{P}_{\mathbf{x}}(\mathbf{y}^l) \leq 1$.

Next, let us bound the expectation over θ^l of $\mathbb{E}_c\left[(\gamma_c^l)^2(\mathcal{P}_{\mathbf{x},c}(\mathbf{y}^l) + 1)\right]$:

$$\begin{aligned} \mathbb{E}_{\theta^l}\left[\mathbb{E}_c\left[(\gamma_c^l)^2(\mathcal{P}_{\mathbf{x},c}(\mathbf{y}^l) + 1)\right]\right] &= \mathbb{E}_c\left[\mathbb{E}_{\theta^l}\left[(\gamma_c^l)^2(\mathcal{P}_{\mathbf{x},c}(\mathbf{y}^l) + 1)\right]\right] \\ &= \mathbb{E}_c\left[\mathbb{E}_{\theta^l}\left[(\gamma_c^l)^2\right]\mathbb{E}_{\theta^l}\left[\mathcal{P}_{\mathbf{x},c}(\mathbf{y}^l) + 1\right]\right] \\ &= \gamma^2\mathbb{E}_{\theta^l}\left[\mathbb{E}_c\left[\mathcal{P}_{\mathbf{x},c}(\mathbf{y}^l) + 1\right]\right] \\ &= \gamma^2\mathbb{E}_{\theta^l}\left[\mathcal{P}_{\mathbf{x}}(\mathbf{y}^l) + 1\right] \\ &\leq 2\gamma^2, \end{aligned}$$

where we used the independence of γ_c^l and $\mathcal{P}_{\mathbf{x},c}(\mathbf{y}^l)$ with respect to θ^l for any c , and again $\mathcal{P}_{\mathbf{x}}(\mathbf{y}^l) \leq 1$.

Markov's inequality then gives for any $\delta > 0$ that

$$\mathbb{P}_{\theta^l}\left[\mathbb{E}_c\left[(\gamma_c^l)^2(\mathcal{P}_{\mathbf{x},c}(\mathbf{y}^l) + 1)\right] \geq \frac{2\gamma^2}{\delta}\right] \leq 2\gamma^2 \frac{\delta}{2\gamma^2} = \delta.$$

Thus, for any $1 \geq \eta > 0$ and any $\delta > 0$, if $C_l \geq N_5(\eta, \delta)$, it holds for any \mathbf{x} with probability greater than $1 - 4\delta$ with respect to θ^l that

$$|\mu_{\mathbf{x}}(\hat{\mathbf{y}}^l)| \leq \eta, \quad (79)$$

$$|\mathcal{P}_{\mathbf{x}}(\hat{\mathbf{y}}^l) - 1| \leq \eta, \quad (80)$$

$$|\mathcal{P}_{\mathbf{x}}(\hat{\mathbf{z}}^l) - F_{\phi}(\gamma^2 + \beta^2)| \leq \eta, \quad (81)$$

$$\mathbb{E}_c\left[(\gamma_c^l)^2(\mathcal{P}_{\mathbf{x},c}(\mathbf{y}^l) + 1)\right] \leq \frac{2\gamma^2}{\delta}. \quad (82)$$

If both inequalities of Eq. (79) and Eq. (80) hold, then

$$\begin{aligned} |\sigma_{\mathbf{x}}(\hat{\mathbf{y}}^l) - 1| &\leq |\sigma_{\mathbf{x}}(\hat{\mathbf{y}}^l) - 1||\sigma_{\mathbf{x}}(\hat{\mathbf{y}}^l) + 1| \\ &\leq |\sigma_{\mathbf{x}}(\hat{\mathbf{y}}^l)^2 - 1| \\ &\leq |\mathcal{P}_{\mathbf{x}}(\hat{\mathbf{y}}^l) - 1| + \mu_{\mathbf{x}}(\hat{\mathbf{y}}^l)^2 \\ &\leq \eta + \eta^2 \leq 2\eta, \\ (\sigma_{\mathbf{x}}(\hat{\mathbf{y}}^l) - 1)^2 &\leq 4\eta^2 \leq 4\eta \\ \mu_{\mathbf{x}}(\hat{\mathbf{y}}^l)^2 &\leq \eta^2 \leq \eta, \end{aligned}$$

where we used $\eta^2 \leq \eta$ due to $\eta \leq 1$.

Injecting this into Eq. (77) and Eq. (78), we get that, if $C_l \geq N_5(\eta, \delta)$, it holds with probability greater than $1 - 4\delta$ with respect to θ^l that

$$\mathcal{P}_{\mathbf{x}}(\hat{\mathbf{y}}^l - \mathbf{y}^l) \leq 10\eta, \quad \mathcal{P}_{\mathbf{x}}(\tilde{\mathbf{z}}^l - \mathbf{z}^l) \leq 20F_\phi\eta\frac{2\gamma^2}{\delta},$$

If we define $N_6(\eta, \delta)$ independently of Θ^{l-1} , l as $N_6(\eta, \delta) = N_5\left(\min(\frac{\eta}{10}, \frac{\eta}{20F_\phi}\frac{\delta}{2\gamma^2}, 1), \frac{\delta}{4|\mathcal{D}|}\right)$, $\forall \eta > 0, \forall \delta > 0$, then if $C_l \geq N_6(\eta, \delta)$, it holds with probability greater than $1 - \delta$ with respect to θ^l that

$$|\mathcal{P}_{\mathbf{x}}(\hat{\mathbf{y}}^l) - 1| \leq \eta, \quad \forall \mathbf{x} \in \mathcal{D} \implies |\mathcal{P}(\hat{\mathbf{y}}^l) - 1| \leq \eta, \quad (83)$$

$$\mathcal{P}_{\mathbf{x}}(\hat{\mathbf{y}}^l - \mathbf{y}^l) \leq \eta, \quad \forall \mathbf{x} \in \mathcal{D} \implies \mathcal{P}(\hat{\mathbf{y}}^l - \mathbf{y}^l) \leq \eta, \quad (84)$$

$$|\mathcal{P}_{\mathbf{x}}(\tilde{\mathbf{z}}^l) - F_\phi(\gamma^2 + \beta^2)| \leq \eta, \quad \forall \mathbf{x} \in \mathcal{D} \implies |\mathcal{P}(\tilde{\mathbf{z}}^l) - F_\phi(\gamma^2 + \beta^2)| \leq \eta, \quad (85)$$

$$\mathcal{P}_{\mathbf{x}}(\tilde{\mathbf{z}}^l - \mathbf{z}^l) \leq \eta, \quad \forall \mathbf{x} \in \mathcal{D} \implies \mathcal{P}(\tilde{\mathbf{z}}^l - \mathbf{z}^l) \leq \eta. \quad (86)$$

If all inequalities of Eq. (83), (84), (85), (86) hold, then

$$\begin{aligned} |\mathcal{P}^{(1)}(\hat{\mathbf{y}}^l) - \mathcal{P}^{(1)}(\mathbf{y}^l)| &\leq \mathcal{P}^{(1)}(\hat{\mathbf{y}}^l - \mathbf{y}^l) + 2\left|\mathbb{E}_c\left[\mu_c(\hat{\mathbf{y}}^l)\mu_c(\hat{\mathbf{y}}^l - \mathbf{y}^l)\right]\right| \\ &\leq \mathcal{P}(\hat{\mathbf{y}}^l - \mathbf{y}^l) + 2\mathbb{E}_c\left[|\mu_c(\hat{\mathbf{y}}^l)||\mu_c(\hat{\mathbf{y}}^l - \mathbf{y}^l)|\right] \\ &\leq \mathcal{P}(\hat{\mathbf{y}}^l - \mathbf{y}^l) + 2\sqrt{\mathbb{E}_c\left[\mu_c(\hat{\mathbf{y}}^l)^2\right]\mathbb{E}_c\left[\mu_c(\hat{\mathbf{y}}^l - \mathbf{y}^l)^2\right]} \\ &\leq \mathcal{P}(\hat{\mathbf{y}}^l - \mathbf{y}^l) + 2\sqrt{\mathcal{P}(\hat{\mathbf{y}}^l)\mathcal{P}(\hat{\mathbf{y}}^l - \mathbf{y}^l)}, \\ &\leq \eta + 2\sqrt{(1 + \eta)\eta}, \end{aligned}$$

where we used $\mathbb{E}_c\left[\mu_c(\hat{\mathbf{y}}^l)^2\right] = \mathcal{P}^{(1)}(\hat{\mathbf{y}}^l) \leq \mathcal{P}(\hat{\mathbf{y}}^l)$, $\mathbb{E}_c\left[\mu_c(\hat{\mathbf{y}}^l - \mathbf{y}^l)^2\right] = \mathcal{P}^{(1)}(\hat{\mathbf{y}}^l - \mathbf{y}^l) \leq \mathcal{P}(\hat{\mathbf{y}}^l - \mathbf{y}^l)$, as well as Jensen's inequality and Cauchy-Schwartz inequality.

Similarly,

$$\begin{aligned} |\mathcal{P}(\hat{\mathbf{y}}^l) - \mathcal{P}(\mathbf{y}^l)| &\leq \mathcal{P}(\hat{\mathbf{y}}^l - \mathbf{y}^l) + 2\mu(|\hat{\mathbf{y}}^l||\hat{\mathbf{y}}^l - \mathbf{y}^l|) \\ &\leq \mathcal{P}(\hat{\mathbf{y}}^l - \mathbf{y}^l) + 2\sqrt{\mathcal{P}(\hat{\mathbf{y}}^l)\mathcal{P}(\hat{\mathbf{y}}^l - \mathbf{y}^l)} \\ &\leq \eta + 2\sqrt{(1 + \eta)\eta}, \end{aligned}$$

A similar calculation with $\tilde{\mathbf{z}}^l, \mathbf{z}^l$ shows that if all inequalities of Eq. (83), (84), (85), (86) hold, then

$$\begin{aligned} |\mathcal{P}^{(1)}(\tilde{\mathbf{z}}^l) - \mathcal{P}^{(1)}(\mathbf{z}^l)| &\leq \eta + 2\sqrt{\eta}\sqrt{F_\phi(\gamma^2 + \beta^2) + \eta}, \\ |\mathcal{P}(\tilde{\mathbf{z}}^l) - \mathcal{P}(\mathbf{z}^l)| &\leq \eta + 2\sqrt{\eta}\sqrt{F_\phi(\gamma^2 + \beta^2) + \eta}. \end{aligned}$$

Given that the three terms η , $\eta + 2\sqrt{(1 + \eta)\eta}$ and $\eta + 2\sqrt{\eta}\sqrt{F_\phi(\gamma^2 + \beta^2) + \eta}$ converge to 0 as $\eta \rightarrow 0$, it follows that there exists a mapping h such that for any $\eta > 0$: $h(\eta) > 0$ and

$$h(\eta) \leq \eta, \quad h(\eta) + 2\sqrt{(1 + h(\eta))h(\eta)} \leq \eta, \quad h(\eta) + 2\sqrt{h(\eta)}\sqrt{F_\phi(\gamma^2 + \beta^2) + h(\eta)} \leq \eta.$$

Thus, if we define N'' independently of Θ^l , l as $N''(\eta, \delta) = N_6(h(\eta), \delta)$, $\forall \eta > 0, \forall \delta > 0$, then for any $\eta > 0$ and any $\delta > 0$, if $C_l \geq N''(\eta, \delta)$, it holds with probability greater than $1 - \delta$ with respect to θ^l that

$$\begin{aligned} |\mathcal{P}^{(1)}(\hat{\mathbf{y}}^l) - \mathcal{P}^{(1)}(\mathbf{y}^l)| &\leq \eta, & |\mathcal{P}^{(1)}(\tilde{\mathbf{z}}^l) - \mathcal{P}^{(1)}(\mathbf{z}^l)| &\leq \eta, \\ |\mathcal{P}(\hat{\mathbf{y}}^l) - \mathcal{P}(\mathbf{y}^l)| &\leq \eta, & |\mathcal{P}(\tilde{\mathbf{z}}^l) - \mathcal{P}(\mathbf{z}^l)| &\leq \eta, \\ |\mathcal{P}_{\mathbf{x}}(\hat{\mathbf{y}}^l) - 1| &\leq \eta, \quad \forall \mathbf{x} \in \mathcal{D}, & |\mathcal{P}_{\mathbf{x}}(\tilde{\mathbf{z}}^l) - F_\phi(\gamma^2 + \beta^2)| &\leq \eta, \quad \forall \mathbf{x} \in \mathcal{D}. \end{aligned} \quad \square$$

Lemma 3. Fix a layer $l \geq 1$, $\nu_\omega, \nu_\beta, \nu_\gamma, \mathcal{D}$ in Definition 1 and model parameters Θ^{l-1} up to layer $l-1$ such that $\mathcal{P}_x(\mathbf{z}^{l-1}) > 0, \forall \mathbf{x}$. Further suppose Norm = LN and suppose that the convolution of Eq. (2) uses periodic boundary conditions.

Then for any $\eta > 0$ and any $\delta > 0$, there exists $N'''(\eta, \delta) \in \mathbb{N}^*$ independent of Θ^{l-1}, l such that if $C_l \geq N'''(\eta, \delta)$, it holds for random nets of Definition 1 with probability greater than $1 - \delta$ with respect to θ^l that

$$\begin{aligned} |\varrho(\mathbf{y}^l) - \varrho(\hat{\mathbf{z}}^{l-1})| &\leq \eta, & |\varrho(\mathbf{z}^l) - \rho\chi(\hat{\mathbf{z}}^{l-1})\varrho(\hat{\mathbf{z}}^{l-1})| &\leq \eta, \\ |\mathcal{P}_x(\mathbf{y}^l) - 1| &\leq \eta, \quad \forall \mathbf{x} \in \mathcal{D}, & |\mathcal{P}_x(\mathbf{z}^l) - F_\phi(\gamma^2 + \beta^2)| &\leq \eta, \quad \forall \mathbf{x} \in \mathcal{D}, \end{aligned}$$

where $F_\phi \equiv \frac{\phi(1)^2 + \phi(-1)^2}{2} > 0$, and where $\rho = \frac{\gamma^2}{\gamma^2 + \beta^2} < 1$ and $\chi(\hat{\mathbf{z}}^{l-1}) \in \mathbb{R}^+$ is dependent on Θ^{l-1} but independent of θ^l such that $\chi(\hat{\mathbf{z}}^{l-1}) \leq 1$ in general and $\chi(\hat{\mathbf{z}}^{l-1}) = 1$ if ϕ = identity.

Proof. First let us note that

$$\begin{aligned} |\mathcal{P}_x(\hat{\mathbf{y}}^l) - 1| &\leq \eta, \quad \forall \mathbf{x} \in \mathcal{D} &\implies & |\mathcal{P}(\hat{\mathbf{y}}^l) - 1| \leq \eta, \\ |\mathcal{P}_x(\check{\mathbf{z}}^l) - F_\phi(\gamma^2 + \beta^2)| &\leq \eta, \quad \forall \mathbf{x} \in \mathcal{D} &\implies & |\mathcal{P}(\check{\mathbf{z}}^l) - F_\phi(\gamma^2 + \beta^2)| \leq \eta. \end{aligned}$$

Combined with Lemma 2, we deduce for any $\eta > 0$ and any $\delta > 0$ that there exists $N''(\eta, \delta) \in \mathbb{N}^*$ independent of Θ^{l-1}, l such that if $C_l \geq N''(\eta, \delta)$, it holds for random nets of Definition 1 with probability greater than $1 - \delta$ with respect to θ^l that

$$|\mathcal{P}^{(1)}(\hat{\mathbf{y}}^l) - \mathcal{P}^{(1)}(\mathbf{y}^l)| \leq \eta, \quad |\mathcal{P}^{(1)}(\check{\mathbf{z}}^l) - \mathcal{P}^{(1)}(\mathbf{z}^l)| \leq \eta, \quad (87)$$

$$|\mathcal{P}(\hat{\mathbf{y}}^l) - \mathcal{P}(\mathbf{y}^l)| \leq \eta, \quad |\mathcal{P}(\check{\mathbf{z}}^l) - \mathcal{P}(\mathbf{z}^l)| \leq \eta, \quad (88)$$

$$|\mathcal{P}(\hat{\mathbf{y}}^l) - 1| \leq \eta, \quad |\mathcal{P}(\check{\mathbf{z}}^l) - F_\phi(\gamma^2 + \beta^2)| \leq \eta, \quad (89)$$

where $F_\phi \equiv \frac{\phi(1)^2 + \phi(-1)^2}{2} > 0$.

If all inequalities of Eq. (87), (88), (89) hold with $\eta \leq \frac{1}{4}F_\phi(\gamma^2 + \beta^2)$, then $\varrho(\mathbf{z}^l) - \varrho(\check{\mathbf{z}}^l)$ may be upper bounded using

$$\begin{aligned} \mathcal{P}(\mathbf{z}^l) - \mathcal{P}^{(1)}(\mathbf{z}^l) &\leq \mathcal{P}(\check{\mathbf{z}}^l) - \mathcal{P}^{(1)}(\check{\mathbf{z}}^l) + |\mathcal{P}^{(1)}(\check{\mathbf{z}}^l) - \mathcal{P}^{(1)}(\mathbf{z}^l)| + |\mathcal{P}(\mathbf{z}^l) - \mathcal{P}(\check{\mathbf{z}}^l)| \\ &\leq \mathcal{P}(\check{\mathbf{z}}^l) - \mathcal{P}^{(1)}(\check{\mathbf{z}}^l) + 2\eta \\ &\leq \varrho(\check{\mathbf{z}}^l)\mathcal{P}(\check{\mathbf{z}}^l) + 2\eta \\ &\leq \varrho(\check{\mathbf{z}}^l)(F_\phi(\gamma^2 + \beta^2) + \eta) + 2\eta \\ &\leq \varrho(\check{\mathbf{z}}^l)F_\phi(\gamma^2 + \beta^2) + 3\eta, \\ \mathcal{P}(\mathbf{z}^l) &\geq \mathcal{P}(\check{\mathbf{z}}^l) - \eta \\ &\geq F_\phi(\gamma^2 + \beta^2) - 2\eta, \\ \varrho(\mathbf{z}^l) &\leq \frac{\varrho(\check{\mathbf{z}}^l)F_\phi(\gamma^2 + \beta^2) + 3\eta}{F_\phi(\gamma^2 + \beta^2) - 2\eta} \\ &\leq \frac{\varrho(\check{\mathbf{z}}^l) + \frac{3\eta}{F_\phi(\gamma^2 + \beta^2)}}{1 - \frac{2\eta}{F_\phi(\gamma^2 + \beta^2)}} \\ &\leq \left(\varrho(\check{\mathbf{z}}^l) + \frac{3\eta}{F_\phi(\gamma^2 + \beta^2)} \right) \left(1 + \frac{8\eta}{F_\phi(\gamma^2 + \beta^2)} \right) \\ &\leq \varrho(\check{\mathbf{z}}^l) + \frac{35\eta}{F_\phi(\gamma^2 + \beta^2)}, \end{aligned}$$

where we used $\varrho(\check{\mathbf{z}}^l) \leq 1$, as well as $\frac{1}{1-x} \leq 1 + 4x$ for $x \leq \frac{1}{2}$ and $\left(\frac{\eta}{F_\phi(\gamma^2 + \beta^2)} \right)^2 \leq \frac{\eta}{F_\phi(\gamma^2 + \beta^2)}$ for $\frac{\eta}{F_\phi(\gamma^2 + \beta^2)} \leq 1$.

Similarly, if all inequalities of Eq. (87), (88), (89) hold with $\eta \leq \frac{1}{4}F_\phi(\gamma^2 + \beta^2)$, then $\varrho(\mathbf{z}^l) - \varrho(\tilde{\mathbf{z}}^l)$ may be lower-bounded using

$$\begin{aligned}
\mathcal{P}(\mathbf{z}^l) - \mathcal{P}^{(1)}(\mathbf{z}^l) &\geq \mathcal{P}(\tilde{\mathbf{z}}^l) - \mathcal{P}^{(1)}(\tilde{\mathbf{z}}^l) - |\mathcal{P}^{(1)}(\tilde{\mathbf{z}}^l) - \mathcal{P}^{(1)}(\mathbf{z}^l)| - |\mathcal{P}(\mathbf{z}^l) - \mathcal{P}(\tilde{\mathbf{z}}^l)| \\
&\geq \mathcal{P}(\tilde{\mathbf{z}}^l) - \mathcal{P}^{(1)}(\tilde{\mathbf{z}}^l) - 2\eta \\
&\geq \varrho(\tilde{\mathbf{z}}^l)\mathcal{P}(\tilde{\mathbf{z}}^l) - 2\eta \\
&\geq \varrho(\tilde{\mathbf{z}}^l)(F_\phi(\gamma^2 + \beta^2) - \eta) - 2\eta \\
&\geq \varrho(\tilde{\mathbf{z}}^l)F_\phi(\gamma^2 + \beta^2) - 3\eta, \\
\mathcal{P}(\mathbf{z}^l) &\leq \mathcal{P}(\tilde{\mathbf{z}}^l) + \eta \leq F_\phi(\gamma^2 + \beta^2) + 2\eta, \\
\varrho(\mathbf{z}^l) &\geq \frac{\max\left(\varrho(\tilde{\mathbf{z}}^l)F_\phi(\gamma^2 + \beta^2) - 3\eta, 0\right)}{F_\phi(\gamma^2 + \beta^2) + 2\eta} \\
&\geq \frac{\max\left(\varrho(\tilde{\mathbf{z}}^l) - \frac{3\eta}{F_\phi(\gamma^2 + \beta^2)}, 0\right)}{1 + \frac{2\eta}{F_\phi(\gamma^2 + \beta^2)}} \\
&\geq \max\left(\left(\varrho(\tilde{\mathbf{z}}^l) - \frac{3\eta}{F_\phi(\gamma^2 + \beta^2)}\right)\left(1 - \frac{2\eta}{F_\phi(\gamma^2 + \beta^2)}\right), 0\right) \\
&\geq \varrho(\tilde{\mathbf{z}}^l) - \frac{5\eta}{F_\phi(\gamma^2 + \beta^2)}.
\end{aligned}$$

where we used $\varrho(\tilde{\mathbf{z}}^l) \leq 1$, as well as $\frac{1}{1+x} \geq 1 - x \geq 0$ for $0 \leq x \leq 1$.

We deduce that if all inequalities of Eq. (87), (88), (89) hold with $\eta \leq \frac{1}{4}F_\phi(\gamma^2 + \beta^2)$, then

$$|\varrho(\mathbf{z}^l) - \varrho(\tilde{\mathbf{z}}^l)| \leq \frac{35\eta}{F_\phi(\gamma^2 + \beta^2)}. \quad (90)$$

The reasoning that yielded Eq. (90) from Eq. (87), (88), (89) can be immediately transposed by replacing \mathbf{z}^l by \mathbf{y}^l , $\tilde{\mathbf{z}}^l$ by $\hat{\mathbf{y}}^l$ and $F_\phi(\gamma^2 + \beta^2)$ by 1.

Consequently, if all inequalities of Eq. (87), (88), (89) hold with $\eta \leq \frac{1}{4}$, then

$$|\varrho(\mathbf{y}^l) - \varrho(\hat{\mathbf{y}}^l)| \leq 35\eta.$$

Lemma 1 also tells us that for any $\eta > 0$ and any $\delta > 0$, there exists $N'(\eta, \delta) \in \mathbb{N}^*$ independent of Θ^{l-1} , l such that if $C_l \geq N'(\eta, \delta)$, it holds with probability greater than $1 - 2\delta$ with respect to θ^l that

$$|\varrho(\hat{\mathbf{y}}^l) - \varrho(\hat{\mathbf{z}}^{l-1})| \leq \eta, \quad |\varrho(\tilde{\mathbf{z}}^l) - \rho\chi(\hat{\mathbf{z}}^{l-1})\varrho(\hat{\mathbf{z}}^{l-1})| \leq \eta,$$

where $\rho = \frac{\gamma^2}{\gamma^2 + \beta^2} < 1$ and $\chi(\hat{\mathbf{z}}^{l-1}) \in \mathbb{R}^+$ is dependent on Θ^{l-1} but independent of θ^l such that $\chi(\hat{\mathbf{z}}^{l-1}) \leq 1$ in general and $\chi(\hat{\mathbf{z}}^{l-1}) = 1$ if $\phi = \text{identity}$.

Let us then define N_7 independently of Θ^{l-1} , l as

$$N_7(\eta, \delta) = \max\left(N'(\eta, \delta), N''\left(\min\left(\eta, \frac{1}{4}, \frac{1}{4}F_\phi(\gamma^2 + \beta^2)\right), \delta\right)\right), \quad \forall \eta > 0, \quad \forall \delta > 0.$$

Then $\forall \eta > 0, \forall \delta > 0$, if $C_l \geq N_7(\eta, \delta)$, it holds with probability greater than $1 - 3\delta$ with respect to θ^l that

$$\begin{aligned}
|\varrho(\mathbf{y}^l) - \varrho(\hat{\mathbf{z}}^{l-1})| &\leq |\varrho(\mathbf{y}^l) - \varrho(\hat{\mathbf{y}}^l)| + |\varrho(\hat{\mathbf{y}}^l) - \varrho(\hat{\mathbf{z}}^{l-1})| \\
&\leq 35\eta + \eta \\
&\leq 36\eta, \\
|\varrho(\mathbf{z}^l) - \rho\chi(\hat{\mathbf{z}}^{l-1})\varrho(\hat{\mathbf{z}}^{l-1})| &\leq |\varrho(\mathbf{z}^l) - \varrho(\tilde{\mathbf{z}}^l)| + |\varrho(\tilde{\mathbf{z}}^l) - \rho\chi(\hat{\mathbf{z}}^{l-1})\varrho(\hat{\mathbf{z}}^{l-1})| \\
&\leq \frac{35\eta}{F_\phi(\gamma^2 + \beta^2)} + \eta \\
&\leq \left(\frac{35 + F_\phi(\gamma^2 + \beta^2)}{F_\phi(\gamma^2 + \beta^2)}\right)\eta,
\end{aligned}$$

Let us define N_8 independently of Θ^{l-1} , l as

$$N_8(\eta, \delta) = N_7 \left(\min \left(\frac{\eta}{36}, \frac{F_\phi(\gamma^2 + \beta^2)}{35 + F_\phi(\gamma^2 + \beta^2)} \eta \right), \frac{\delta}{3} \right), \quad \forall \eta > 0, \quad \forall \delta > 0.$$

Then $\forall \eta > 0, \delta > 0$, if $C_l \geq N_8(\eta, \delta)$, it holds with probability greater than $1 - \delta$ with respect to θ^l that

$$|\varrho(\mathbf{y}^l) - \varrho(\hat{\mathbf{z}}^{l-1})| \leq \eta, \quad |\varrho(\mathbf{z}^l) - \rho\chi(\hat{\mathbf{z}}^{l-1})\varrho(\hat{\mathbf{z}}^{l-1})| \leq \eta.$$

Next, as in the proof of Lemma 2, we note that $\hat{\mathbf{y}}^l$ and $\hat{\mathbf{z}}^l$ depend only on \mathbf{x} and not on other inputs in the dataset. We may thus apply Lemma 2 in the case of datasets $\mathcal{D}_{\mathbf{x}} = \{\mathbf{x}\}$ with single inputs \mathbf{x} . This gives, for any $\eta > 0$ and any $\delta > 0$, that if $C_l \geq N''(\eta, \delta)$, it holds for any $\mathbf{x} \in \mathcal{D}$ that with probability greater than $1 - 2\delta$ with respect to θ^l :

$$\begin{aligned} |\mathcal{P}_{\mathbf{x}}(\mathbf{y}^l) - 1| &\leq |\mathcal{P}_{\mathbf{x}}(\mathbf{y}^l) - \mathcal{P}_{\mathbf{x}}(\hat{\mathbf{y}}^l)| + |\mathcal{P}_{\mathbf{x}}(\hat{\mathbf{y}}^l) - 1| \\ &\leq 2\eta, \\ |\mathcal{P}_{\mathbf{x}}(\mathbf{z}^l) - F_\phi(\gamma^2 + \beta^2)| &\leq |\mathcal{P}_{\mathbf{x}}(\mathbf{z}^l) - \mathcal{P}_{\mathbf{x}}(\hat{\mathbf{z}}^l)| + |\mathcal{P}_{\mathbf{x}}(\hat{\mathbf{z}}^l) - F_\phi(\gamma^2 + \beta^2)| \\ &\leq 2\eta. \end{aligned}$$

This means that, if $C_l \geq N''(\eta, \delta)$, it holds with probability greater than $1 - 2|\mathcal{D}|\delta$ with respect to θ^l that

$$\begin{aligned} |\mathcal{P}_{\mathbf{x}}(\mathbf{y}^l) - 1| &\leq 2\eta, \quad \forall \mathbf{x} \in \mathcal{D}, \\ |\mathcal{P}_{\mathbf{x}}(\mathbf{z}^l) - F_\phi(\gamma^2 + \beta^2)| &\leq 2\eta, \quad \forall \mathbf{x} \in \mathcal{D}. \end{aligned}$$

Let us finally define N''' independently of Θ^{l-1} , l as $N'''(\eta, \delta) = \max \left(N_8(\eta, \frac{\delta}{2}), N''(\frac{\eta}{2}, \frac{1}{2|\mathcal{D}|} \frac{\delta}{2}) \right)$, $\forall \eta > 0, \forall \delta > 0$. Then, for any $\eta > 0$ and any $\delta > 0$, if $C_l \geq N'''(\eta, \delta)$, it holds with probability greater than $1 - \delta$ with respect to θ^l that

$$\begin{aligned} |\varrho(\mathbf{y}^l) - \varrho(\hat{\mathbf{z}}^{l-1})| &\leq \eta, & |\varrho(\mathbf{z}^l) - \rho\chi(\hat{\mathbf{z}}^{l-1})\varrho(\hat{\mathbf{z}}^{l-1})| &\leq \eta, \\ |\mathcal{P}_{\mathbf{x}}(\mathbf{y}^l) - 1| &\leq \eta, \quad \forall \mathbf{x} \in \mathcal{D}, & |\mathcal{P}_{\mathbf{x}}(\mathbf{z}^l) - F_\phi(\gamma^2 + \beta^2)| &\leq \eta, \quad \forall \mathbf{x} \in \mathcal{D}. \end{aligned} \quad \square$$

E.3 Proof of Theorem 1

Theorem 1. Fix a layer $l \geq 1$ and $\nu_\omega, \nu_\beta, \nu_\gamma, \mathcal{D}$ in Definition 1. Further suppose Norm = LN and suppose that the convolution of Eq. (2) uses periodic boundary conditions.

Then for any $\eta > 0$ and any $\delta > 0$, there exists $N(\eta, \delta) \in \mathbb{N}^*$ such that if $\min_{1 \leq k \leq l} C_k \geq N(\eta, \delta)$, it holds for random nets of Definition 1 with probability greater than $1 - \delta$ with respect to Θ^l that

$$\mathcal{P}(\mathbf{y}^l) - \mathcal{P}^{(1)}(\mathbf{y}^l) \leq \rho^{l-1} + \eta, \quad \mathcal{P}(\mathbf{y}^l) = 1, \quad (91)$$

where $\rho \equiv \frac{\gamma^2}{\gamma^2 + \beta^2} < 1$.

Proof. For fixed Θ^{l-1} such that $\mathcal{P}_{\mathbf{x}}(\mathbf{z}^{l-1}) > 0, \forall \mathbf{x} \in \mathcal{D}$, Lemma 3 tells us that for any $\delta > 0$, if $C_l \geq N''' \left(\min \left(\frac{1}{2}, \frac{F_\phi(\gamma^2 + \beta^2)}{2} \right), \delta \right)$ with $F_\phi \equiv \frac{\phi(1)^2 + \phi(-1)^2}{2} > 0$, it holds for random nets of Definition 1 with probability greater than $1 - \delta$ with respect to θ^l that $\forall \mathbf{x} \in \mathcal{D}$:

$$\begin{aligned} |\mathcal{P}_{\mathbf{x}}(\mathbf{y}^l) - 1| &\leq \frac{1}{2} \implies \mathcal{P}_{\mathbf{x}}(\mathbf{y}^l) \geq 1 - \frac{1}{2} > 0, \\ |\mathcal{P}_{\mathbf{x}}(\mathbf{z}^l) - F_\phi(\gamma^2 + \beta^2)| &\leq \frac{F_\phi(\gamma^2 + \beta^2)}{2} \implies \mathcal{P}_{\mathbf{x}}(\mathbf{z}^l) \geq F_\phi(\gamma^2 + \beta^2) - \frac{F_\phi(\gamma^2 + \beta^2)}{2} > 0. \end{aligned}$$

If we define the event $A^{l-1} \equiv (\mathcal{P}_{\mathbf{x}}(\mathbf{y}^{l-1}) > 0, \forall \mathbf{x} \in \mathcal{D}) \wedge (\mathcal{P}_{\mathbf{x}}(\mathbf{z}^{l-1}) > 0, \forall \mathbf{x} \in \mathcal{D})$, given that N''' is independent of Θ^{l-1} , l , this implies for $C_l \geq N''' \left(\min \left(\frac{1}{2}, \frac{F_\phi(\gamma^2 + \beta^2)}{2} \right), \delta \right)$ that

$$\mathbb{P}_{\Theta^l} \left[\left(\mathcal{P}_{\mathbf{x}}(\mathbf{y}^l) > 0, \forall \mathbf{x} \in \mathcal{D} \right) \wedge \left(\mathcal{P}_{\mathbf{x}}(\mathbf{z}^l) > 0, \forall \mathbf{x} \in \mathcal{D} \right) \middle| A^{l-1} \right] \geq 1 - \delta.$$

Using the fact that $\mathcal{P}(\mathbf{x}) > 0, \forall \mathbf{x} \in \mathcal{D}$ by Definition 1, this implies for $\min_{1 \leq k \leq l} C_k \geq N''' \left(\min \left(\frac{1}{2}, \frac{F_\phi(\gamma^2 + \beta^2)}{2} \right), \delta \right)$ that

$$\mathbb{P}_{\Theta^l} \left[\left(\mathcal{P}_{\mathbf{x}}(\mathbf{y}^l) > 0, \forall \mathbf{x} \in \mathcal{D} \right) \wedge \left(\mathcal{P}_{\mathbf{x}}(\mathbf{z}^l) > 0, \forall \mathbf{x} \in \mathcal{D} \right) \right] \geq (1 - \delta)^l.$$

Thus, for any $\delta > 0$ there exists $N_9(\delta) \in \mathbb{N}^*$ such that, if $\min_{1 \leq k \leq l} C_k \geq N_9(\delta)$, it holds with probability greater than $1 - \delta$ with respect to Θ^l that

$$\begin{aligned} \left(\mathcal{P}_{\mathbf{x}}(\mathbf{y}^l) > 0, \forall \mathbf{x} \in \mathcal{D} \right) \wedge \left(\mathcal{P}_{\mathbf{x}}(\mathbf{z}^l) > 0, \forall \mathbf{x} \in \mathcal{D} \right) &\implies \mathcal{P}_{\mathbf{x}}(\mathbf{y}^l) = 1, \forall \mathbf{x} \in \mathcal{D} \\ &\implies \mathcal{P}(\mathbf{y}^l) = 1. \end{aligned}$$

Lemma 3 also tells us that for any $1 > \eta > 0$ and $\delta > 0$, if $C_l \geq N''' \left(\min \left(\eta, F_\phi(\gamma^2 + \beta^2)\eta \right), \delta \right)$, it holds for random nets of Definition 1 with probability greater than $1 - \delta$ with respect to θ^l that

$$\begin{aligned} F_\phi(\gamma^2 + \beta^2)(1 - \eta) &\leq \mathcal{P}_{\mathbf{x}}(\mathbf{z}^l) \leq F_\phi(\gamma^2 + \beta^2)(1 + \eta) \quad \forall \mathbf{x} \in \mathcal{D}, \\ F_\phi(\gamma^2 + \beta^2)(1 - \eta) &\leq \mathcal{P}(\mathbf{z}^l) \leq F_\phi(\gamma^2 + \beta^2)(1 + \eta), \end{aligned} \quad (92)$$

$$\begin{aligned} \sqrt{\frac{1 - \eta}{1 + \eta}} &\leq \sqrt{\frac{\mathcal{P}(\mathbf{z}^l)}{\mathcal{P}_{\mathbf{x}}(\mathbf{z}^l)}} \leq \sqrt{\frac{1 + \eta}{1 - \eta}} \quad \forall \mathbf{x} \in \mathcal{D}, \\ \left(\sqrt{\frac{\mathcal{P}(\mathbf{z}^l)}{\mathcal{P}_{\mathbf{x}}(\mathbf{z}^l)}} - 1 \right)^2 &\leq g(\eta) \equiv \max \left(\left(\sqrt{\frac{1 - \eta}{1 + \eta}} - 1 \right)^2, \left(\sqrt{\frac{1 + \eta}{1 - \eta}} - 1 \right)^2 \right) \quad \forall \mathbf{x} \in \mathcal{D}. \end{aligned} \quad (93)$$

If Eq. (93) holds, then

$$\begin{aligned} \hat{\mathbf{z}}_{\alpha,c}^l - \mathbf{z}_{\alpha,c}^l &= \left(\sqrt{\frac{\mathcal{P}(\mathbf{z}^l)}{\mathcal{P}_{\mathbf{x}}(\mathbf{z}^l)}} - 1 \right) \mathbf{z}_{\alpha,c}^l, \\ \mathcal{P}_{\mathbf{x}}(\hat{\mathbf{z}}^l - \mathbf{z}^l) &= \left(\sqrt{\frac{\mathcal{P}(\mathbf{z}^l)}{\mathcal{P}_{\mathbf{x}}(\mathbf{z}^l)}} - 1 \right)^2 \mathcal{P}_{\mathbf{x}}(\mathbf{z}^l) \leq g(\eta) \mathcal{P}_{\mathbf{x}}(\mathbf{z}^l), \\ \mathcal{P}(\hat{\mathbf{z}}^l - \mathbf{z}^l) &\leq g(\eta) \mathcal{P}(\mathbf{z}^l). \end{aligned}$$

In turn, this implies that if both Eq. (92) and Eq. (93) hold, then

$$\begin{aligned} |\mathcal{P}(\hat{\mathbf{z}}^l) - \mathcal{P}(\mathbf{z}^l)| &\leq \mathcal{P}(\hat{\mathbf{z}}^l - \mathbf{z}^l) + 2\mu(|\hat{\mathbf{z}}^l - \mathbf{z}^l| |\mathbf{z}^l|) \\ &\leq \mathcal{P}(\hat{\mathbf{z}}^l - \mathbf{z}^l) + 2\sqrt{\mathcal{P}(\hat{\mathbf{z}}^l - \mathbf{z}^l) \mathcal{P}(\mathbf{z}^l)} \\ &\leq \left(g(\eta) + 2\sqrt{g(\eta)} \right) \mathcal{P}(\mathbf{z}^l) \\ &\leq \left(g(\eta) + 2\sqrt{g(\eta)} \right) F_\phi(\gamma^2 + \beta^2)(1 + \eta), \\ |\mathcal{P}^{(1)}(\hat{\mathbf{z}}^l) - \mathcal{P}^{(1)}(\mathbf{z}^l)| &\leq \mathcal{P}^{(1)}(\hat{\mathbf{z}}^l - \mathbf{z}^l) + 2 \left| \mathbb{E}_c \left[\mu_c(\hat{\mathbf{z}}^l - \mathbf{z}^l) \mu_c(\hat{\mathbf{z}}^l) \right] \right| \\ &\leq \mathcal{P}(\hat{\mathbf{z}}^l - \mathbf{z}^l) + 2 \mathbb{E}_c \left[\left| \mu_c(\hat{\mathbf{z}}^l - \mathbf{z}^l) \right| \left| \mu_c(\hat{\mathbf{z}}^l) \right| \right] \\ &\leq \mathcal{P}(\hat{\mathbf{z}}^l - \mathbf{z}^l) + 2 \sqrt{\mathbb{E}_c \left[\mu_c(\hat{\mathbf{z}}^l - \mathbf{z}^l)^2 \right] \mathbb{E}_c \left[\mu_c(\hat{\mathbf{z}}^l)^2 \right]} \\ &\leq \mathcal{P}(\hat{\mathbf{z}}^l - \mathbf{z}^l) + 2\sqrt{\mathcal{P}(\hat{\mathbf{z}}^l - \mathbf{z}^l) \mathcal{P}(\hat{\mathbf{z}}^l)} \\ &\leq \left(g(\eta) + 2\sqrt{g(\eta)} \right) F_\phi(\gamma^2 + \beta^2)(1 + \eta). \end{aligned}$$

Since $(g(\eta) + 2\sqrt{g(\eta)}) F_\phi(\gamma^2 + \beta^2)(1 + \eta) \rightarrow 0$ as $\eta \rightarrow 0$, we deduce for any $\eta > 0$ and any $\delta > 0$ that there exists $N_{10}(\eta, \delta) \in \mathbb{N}^*$, such that, if $C_l \geq N_{10}(\eta, \delta)$, it holds with probability greater than

$1 - \delta$ with respect to θ^l that

$$\begin{aligned} |\mathcal{P}_{\mathbf{x}}(\mathbf{z}^l) - F_\phi(\gamma^2 + \beta^2)| &\leq \eta \quad \forall \mathbf{x} \in \mathcal{D} \implies |\mathcal{P}(\mathbf{z}^l) - F_\phi(\gamma^2 + \beta^2)| \leq \eta, \\ |\mathcal{P}(\hat{\mathbf{z}}^l) - \mathcal{P}(\mathbf{z}^l)| &\leq \eta, \\ |\mathcal{P}^{(1)}(\hat{\mathbf{z}}^l) - \mathcal{P}^{(1)}(\mathbf{z}^l)| &\leq \eta. \end{aligned}$$

Defining N_{11} independently of Θ^{l-1} , l as $N_{11}(\eta, \delta) = \max\left(N'''(\eta, \frac{\delta}{2}), N_{10}(\eta, \frac{\delta}{2})\right)$, $\forall \eta > 0$, $\forall \delta > 0$, we deduce for any $\eta > 0$ and any $\delta > 0$ that, if $C_l \geq N_{11}(\eta, \delta)$, it holds with probability greater than $1 - \delta$ with respect to θ^l that

$$\begin{aligned} |\varrho(\mathbf{y}^l) - \varrho(\hat{\mathbf{z}}^{l-1})| &\leq \eta, \\ |\varrho(\mathbf{z}^l) - \rho\chi(\hat{\mathbf{z}}^{l-1})\varrho(\hat{\mathbf{z}}^{l-1})| &\leq \eta, \\ |\mathcal{P}(\mathbf{z}^l) - F_\phi(\gamma^2 + \beta^2)| &\leq \eta, \\ |\mathcal{P}(\hat{\mathbf{z}}^l) - \mathcal{P}(\mathbf{z}^l)| &\leq \eta, \\ |\mathcal{P}^{(1)}(\hat{\mathbf{z}}^l) - \mathcal{P}^{(1)}(\mathbf{z}^l)| &\leq \eta. \end{aligned}$$

The reasoning that yielded Eq. (90) from Eq. (87), (88), (89) can be immediately transposed by replacing $\hat{\mathbf{z}}^l$ by \mathbf{z}^l and \mathbf{z}^l by $\hat{\mathbf{z}}^l$.

Thus, if $C_l \geq N_{11}(\eta, \delta)$, it holds with probability greater than $1 - \delta$ with respect to θ^l that

$$\begin{aligned} |\varrho(\mathbf{y}^l) - \varrho(\hat{\mathbf{z}}^{l-1})| &\leq \eta, \\ |\varrho(\mathbf{z}^l) - \rho\chi(\hat{\mathbf{z}}^{l-1})\varrho(\hat{\mathbf{z}}^{l-1})| &\leq \eta, \\ |\varrho(\hat{\mathbf{z}}^l) - \varrho(\mathbf{z}^l)| &\leq \frac{35\eta}{F_\phi(\gamma^2 + \beta^2)}, \\ |\varrho(\hat{\mathbf{z}}^l) - \rho\chi(\hat{\mathbf{z}}^{l-1})\varrho(\hat{\mathbf{z}}^{l-1})| &\leq \eta + \frac{35\eta}{F_\phi(\gamma^2 + \beta^2)} = \frac{F_\phi(\gamma^2 + \beta^2) + 35}{F_\phi(\gamma^2 + \beta^2)}\eta. \end{aligned}$$

Defining N_{12} independently of Θ^{l-1} , l as $N_{12}(\eta, \delta) = N_{11}\left(\frac{F_\phi(\gamma^2 + \beta^2)}{F_\phi(\gamma^2 + \beta^2) + 35}\eta, \delta\right)$, $\forall \eta > 0$, $\forall \delta > 0$, we deduce for any $\eta > 0$ and any $\delta > 0$ that, if $C_l \geq N_{12}(\eta, \delta)$, it holds that

$$\begin{aligned} \mathbb{P}_{\theta^l} \left[|\varrho(\mathbf{y}^l) - \varrho(\hat{\mathbf{z}}^{l-1})| \leq \eta \right] &\geq \mathbb{P}_{\theta^l} \left[|\varrho(\mathbf{y}^l) - \varrho(\hat{\mathbf{z}}^{l-1})| \leq \frac{F_\phi(\gamma^2 + \beta^2)}{F_\phi(\gamma^2 + \beta^2) + 35}\eta \right] \geq 1 - \delta, \\ \mathbb{P}_{\theta^l} \left[|\varrho(\hat{\mathbf{z}}^l) - \rho\chi(\hat{\mathbf{z}}^{l-1})\varrho(\hat{\mathbf{z}}^{l-1})| \leq \eta \right] &\geq 1 - \delta. \end{aligned}$$

Consequently, for any layer k and for any $\eta > 0$ and any $\delta > 0$, if $C_k \geq N_{12}(\eta, \delta)$, it holds for random nets of Definition 1 that

$$\begin{aligned} \mathbb{P}_{\Theta^k} \left[|\varrho(\mathbf{y}^k) - \varrho(\hat{\mathbf{z}}^{k-1})| \leq \eta \right] &\geq 1 - \delta, \\ \mathbb{P}_{\Theta^k} \left[|\varrho(\hat{\mathbf{z}}^k) - \rho\chi(\hat{\mathbf{z}}^{k-1})\varrho(\hat{\mathbf{z}}^{k-1})| \leq \eta \right] &\geq 1 - \delta. \end{aligned}$$

Thus, for any $\eta > 0$ and any $\delta > 0$, if $\min_{1 \leq k \leq l} C_k \geq N_{12}(\eta, \delta)$, it holds for random nets of Definition 1 with probability greater than $1 - l\delta$ with respect to Θ^l that

$$|\varrho(\hat{\mathbf{z}}^k) - \rho\chi(\hat{\mathbf{z}}^{k-1})\varrho(\hat{\mathbf{z}}^{k-1})| \leq \eta, \quad \forall k \leq l - 1, \quad (94)$$

$$|\varrho(\mathbf{y}^l) - \varrho(\hat{\mathbf{z}}^{l-1})| \leq \eta. \quad (95)$$

Given $\chi(\hat{\mathbf{z}}^{k-1}) \leq 1, \forall k$ and given $\varrho(\mathbf{z}^0) = \varrho(\mathbf{x}) \leq 1$, we note that if Eq. (94) and Eq. (95) hold, then

$$\begin{aligned}
\varrho(\hat{\mathbf{z}}^1) &\leq \rho\chi(\mathbf{z}^0)\varrho(\mathbf{z}^0) + \eta \leq \rho + \eta, \\
\varrho(\hat{\mathbf{z}}^2) &\leq \rho\chi(\hat{\mathbf{z}}^1)\varrho(\hat{\mathbf{z}}^1) + \eta \leq \rho^2 + \rho\eta + \eta, \\
&\vdots \\
\varrho(\hat{\mathbf{z}}^{l-1}) &\leq \rho\chi(\hat{\mathbf{z}}^{l-2})\varrho(\hat{\mathbf{z}}^{l-2}) + \eta \leq \rho^{l-1} + \left(\sum_{k=0}^{l-2} \rho^k\right)\eta \leq \rho^{l-1} + \frac{1}{1-\rho}\eta, \\
\varrho(\mathbf{y}^l) &\leq \varrho(\hat{\mathbf{z}}^{l-1}) + \eta \leq \rho^{l-1} + \frac{1}{1-\rho}\eta + \eta \leq \rho^{l-1} + \left(\frac{2-\rho}{1-\rho}\right)\eta.
\end{aligned} \tag{96}$$

Defining N_{13} such that $N_{13}(\eta, \delta) = N_{12}\left(\frac{1-\rho}{2-\rho}\eta, \frac{1}{l}\delta\right)$, $\forall \eta > 0, \forall \delta > 0$, we deduce for any $\eta > 0$ and any $\delta > 0$ that, if $\min_{1 \leq k \leq l} C_k \geq N_{13}(\eta, \delta)$, it holds for random nets of Definition 1 with probability greater than $1 - \delta$ with respect to Θ^l that

$$\varrho(\mathbf{y}^l) \leq \rho^{l-1} + \eta.$$

Finally, let us define N such that $N(\eta, \delta) = \max\left(N_9\left(\frac{\delta}{2}\right), N_{13}(\eta, \frac{\delta}{2})\right)$, $\forall \eta > 0, \forall \delta > 0$. Then for any $\eta > 0$ and any $\delta > 0$, if $\min_{1 \leq k \leq l} C_k \geq N(\eta, \delta)$, it holds with probability greater than $1 - \delta$ with respect to Θ^l that

$$\varrho(\mathbf{y}^l) = \mathcal{P}(\mathbf{y}^l) - \mathcal{P}^{(1)}(\mathbf{y}^l) \leq \rho^{l-1} + \eta, \quad \mathcal{P}(\mathbf{y}^l) = 1. \quad \square$$

E.4 Case $\phi = \text{identity}$

Proposition 6. Fix a layer $l \geq 1$ and $\nu_\omega, \nu_\beta, \nu_\gamma, \mathcal{D}$ in Definition 1, with \mathcal{D} “centered” such that $\mathcal{P}^{(1)}(\mathbf{x}) = 0$. Further suppose Norm = LN and $\phi = \text{identity}$, and suppose that the convolution of Eq. (2) uses periodic boundary conditions.

Then for any $\eta > 0$ and any $\delta > 0$, there exists $N(\eta, \delta) \in \mathbb{N}^*$ such that if $\min_{1 \leq k \leq l} C_k \geq N(\eta, \delta)$, it holds for random nets of Definition 1 with probability greater than $1 - \delta$ with respect to Θ^l that

$$|\mathcal{P}(\mathbf{y}^l) - \mathcal{P}^{(1)}(\mathbf{y}^l) - \rho^{l-1}| \leq \eta, \quad \mathcal{P}(\mathbf{y}^l) = 1,$$

where $\rho \equiv \frac{\gamma^2}{\gamma^2 + \beta^2} < 1$.

Proof. Since $\phi = \text{identity}$ is a particular case of positive homogeneous activation function, the whole proof of Theorem 1 still applies. Let us then define N_9, N_{12} as in the proof of Theorem 1.

Then for any $\delta > 0$, if $\min_{1 \leq k \leq l} C_k \geq N_9(\delta)$, it holds with probability greater than $1 - \delta$ with respect to Θ^l that

$$\mathcal{P}(\mathbf{y}^l) = 1.$$

In addition, for any $\eta > 0$ and any $\delta > 0$, if $\min_{1 \leq k \leq l} C_k \geq N_{12}(\eta, \delta)$, it holds for random nets of Definition 1 with probability greater than $1 - \delta$ with respect to Θ^l that

$$\begin{aligned}
|\varrho(\hat{\mathbf{z}}^k) - \rho\chi(\hat{\mathbf{z}}^{k-1})\varrho(\hat{\mathbf{z}}^{k-1})| &= |\varrho(\hat{\mathbf{z}}^k) - \rho\varrho(\hat{\mathbf{z}}^{k-1})| \leq \eta, \quad \forall k \leq l-1, \\
|\varrho(\mathbf{y}^l) - \varrho(\hat{\mathbf{z}}^{l-1})| &\leq \eta,
\end{aligned}$$

where we used the fact that $\chi(\hat{\mathbf{z}}^{k-1}) = 1, \forall k$ when $\phi = \text{identity}$.

Next we note that: (i) the assumptions that $\mathcal{P}^{(1)}(\mathbf{x}) = 0$ and that $\mathcal{P}_x(\mathbf{x}) > 0, \forall \mathbf{x}$ (cf Definition 1) together imply $\varrho(\mathbf{z}^0) = \varrho(\mathbf{x}) = 1$; (ii) the reasoning yielding Eq. (96) from Eq. (94), (95) still applies.

Thus, if $\min_{1 \leq k \leq l} C_k \geq N_{12}(\eta, \delta)$, it holds for random nets of Definition 1 with probability greater than $1 - l\delta$ with respect to Θ^l that

$$\begin{aligned}
\varrho(\hat{\mathbf{z}}^1) &\geq \rho\varrho(\mathbf{x}) - \eta = \rho - \eta, \\
\varrho(\hat{\mathbf{z}}^2) &\geq \rho\varrho(\hat{\mathbf{z}}^1) - \eta \geq \rho^2 - \rho\eta - \eta, \\
&\vdots \\
\varrho(\hat{\mathbf{z}}^{l-1}) &\geq \rho\varrho(\hat{\mathbf{z}}^{l-2}) - \eta \geq \rho^{l-1} - \left(\sum_{k=0}^{l-2} \rho^k\right)\eta \geq \rho^{l-1} - \frac{1}{1-\rho}\eta, \\
\varrho(\mathbf{y}^l) &\geq \varrho(\hat{\mathbf{z}}^{l-1}) - \eta \geq \rho^{l-1} - \frac{1}{1-\rho}\eta - \eta \geq \rho^{l-1} - \left(\frac{2-\rho}{1-\rho}\right)\eta, \\
\varrho(\mathbf{y}^l) &\leq \rho^{l-1} + \left(\frac{2-\rho}{1-\rho}\right)\eta, \\
|\varrho(\mathbf{y}^l) - \rho^{l-1}| &\leq \left(\frac{2-\rho}{1-\rho}\right)\eta,
\end{aligned} \tag{97}$$

where Eq. (97) follows from Eq. (96).

As in the proof of Theorem 1, defining N_{13} such that $N_{13}(\eta, \delta) = N_{12}\left(\frac{1-\rho}{2-\rho}\eta, \frac{1}{l}\delta\right)$, we deduce for any $\eta > 0$ and any $\delta > 0$ that, if $\min_{1 \leq k \leq l} C_k \geq N_{13}(\eta, \delta)$, it holds for random nets of Definition 1 with probability greater than $1 - \delta$ with respect to Θ^l that

$$|\varrho(\mathbf{y}^l) - \rho^{l-1}| \leq \eta.$$

As in the proof of Theorem 1, defining N such that $N(\eta, \delta) = \max\left(N_9\left(\frac{\delta}{2}\right), N_{13}\left(\eta, \frac{\delta}{2}\right)\right)$, $\forall \eta > 0$, $\forall \delta > 0$, we deduce for any $\eta > 0$ and any $\delta > 0$ that, if $\min_{1 \leq k \leq l} C_k \geq N(\eta, \delta)$, it holds with probability greater than $1 - \delta$ with respect to Θ^l that

$$|\varrho(\mathbf{y}^l) - \rho^{l-1}| = |\mathcal{P}(\mathbf{y}^l) - \mathcal{P}^{(1)}(\mathbf{y}^l) - \rho^{l-1}| \leq \eta, \quad \mathcal{P}(\mathbf{y}^l) = 1. \quad \square$$

F Proof of Theorem 2

Theorem 2. Fix a layer $l \in \{1, \dots, L\}$ and lift any assumption on ϕ . Further suppose $\text{Norm} = \text{IN}$, with Eq. (3) having nonzero denominator at layer l for all inputs and channels.

Then it holds that

- \mathbf{y}^l is normalized in each channel c with

$$\mathcal{P}_c^{(1)}(\mathbf{y}^l) = 0, \quad \mathcal{P}_c(\mathbf{y}^l) = 1;$$

- \mathbf{y}^l lacks variability in instance statistics in each channel c with

$$\mathcal{P}_c^{(2)}(\mathbf{y}^l) = 0, \quad \mathcal{P}_c^{(3)}(\mathbf{y}^l) = 1, \quad \mathcal{P}_c^{(4)}(\mathbf{y}^l) = 0.$$

Proof. With $\text{Norm} = \text{IN}$, if $\sigma_{\mathbf{x},c}(\mathbf{x}^l) > 0$, $\forall \mathbf{x}, c$, the instance statistics are given by

$$\begin{aligned}
\mu_{\mathbf{x},c}(\mathbf{y}^l) &= \mathbb{E}_\alpha[\mathbf{y}_{\alpha,c}^l] = \frac{\mathbb{E}_\alpha[\mathbf{x}_{\alpha,c}^l] - \mu_{\mathbf{x},c}(\mathbf{x}^l)}{\sigma_{\mathbf{x},c}(\mathbf{x}^l)} = \frac{\mu_{\mathbf{x},c}(\mathbf{x}^l) - \mu_{\mathbf{x},c}(\mathbf{x}^l)}{\sigma_{\mathbf{x},c}(\mathbf{x}^l)} = 0, \\
\mathcal{P}_{\mathbf{x},c}(\mathbf{y}^l) &= \mathbb{E}_\alpha[(\mathbf{y}_{\alpha,c}^l)^2] = \frac{\mathbb{E}_\alpha[(\mathbf{x}_{\alpha,c}^l - \mu_{\mathbf{x},c}(\mathbf{x}^l))^2]}{\sigma_{\mathbf{x},c}(\mathbf{x}^l)^2} = \frac{\sigma_{\mathbf{x},c}(\mathbf{x}^l)^2}{\sigma_{\mathbf{x},c}(\mathbf{x}^l)^2} = 1, \\
\sigma_{\mathbf{x},c}(\mathbf{y}^l) &= \sqrt{\mathcal{P}_{\mathbf{x},c}(\mathbf{y}^l) - \mu_{\mathbf{x},c}(\mathbf{y}^l)^2} = 1.
\end{aligned}$$

In turn, this implies for the different power terms:

$$\begin{aligned}\mathcal{P}_c(\mathbf{y}^l) &= \mathbb{E}_{\mathbf{x}}[\mathcal{P}_{\mathbf{x},c}(\mathbf{y}^l)] = \mathbb{E}_{\mathbf{x}}[1] = 1, \\ \mathcal{P}_c^{(1)}(\mathbf{y}^l) &= \mathbb{E}_{\mathbf{x}}[\mu_{\mathbf{x},c}(\mathbf{y}^l)]^2 = \mathbb{E}_{\mathbf{x}}[0]^2 = 0, \quad \mathcal{P}_c^{(2)}(\mathbf{y}^l) = \text{Var}_{\mathbf{x}}[\mu_{\mathbf{x},c}(\mathbf{y}^l)] = \text{Var}_{\mathbf{x}}[0] = 0, \\ \mathcal{P}_c^{(3)}(\mathbf{y}^l) &= \mathbb{E}_{\mathbf{x}}[\sigma_{\mathbf{x},c}(\mathbf{y}^l)]^2 = \mathbb{E}_{\mathbf{x}}[1]^2 = 1, \quad \mathcal{P}_c^{(4)}(\mathbf{y}^l) = \text{Var}_{\mathbf{x}}[\sigma_{\mathbf{x},c}(\mathbf{y}^l)] = \text{Var}_{\mathbf{x}}[1] = 0. \quad \square\end{aligned}$$

G Proof of Theorem 3

Theorem 3. Fix a layer $l \in \{1, \dots, L\}$ and lift any assumptions on ϕ and \mathbf{x} 's distribution. Further suppose that the neural network implements Eq. (2), (3), (7) at every layer up to depth L , with $\epsilon = 0$ and Eq. (3), (7) having nonzero denominators for all layers, inputs and channels.

Now suppose that

- The proxy-normalized post-activations $\tilde{\mathbf{z}}^{l-1}$ at layer $l-1$ are normalized in each channel c :

$$\mathcal{P}_c^{(1)}(\tilde{\mathbf{z}}^{l-1}) = 0, \quad \mathcal{P}_c(\tilde{\mathbf{z}}^{l-1}) = 1;$$

- The convolution and normalization steps at layer l do not cause any aggravation of channel-wise collapse and channel imbalance, i.e. $\forall c, c'$:

$$\mathcal{P}_c^{(1)}(\mathbf{y}^l) = 0, \quad \mathcal{P}_c(\mathbf{y}^l) = \mathcal{P}_{c'}(\mathbf{y}^l);$$

- The pre-activations \mathbf{y}^l at layer l are Gaussian in each channel c and PN's additional parameters $\tilde{\beta}^l, \tilde{\gamma}^l$ are zero.

Then both the pre-activations \mathbf{y}^l and the proxy-normalized post-activations $\tilde{\mathbf{z}}^l$ at layer l are normalized in each channel c :

$$\mathcal{P}_c^{(1)}(\mathbf{y}^l) = 0, \quad \mathcal{P}_c(\mathbf{y}^l) = 1, \quad (98)$$

$$\mathcal{P}_c^{(1)}(\tilde{\mathbf{z}}^l) = 0, \quad \mathcal{P}_c(\tilde{\mathbf{z}}^l) = 1. \quad (99)$$

Proof of Eq. (98). If the denominator of Eq. (3) is nonzero for all layers, inputs and channels, it follows from Proposition 3 that $\mathcal{P}(\mathbf{y}^l) = \mathbb{E}_c[\mathcal{P}_c(\mathbf{y}^l)] = 1$.

Combined with $\mathcal{P}_c^{(1)}(\mathbf{y}^l) = 0, \forall c$ and $\mathcal{P}_c(\mathbf{y}^l) = \mathcal{P}_{c'}(\mathbf{y}^l), \forall c, c'$, we deduce that in each channel c :

$$\mathcal{P}_c^{(1)}(\mathbf{y}^l) = 0, \quad \mathcal{P}_c(\mathbf{y}^l) = 1. \quad \square$$

Proof of Eq. (99). Given Eq. (98) and given that \mathbf{y}^l is Gaussian in each channel c , it follows that $\forall c$:

$$\mathbf{y}_{\alpha,c}^l \underset{\mathbf{x},\alpha}{\sim} \mathcal{N}(0, 1).$$

We deduce that the distribution of $\mathbf{z}_{\alpha,c}^l = \phi(\gamma_c^l \mathbf{y}_{\alpha,c}^l + \beta_c^l)$ with respect to (\mathbf{x}, α) and the distribution of $\phi(\gamma_c^l Y_c^l + \beta_c^l)$ with respect to $Y_c^l \sim \mathcal{N}(\tilde{\beta}_c^l, (1 + \tilde{\gamma}_c^l)^2) = \mathcal{N}(0, 1)$ are equal.

We then get from Eq. (7) at layer l that

$$\tilde{\mathbf{z}}_{\alpha,c}^l = \frac{\mathbf{z}_{\alpha,c}^l - \mathbb{E}_{Y_c^l}[\phi(\gamma_c^l Y_c^l + \beta_c^l)]}{\sqrt{\text{Var}_{Y_c^l}[\phi(\gamma_c^l Y_c^l + \beta_c^l)] + \epsilon}} = \frac{\mathbf{z}_{\alpha,c}^l - \mathbb{E}_{\mathbf{x},\alpha}[\mathbf{z}_{\alpha,c}^l]}{\sqrt{\text{Var}_{\mathbf{x},\alpha}[\mathbf{z}_{\alpha,c}^l]}} = \frac{\mathbf{z}_{\alpha,c}^l - \mu_c(\mathbf{z}^l)}{\sigma_c(\mathbf{z}^l)},$$

where we used $\epsilon = 0$.

We deduce that in each channel c :

$$\begin{aligned}\mu_c(\tilde{\mathbf{z}}^l) &= 0, & \sigma_c(\tilde{\mathbf{z}}^l) &= 1, \\ \mathcal{P}_c^{(1)}(\tilde{\mathbf{z}}^l) &= \mu_c(\tilde{\mathbf{z}}^l)^2 = 0, & \mathcal{P}_c(\tilde{\mathbf{z}}^l) &= \sigma_c(\tilde{\mathbf{z}}^l)^2 + \mu_c(\tilde{\mathbf{z}}^l)^2 = 1. \quad \square\end{aligned}$$